



UNIVERSIDAD  
DE MÁLAGA

ESCUELA DE INGENIERÍAS INDUSTRIALES  
DOCTORADO EN SISTEMAS DE ENERGÍA ELÉCTRICA

DOCTORAL DISSERTATION

---

TIGHT AND COMPACT MODELS  
FOR POWER SYSTEMS OPERATION

---

*Author*

*Álvaro Porras Cabrera*

*Supervisors*

Prof. Dr. *Juan Miguel Morales González*

Prof. Dr. *Salvador Pineda Morente*

Universidad de Málaga, 2023





## DECLARACIÓN DE AUTORÍA Y ORIGINALIDAD DE LA TESIS PRESENTADA PARA OBTENER EL TÍTULO DE DOCTOR

D./Dña ÁLVARO PORRAS CABRERA

Estudiante del programa de doctorado SISTEMAS DE ENERGÍA ELÉCTRICA de la Universidad de Málaga, autor/a de la tesis, presentada para la obtención del título de doctor por la Universidad de Málaga, titulada: TIGHT AND COMPACT MODELS FOR POWER SYSTEMS OPERATION

Realizada bajo la tutorización de SALVADOR PINEDA MORENTE y dirección de JUAN MIGUEL MORALES GONZÁLEZ Y SALVADOR PIENDA MORENTE (si tuviera varios directores deberá hacer constar el nombre de todos)

DECLARO QUE:

La tesis presentada es una obra original que no infringe los derechos de propiedad intelectual ni los derechos de propiedad industrial u otros, conforme al ordenamiento jurídico vigente (Real Decreto Legislativo 1/1996, de 12 de abril, por el que se aprueba el texto refundido de la Ley de Propiedad Intelectual, regularizando, aclarando y armonizando las disposiciones legales vigentes sobre la materia), modificado por la Ley 2/2019, de 1 de marzo.

Igualmente asumo, ante a la Universidad de Málaga y ante cualquier otra instancia, la responsabilidad que pudiera derivarse en caso de plagio de contenidos en la tesis presentada, conforme al ordenamiento jurídico vigente.

En Málaga, a 24 de JULIO de 2023

Fdo.: ÁLVARO PORRAS CABRERA Doctorando/a	Fdo.: SALVADOR PINEDA MORENTE Tutor/a
Fdo.: JUAN MIGUEL MORALES GONZÁLEZ, SALVADOR PINEDA MORENTE Director/es de tesis	







UNIVERSIDAD  
DE MÁLAGA

Dr. Juan Miguel Morales González, profesor titular del departamento de Matemática Aplicada de la Universidad de Málaga, en calidad de director y Dr. Salvador Pineda Morente, profesor del departamento de Ingeniería Eléctrica de la Universidad de Málaga, en calidad de director y tutor de la tesis de título “TIGHT AND COMPACT MODELS FOR POWER SYSTEMS OPERATION” realizada por el doctorando Álvaro Porrás Cabrera dentro del programa de doctorado de Sistemas de Energía Eléctrica, certifican que:

- Han procedido a la revisión de la presente memoria y reúne los requisitos necesarios para ser sometida al juicio de la Comisión correspondiente.
- Las publicaciones que avalan la mencionada tesis no han sido utilizadas en tesis doctorales anteriores.

Y para que conste a efectos de lo establecido en el artículo octavo del Real Decreto 99/2011, autorizan la presentación y defensa de este trabajo para optar al Grado de Doctor por la Universidad de Málaga.

En Málaga, a 24 de julio de 2023

Fdo. JUAN MIGUEL MORALES GONZÁLEZ

Director de la tesis

Fdo. SALVADOR PINEDA MORENTE

Director y tutor de la tesis



*A la memoria de mis abuelos,  
Dolores y Eusebio,  
Rosario y Mariano.*

*A mis padres,  
Paula y Mariano.*



# Acknowledgments

With this thesis, I am fulfilling one of the numerous aspirations I have held since childhood. I could not let this occasion pass by without expressing my heartfelt gratitude to those individuals who have made this achievement possible.

My deepest thanks to my supervisors, Dr. Juan M. Morales, and Dr. Salvador Pineda. Your unwavering dedication, active involvement, and insightful guidance have encouraged me to grow as a researcher. With your invaluable support, I have been able to embrace this experience fully and delve into fascinating realms of research such as power systems and optimization. Without doubt, you serve as an inspiration, both personally and professionally.

Thanks to the rest of the members of the OASYS research group, a piece of all of you is in this thesis. Ricardo, I am deeply grateful for your invaluable assistance during my early days at OASYS, which allowed me to embark on this journey with confidence. Miguel Ángel, thank you for your willingness to help me and for the great discussions we have had. A special mention goes to Adrián, whose friendship has become an integral part of this stage of my life. You are truly unique, and this experience would have been utterly different without you.

I would also thank Dr. Line Roald, who kindly hosted me in her research group, WISPO, during my research stay. Your work has been a remarkable source of inspiration for this thesis. I would also like to acknowledge the other members of WISPO for fostering a welcoming environment, especially Aditya and Yasmine. Aditya, I appreciate your companionship in the office and our enlightening conversations. Yasmine, thank you for being a true friend and for your support.

Finally, I would like to thank Prof. Mario Durán for introducing me to the world of research when I was an undergraduate student, and Dr. Ignacio González for sharing his passion for this profession with me.

También quiero agradecer a las personas de mi entorno que, a pesar de no estar involucradas con el mundo de la investigación, han formado parte de este camino.

*A mis padres, Paula y Mariano.* De vosotros aprendí que el éxito es superar y no conseguir. Vuestra vida es un ejemplo, es éxito. Gracias por todo lo que me habéis dado.

*A Paloma, mi compañera de vida.* Siempre agradeceré al destino que aparecieses en mi camino. Gracias por tu tiempo y por adaptarte. Gracias por las aventuras, aprendí a exprimir cada momento y a conectar con cada lugar. Gracias por apoyarme y quererme sin importar las circunstancias.

*A mis hermanos, Mariano y David.* Pasarán los años y siempre seré el pequeño, gracias por protegerme.

*A mis sobrinos, Bruno y Mateo.* La alegría de la casa y parte de la mía. Gracias por vuestro amor y vuestra nobleza.

*A Pilar, Fran y Francisco.* Gracias por abrirme las puertas de vuestra casa y tratarme como uno más, en pocas palabras, por ser una segunda familia. Por supuesto, no me olvido de *Tita Carmen*, gracias por tanto cariño y tantos momentos divertidos.

Por último, quiero hacer una mención especial para la generación de mis abuelos y la generación de mis padres, campesinos y obreros. Generaciones que aceptaron su destino, trabajaron sin descanso y se sacrificaron por brindarnos las oportunidades que nunca tuvieron. Gracias de corazón.



# Resumen

## Motivación

Los sistemas eléctricos son unas de las estructuras ingenieriles más complejas y colosales en la sociedad actual, cuya operación requiere de la coordinación de múltiples unidades de generación para garantizar un suministro de energía seguro y fiable. Esta coordinación implica considerar varios aspectos técnicos de los generadores, tales como los límites en los niveles de producción y en las rampas, así como diversos aspectos del sistema eléctrico como las restricciones de red.

En las últimas décadas, se han producido cambios significativos en los sistemas eléctricos de numerosas regiones del mundo con el propósito de transitar a sistemas sostenibles con cero emisiones netas de gases de efecto invernadero. En particular, la integración de fuentes de energía renovable ha planteado desafíos en la operación de los sistemas eléctricos debido a su naturaleza inherentemente incierta y el cambio producido hacia un sistema eléctrico geográficamente más disperso [1]. Además, la transición hacia la sostenibilidad implica que la operación de los sistemas eléctricos se enfrente a futuros retos como la integración de pequeños recursos energéticos distribuidos en los sistemas de distribución, el desarrollo de un enfoque centrado en el usuario final donde se garantice la participación activa de los consumidores junto con el conocimiento de las necesidades de los sistemas eléctricos, las transacciones locales de energía y la integración a gran escala de los sistemas de almacenamiento de energía [2]. Esto exige el desarrollo de nuevas vías de investigación para acelerar la transición mediante la mejora de la operación de los sistemas de energía.

En este contexto, esta tesis aborda dos de los problemas más relevantes en la operación de los sistemas eléctricos, como son el problema de la programación horaria de centrales eléctricas (conocido por sus siglas en inglés UC, *unit commitment*) y el flujo de cargas óptimo (conocido por sus siglas en inglés OPF, *optimal power flow*). Estos dos problemas representan una pieza fundamental en los mercados eléctricos en todo el mundo [3–5].

El UC y el OPF constituyen problemas de optimización cuya solución supone un gran reto computacional por numerosas razones. En esta tesis, nos centramos en dos

retos específicos: el primero es la necesidad de usar en el UC variables binarias para modelar el estado de encendido/apagado de cada generador, lo que conlleva un proceso combinatorio de toma de decisiones incurriendo en una gran carga computacional. El segundo reto, más relacionado con el OPF, es la incorporación de factores aleatorios, como la demanda eléctrica y la generación renovable, que necesitan de modelos más sofisticados donde se pueda capturar su impacto en la fiabilidad de la operación de los sistemas eléctricos. Además, la solución de ambos problemas se complica sustancialmente al modelar las leyes físicas que regulan el flujo de potencia a través de las líneas de transporte. Esta tarea es particularmente ardua tanto en la versión de corriente alterna (conocida por sus siglas en inglés AC, *alternating current*), como en su aproximación lineal (conocida por sus siglas en inglés DC, *direct current*) [6].

Dado el papel crítico de estos problemas en los mercados eléctricos, cualquier mejora en sus algoritmos va a tener un impacto económico sustancial, implicando grandes beneficios. En esta tesis, presentamos mejoras a los modelos de optimización de ambos problemas en términos de una carga computacional reducida y un mejor equilibrio entre coste y fiabilidad del sistema.

A lo largo de esta tesis, todas las formulaciones de los problemas UC y OPF se desarrollan como programas enteros mixtos (conocidos por sus siglas en inglés como MIPs, *mixed-integer programs*), es decir, estas formulaciones incorporan variables binarias o enteras además de variables continuas. Los esfuerzos en la literatura reciente se han dirigido a mejorar el rendimiento de las formulaciones MIP centrándose en dos aspectos clave: el **ajuste** y la **compacidad** [7]. El **ajuste** de una formulación MIP mide la extensión del espacio de búsqueda que el solucionador de problemas de optimización necesita para explorar con el objetivo de identificar soluciones óptimas dentro del dominio entero. Una formulación más ajustada implica un espacio de búsqueda menor, lo que acelera la solución. Lograr formulaciones más ajustadas incluye modificar constantes (límites) y coeficientes (que multiplican a las variables binarias o enteras), o incorporar restricciones adicionales que reducen el espacio de búsqueda, llamadas *desigualdades válidas*. Por otro lado, la **compacidad** de una formulación MIP se refiere a su tamaño, que está influenciado por el número de variables, restricciones y elementos distintos de cero. Así, una formulación es más compacta si su tamaño es menor, lo que se traduce en una aceleración del tiempo de cálculo. La mejor forma de compactar una formulación es a través de la eliminación de restricciones o variables superfluas, sin las cuales la solución óptima del problema no cambia. Por lo tanto, la investigación llevada a cabo en esta tesis se ha centrado en encontrar modelos de optimización novedosos, ajustados y compactos para estos problemas con el objetivo de representar mejor la operación de sistemas eléctricos, a la vez que se reduce su carga computacional.

## Programación Horaria de Centrales Eléctricas

La solución del UC corresponde a la programación horaria de las centrales eléctricas más económica posible, y viene dada por sus estados de encendido/apagado y sus niveles de producción. El UC se ejecuta con un día de antelación, ya que algunas centrales eléctricas necesitan de varias horas para arrancar. El objetivo del problema UC es minimizar los costes de operación del sistema, mientras se satisfacen restricciones físicas e ingenieriles, como los niveles mínimos/máximos de producción, límites de rampa, tiempos mínimos de encendido y apagado o restricciones de red [8].

Matemáticamente, el problema UC es típicamente formulado como un problema MIP de gran escala, que pertenece a la clase de problemas que no se resuelven en tiempo polinómico (conocido como NP-difícil), incluso para un solo período de tiempo [9]. Por esta razón, el desarrollo de estrategias para solucionar este problema hasta optimalidad de una forma computacionalmente eficiente ha sido y aún es un tema actual de investigación [10].

Es bien sabido que i) tratar con las restricciones de red en la formulación del UC complica considerablemente la obtención y certificación de una solución óptima, y ii) en muchos sistemas eléctricos la mayoría de las líneas de transporte están sobredimensionadas (bajo un estado de precontingencia), por lo tanto, raramente congestionadas. Por esta razón, los esfuerzos de investigación se han centrado en estrategias para conseguir formulaciones del UC más reducidas, es decir, compactas, mediante la eliminación de restricciones de líneas superfluas [11], lo que acaba acelerando su solución. Como se señala en [12], el proceso de cribado se basa en identificar restricciones de línea redundantes e inactivas que pueden ser eliminadas con seguridad del UC sin afectar a su solución óptima.

Hay una amplia literatura sobre eliminación de restricciones para problemas operacionales en sistemas eléctricos. Por ejemplo, inspirados por el reciente auge del aprendizaje automático y la inteligencia artificial, un gran número de estrategias basadas en datos han sido propuestas para detectar muy rápido restricciones redundantes e inactivas aprendiendo de instancias del problema resueltas previamente [12–17]. Aunque computacionalmente no son costosos, los métodos de cribado de restricciones puramente basados en aprendizaje automático conllevan un riesgo de identificación errónea y, por lo tanto, pueden dar lugar a problemas reducidos que no son equivalentes a la formulación original. Esto significa que, por construcción, existe una probabilidad no nula de que la solución del problema reducido sea subóptima o infactible en el problema original. Estas infactibilidades pueden ser eliminadas combinando el método de aprendizaje automático con un algoritmo de generación de restricciones, como propone [12], a coste de aumentar el tiempo computacional.

Por otro lado, la literatura técnica también incluye una familia de métodos de cribado de restricciones que buscan reducir el modelo del UC tanto como sea posible asegurando

la equivalencia entre el modelo reducido y el original. Para este propósito, estos métodos generalmente incluyen, de una forma u otra, alguna forma de optimización y por lo tanto, son en general más exigentes desde el punto de vista computacional. Quizás, el método más conocido dentro de esta familia es un procedimiento iterativo basado en la generación de restricciones, [18]. En este método, las restricciones violadas del problema UC original se añaden gradualmente al reducido hasta que la solución de este último es factible en el primero. Este procedimiento se ha utilizado, por ejemplo, en [19, 20] para aligerar la carga computacional del problema UC con restricciones de seguridad (conocido por sus siglas en inglés SCUC, *security constrained UC*), cuyo objeto es ser robusto ante el fallo de alguna línea de transporte. La principal desventaja de los métodos basados en la generación de restricciones es que pueden llegar a ser costosos computacionalmente, si el número de iteraciones que se necesitan para garantizar la factibilidad de la solución es demasiado grande.

Existe otro grupo de métodos basados en optimización que se concentra en identificar las restricciones *redundantes*, también denominadas en inglés *non-umbrella* en [21]. Estas son las restricciones que, si se eliminan, la región de factibilidad del problema UC original se preserva. La idea básica de estos métodos es, por tanto, comprobar si las restricciones candidatas a ser eliminadas se violan o no sobre una relajación lineal de esta región. Si no se violan, pueden descartarse con seguridad. En general, esta comprobación requiere optimización, ya que suele traducirse en la resolución de una serie de problemas de acotación sobre la región factible relajada y, lógicamente, tiene sentido siempre que estos problemas de acotación sean mucho más fáciles de resolver que el problema de optimización objetivo. Ejemplos de trabajos que siguen este *modus operandi* para resolver el problema UC son [22–25]. Estos métodos basados en cálculos de cotas pretenden eliminar tantas restricciones redundantes como sea posible de la formulación UC completa. Sin embargo, incluso si todas las restricciones redundantes se identifican con éxito y se eliminan, todavía puede quedar un número de restricciones en el problema de UC reducido que no son necesarias porque no afectan a la minimización del coste de operación del UC. En otras palabras, es la función objetivo del problema UC, y no su región factible, la que hace superfluas dichas restricciones. Utilizamos el calificativo de “*inactivas*” para referirnos a estas restricciones. Se han utilizado ideas análogas en el contexto del problemas de flujo de cargas óptimo en su versión DC con restricciones de seguridad; véase, por ejemplo, [21, 26] y sus referencias.

En esta tesis, proponemos un procedimiento para aumentar sustancialmente las restricciones de línea que son filtradas por los métodos basados en optimización sin poner en peligro su atractiva capacidad de preservar la factibilidad. Nuestro enfoque se basa en reforzar la relajación lineal que utiliza el método basado en la optimización con una desigualdad válida relacionada con la función objetivo del problema UC y, por tanto, de naturaleza económica. El resultado es que el método basado en optimización

es reforzado e identifica no sólo las restricciones de línea redundantes, sino también las *inactivas*, lo que conduce a formulaciones de UC más reducidas y, por lo tanto, más fáciles de resolver.

## Flujo de Cargas Óptimo

El problema OPF trata de determinar el despacho de los generadores más económico para satisfacer la demanda (neta) del sistema, respetando los límites técnicos de la producción y del equipamiento de la red [27]. Este problema suele utilizar como información de entrada el estado de encendido/apagado de los generadores que resulta del UC descrito anteriormente. El OPF es ampliamente aplicable, y su solución es requerida por el operador del sistema con frecuencias que varían desde un día hasta cada cinco minutos antes de la entrega de energía. La utilidad del OPF trasciende tanto las redes de transporte como las de distribución.

La creciente integración de las fuentes de energía renovables en los sistemas eléctricos aumenta la variabilidad y la incertidumbre en la generación y los flujos de potencia de las líneas de transporte, que ya eran originadas previamente debido a los patrones dinámicos de la demanda eléctrica. Comprender y cuantificar el impacto de esta incertidumbre en los problemas de toma de decisiones como el OPF es crucial para garantizar el funcionamiento seguro de los sistemas eléctricos de potencia [28].

El problema OPF puede transformarse en un problema de optimización estocástica para integrar la incertidumbre en los valores predichos de la demanda eléctrica y la generación renovable, lo que se conoce como problema OPF estocástico (conocido por sus siglas en inglés SOPF, *stochastic* OPF). El objetivo del SOPF es minimizar el coste de operación esperado y evitar la violación de las restricciones, teniendo en cuenta la incertidumbre asociada a sus parámetros aleatorios. Los trabajos existentes tratan la incertidumbre en el SOPF utilizando diferentes enfoques como la programación estocástica multietapa [29], la optimización robusta [30–32] o la programación con restricciones probabilistas [33–40]. El mayor reto consiste en diseñar un modelo que capte el riesgo de violación de las restricciones y refleje con precisión el funcionamiento de los sistemas eléctricos, manteniendo al mismo tiempo la tratabilidad computacional.

Un aspecto crítico en la resolución del SOPF es el equilibrio entre fiabilidad y coste. Garantizar un funcionamiento seguro y fiable de los sistemas eléctricos en todo el espectro de posibles realizaciones de la incertidumbre suele conducir a una planificación de la operación conservadora y cara. Como alternativa, una práctica habitual y más económica consiste en modelar el problema del SOPF descartando el cumplimiento de las restricciones técnicas en circunstancias altamente improbables y críticas, por lo tanto, costosas. Para lograrlo, los trabajos existentes hacen uso de restricciones probabilistas individuales o conjuntas para abordar la satisfacción de una restricción o de un grupo de restricciones con un nivel aceptable de probabilidad de violación [41]. La programación

con restricciones probabilistas se adapta a aplicaciones donde se toman decisiones en función de parámetros aleatorios. En estas situaciones, es deseable garantizar la viabilidad del sistema de forma casi segura, pero apenas hay decisiones que la garanticen en caso de sucesos extremos o circunstancias inesperadas. En este contexto, la versión probabilística del OPF (conocida por sus siglas en inglés CC-OPF, *chance-constrained OPF*) trata de minimizar el coste de operación esperado imponiendo el cumplimiento de las restricciones técnicas para un nivel de probabilidad especificado (alto). De este modo, una mayor probabilidad aceptable de violación (determinada por el operador del sistema) implica una reducción en el coste de operación, al mismo tiempo que disminuye la seguridad del sistema eléctrico ante sucesos extremos.

Para abordar el problema CC-OPF, varios trabajos de la bibliografía (por ejemplo, [42]) trabajan directamente con restricciones probabilistas individuales para cada restricción técnica. Sin embargo, el principal inconveniente de este enfoque de modelización es que, incluso en aquellos casos en los que la probabilidad de violar cada restricción individual parece más que tolerable, el *riesgo conjunto* resultante (es decir, la probabilidad de que se infrinja *cualquiera* de las restricciones técnicas) puede seguir siendo excesivo e inadmisibles. Esta es la motivación clave que subyace al uso de una restricción probabilista conjunta para abordar el problema CC-OPF (véase, por ejemplo, [39]).

La versión del OPF con una restricción de probabilidad conjunta (conocida por sus siglas en inglés JCC-OPF, *joint CC-OPF*) ha ganado más adeptos en los últimos años, ya que permite al operador equilibrar la seguridad y el coste de manera eficaz ajustando la probabilidad de violación aceptable del conjunto restricciones técnicas, y, además, esta opción es intuitiva en términos de modelado. Sin embargo, sigue siendo un problema complejo que requiere una investigación continua, ya que no existe una reformulación finita y tratable del mismo. En la literatura, se han propuesto diversos enfoques para aproximar la región factible determinada por estas restricciones. Sin embargo, las formulaciones resultantes a menudo sufren de una disyuntiva entre ser manejables o conservadoras. Por ejemplo, Vrakopoulou *et al.* [34] adoptan un enfoque basado en escenarios para aproximarse a la solución del JCC-OPF, mientras que Chen *et al.* [43] proponen un método heurístico basado en datos que implica hacer cumplir la satisfacción de las restricciones técnicas para un conjunto de incertidumbre rectangular. Este conjunto se infiere mediante técnicas de aprendizaje automático. Hou y Roald [38] proponen un algoritmo iterativo de tuneo de parámetros para resolver una reformulación robusta del problema JCC-OPF. Esteban-Pérez y Morales [40] introducen un modelo JCC-OPF distribucionalmente robusto que tiene en cuenta información contextual utilizando un conjunto de ambigüedad basado en recortes de probabilidad. Para hacer su modelo tratable, recurren a la conocida aproximación basada en el valor en riesgo condicional (conocido por sus siglas en inglés CVaR, *conditional value-at-risk*) de la

restricción probabilista conjunta.

En esta tesis, resolvemos el problema JCC-OPF adoptando una reformulación determinista basada en datos, concretamente la aproximación por media muestral (conocida por sus siglas en inglés SAA, *sample average approximation*), que ha demostrado ofrecer un mejor rendimiento en términos de costes en comparación con las otras aproximaciones de la literatura. Sin embargo, esta aproximación plantea un gran reto computacional porque requiere el uso de variables binarias, transformando el problema en un MIP mediante el uso de grandes constantes (denominadas en inglés *big-M*). Cabe destacar que a mayor valor de la *big-M*, más pobre es el rendimiento computacional del MIP, por esta razón, ser preciso en la determinación de su valor es crucial. Lejeune y Dehghanian [44] proponen una metodología para resolver el SAA del JCC-OPF, pero sin incluir las ecuaciones de flujo de potencia en la restricción de probabilidad conjunta. Hasta donde sabemos, el trabajo en esta tesis constituye el primer intento de resolver el problema JCC-OPF mediante el enfoque SAA, utilizando una reformulación MIP e incluyendo las arduas restricciones de flujo de potencia. En concreto, en esta tesis, desarrollamos una metodología basada en un procedimiento iterativo, que ajusta las *big-Ms* eliminando a la vez restricciones redundantes, y desigualdades válidas. Esto conduce a un modelo ajustado y compacto que resuelve eficientemente la aproximación SAA del problema JCC-OPF.

Tradicionalmente, en los modelos JCC-OPF, la incertidumbre se incorpora asumiendo que los errores en la predicción de la demanda eléctrica o de la generación renovable se balancean mediante el despliegue de reservas de generación y, en particular, mediante sistemas como el control automático de generación (conocido por sus siglas en inglés AGC, *automatic generation control*) [45]. Una ventaja de modelar el balance del sistema mediante AGC es que se representa de forma natural como una regla de decisión afín, en concreto, los generadores responden proporcionalmente al error global de predicción del sistema, lo que también simplifica la solución del problema de optimización. En consecuencia, estos modelos utilizan AGC para lidiar con los errores de predicción al tiempo que garantizan que las restricciones técnicas se cumplan con una alta probabilidad. Sin embargo, este tipo de planificación operativa no tiene en cuenta la factibilidad en escenarios poco probables, pero altamente perjudiciales, que exponen al sistema a posibles vulnerabilidades. Por otro lado, garantizar la satisfacción de las restricciones técnicas para cualquier realización de incertidumbre utilizando AGC implica un mayor coste de operación, ya que restringe mucho las posibles soluciones del problema.

La aplicación de estos enfoques se ve dificultada porque proporcionan una representación insuficiente e inexacta de la operación del sistema eléctrico. De hecho, en situaciones extremas, en las que usar AGC podría poner en peligro la fiabilidad del sistema o acarrear costes significativos de operación, los operadores del sistema pueden

optar por interrumpir el uso de AGC y establecer manualmente nuevos puntos de operación de los generadores. Para resolver este problema, en esta tesis proponemos un nuevo modelo SOPF que distingue explícitamente entre “funcionamiento normal”, en el que usar AGC es suficiente para garantizar la seguridad del sistema, y “funcionamiento adverso”, en el que el operador del sistema debe tomar medidas adicionales, por ejemplo, el despliegue de reservas manuales. Este modelo proporciona soluciones más seguras que las formulaciones JCC-OPF estándar, pero menos costosas que las soluciones que garantizan una factibilidad robusta solo con AGC.

## Contribuciones

Las principales contribuciones de esta tesis son:

1. La revisión de los principales retos de modelado del problema UC y los métodos para acelerar su solución eliminando restricciones de línea superfluas;
2. El desarrollo de un método de optimización basado en costes para eliminar las restricciones de flujo de potencia redundantes *e inactivas* de la formulación del UC, a diferencia de los métodos de optimización estándar que sólo identifican restricciones redundantes. Por otra parte, la idea de esta técnica basada en costes se utiliza para ajustar aún más las constantes big-M para las formulaciones OPF implementadas a lo largo de esta tesis, lo que resulta en modelos más ajustados y compactos;
3. El método propuesto para la eliminación de restricciones basado en costes puede resolverse de manera eficiente para horizontes temporales extensos, al considerar un conjunto variado de demandas netas. Esto se consigue modelando la demanda neta como una combinación convexa de instancias históricas, en contraste con las restricciones rectangulares utilizadas convencionalmente en la literatura. Como resultado, este enfoque aumenta la capacidad de eliminación del método, mejorando así su eficacia;
4. El método de eliminación basado en costes se evalúa en un ejemplo ilustrativo y en un sistema eléctrico realista, que incluye condiciones extremas. Los resultados revelan que el método propuesto supera a los métodos convencionales basados en optimización, al tiempo que es más fiable que los algoritmos de aprendizaje automático. El enfoque propuesto reduce el número de restricciones que se imponen y el tiempo de resolución un 15% y un 45%, respectivamente, comparado con métodos convencionales de cribado de restricciones.
5. Una revisión exhaustiva de los problemas SOPF, los programas con restricciones

de probabilidad, la reformulación SAA y los problemas CC-OPF, así como sus principales retos de modelización;

6. Una metodología para resolver eficientemente la reformulación SAA del JCC-OPF. Nuestro método da como resultado un modelo ajustado y compacto que resuelve la reformulación MIP hasta optimalidad. Más concretamente, esta metodología consiste en:
  - (a) Un algoritmo iterativo que ajusta las constantes Big-M. Además, este algoritmo se mejora para filtrar restricciones redundantes;
  - (b) El desarrollo de desigualdades válidas para reforzar la reformulación MIP basada en la aproximación SAA del JCC-OPF. Además, estas desigualdades válidas, combinadas con el procedimiento de ajuste de big-Ms y eliminación de restricciones, reducen significativamente la carga computacional.
7. La metodología propuesta se evalúa mediante amplios estudios computacionales utilizando cinco sistemas eléctricos estándar disponibles en la literatura relacionada. La combinación de las desigualdades válidas con el ajuste de las Big-Ms y el cribado de restricciones nos permite resolver eficazmente hasta optimalidad instancias que no se resuelven con la formulación SAA original, ya que la combinación de ambas técnicas reduce ostensiblemente su tamaño y dificultad. La metodología propuesta es capaz de lograr factores de aceleración entre 8.5x y 1470x. Nuestro enfoque también se compara con aproximaciones del estado del arte, proporcionando el mejor rendimiento en términos de coste en tiempos computacionales competitivos.
8. Una nueva formulación del SOPF que integra varias acciones de reserva empleadas en la operación actual de los sistemas eléctricos, como AGC y la reserva manual;
9. El uso de una restricción probabilista conjunta para restringir la probabilidad de que se produzcan ajustes manuales en los generadores del sistema, en lugar de limitar la probabilidad de violación de las restricciones técnicas como se hace tradicionalmente en los problemas con restricciones de probabilidad. De ahí que se considere un escenario más realista en el que la reserva AGC funciona en condiciones ordinarias del sistema y los ajustes manuales, que no son automáticos, se aplican en escenarios adversos;
10. El modelo SOPF propuesto se analiza en profundidad utilizando un ejemplo ilustrativo y un sistema eléctrico estándar. El enfoque propuesto ofrece soluciones más fiables que el JCC-OPF convencional, pero menos costosas que los enfoques que garantizan una factibilidad robusta solo usando AGC.

## Estructura de la tesis

Los capítulos de esta tesis se resumen a continuación:

- El Capítulo 1 expone la motivación de esta tesis y sus antecedentes.
- En el Capítulo 2, se describe la formulación del UC y los métodos estándar basados en optimización para el cribado de restricciones superfluas de flujo de potencia en líneas. Además, introduce una mejora en los métodos tradicionales basados en optimización mediante la incorporación de información de la función objetivo a través de una desigualdad válida que sobreestima el coste del UC. Mediante dos casos de estudio, exploramos la viabilidad del método basado en costes para eliminar restricciones de línea superfluas en contraste con los enfoques convencionales. Además, verificamos su aplicabilidad en condiciones desfavorables.
- El Capítulo 3 comienza con la formulación JCC-OPF, junto con su reformulación SAA. Posteriormente, se profundiza en la aplicación de un algoritmo iterativo para ajustar las constantes big-M y eliminar restricciones redundantes. Además, se introducen nuevas desigualdades válidas para reforzar la reformulación SAA aprovechando la estructura de la matriz de restricciones. El capítulo concluye con un caso de estudio exhaustivo, en el que la metodología propuesta se prueba en cinco sistemas de potencia estándar, y su rendimiento se compara con métodos alternativos disponibles en la bibliografía existente.
- El Capítulo 4 empieza con una formulación ampliada y realista del JCC-OPF, que posteriormente se mejora integrando reservas automáticas y manuales, equilibrando así fiabilidad y coste. Por último, se evalúa la eficacia de nuestra propuesta en términos de coste y fiabilidad en un sistema eléctrico estándar.
- El Capítulo 5 concluye esta tesis y ofrece sugerencias para futuros trabajos.

## Conclusiones

El UC y el OPF son herramientas fundamentales para la operación de los sistemas eléctricos, ampliamente utilizadas en las rutinas de funcionamiento de los mercados eléctricos. El UC y el OPF son problemas de optimización computacionalmente desafiantes por varias razones y, dado su papel crítico en los mercados eléctricos, cualquier mejora de los mismos puede resultar en beneficios significativos. En esta tesis, nos centramos en abordar los siguientes retos:

1. **Carga computacional del problema UC.** El estado de encendido/apagado de los generadores se modela como variables binarias que dan lugar a un proceso

combinatorio de toma de decisiones que requiere un tiempo de cálculo considerable.

2. **Incorporación de la incertidumbre asociada con la demanda eléctrica y la generación renovable en el problema OPF.** Cuantificar con precisión el impacto de la incertidumbre es esencial en el OPF para garantizar la operación segura de los sistemas eléctricos. En consecuencia, surgen modelos estocásticos del OPF (SOPF) que presentan dificultades a la hora de establecer un equilibrio entre fiabilidad y coste, además de ser tratables.

Para hacer frente a estos problemas, en esta tesis se han estudiado varios temas y herramientas:

- **Compactación de la formulación del UC.** Se sabe que las restricciones de red complican la solución del problema UC. En los sistemas eléctricos actuales, la mayoría de las líneas de transporte están sobredimensionadas (bajo un estado de precontingencia), lo que hace que las restricciones que imponen sean redundantes. En esta tesis, profundizamos en métodos que aceleran la solución del UC eliminando restricciones de transporte superfluas.
- **OPF con restricciones probabilistas conjuntas (JCC-OPF).** Este modelo reduce el coste de operación esperado al descartar la satisfacción de las restricciones técnicas para un porcentaje determinado de realizaciones de incertidumbre, garantizando la seguridad del sistema para el resto. Cabe destacar la adaptabilidad y practicidad del modelo, ya que el operador del sistema puede ajustar la proporción de escenarios violados, influyendo así tanto en la fiabilidad del sistema como en los costes de operación. Como inconveniente, este problema de optimización carece de una reformulación finita y tratable. Entre las aproximaciones existentes, esta tesis se centra en investigar la aproximación SAA, que ofrece el rendimiento menos conservador en términos de coste. El inconveniente de la reformulación SAA es que requiere de un tiempo computacional significativo debido a la presencia de variables binarias, es decir, requiere resolver un MIP.
- **Integración de varios tipos de reserva.** En los modelos SOPF, en particular en los problemas JCC-OPF, es habitual suponer que los errores de predicción de la demanda eléctrica y la generación renovable se balancean mediante el despliegue de reservas, como el *control automático de la generación* (AGC). La reserva AGC se modela como una regla de decisión afín, por lo que su implementación simplifica la solución del problema de optimización. Sin embargo, en escenarios extremos, el uso de AGC puede poner en peligro la fiabilidad del sistema o incurrir en costes significativos. En la práctica, en esos casos, los operadores del sistema pueden recurrir a recursos adicionales, por ejemplo, la reserva manual. Por ello,

estudiamos la integración del uso de AGC y reserva manual como herramienta para equilibrar fiabilidad y coste en problemas SOPF.

En esta tesis, hemos desarrollado varios modelos de optimización ajustados y compactos para problemas UC y OPF que contribuyen a estos retos de investigación. Los contenidos de esta tesis se incluyen en los artículos [46], [47] y [48].

- En el artículo [46], presentamos una metodología para reducir el tiempo computacional del UC eliminando restricciones de línea superfluas. Los métodos basados en optimización propuestos en la literatura solo eliminan restricciones redundantes y, por tanto, suponen un ahorro computacional moderado. Este trabajo presenta una nueva metodología de cribado de restricciones que elimina tanto restricciones redundantes como *inactivas* y reduce aún más la carga computacional de este problema. Al igual que los enfoques existentes, el que proponemos se basa en el cálculo de los máximos flujos de potencia a través de las líneas en una relajación LP del UC. Como característica destacada de nuestro trabajo, proponemos ajustar esta relajación LP para excluir las condiciones de operación no económicas. De este modo, nuestra metodología es capaz de filtrar un mayor número de restricciones de línea. Los resultados de la simulación con una red de 2000 nodos muestran que nuestra propuesta reduce el número de restricciones retenidas y el tiempo de solución en un 15% y un 45%, respectivamente, en comparación con los métodos de referencia existentes. Además, la tasa de cribado de restricciones de nuestro enfoque permanece bastante similar cuando se consideran cambios topológicos de la red.
- En el trabajo [47] proponemos una novedosa técnica de resolución exacta para la reformulación SAA del problema JCC-OPF. Nuestra metodología incluye un método de cribado para eliminar restricciones superfluas basado en un procedimiento iterativo para ajustar las Big-Ms presentes en el MIP. Estos procedimientos se combinan con la adición de desigualdades válidas basadas en la estructura especial de la matrix de restricciones. Dichas desigualdades refuerzan su relajación lineal y permiten un filtrado adicional de restricciones. De este modo, el modelo resultante es más compacto y más ajustado. En el caso de estudio, probamos sistemas eléctricos de diferentes tamaños y se demuestra que, en comparación con el modelo de referencia SAA, nuestra metodología proporciona resultados notables en términos de la cota de la relajación lineal, memoria RAM necesaria para resolver las instancias y el tiempo total de cómputo. En concreto, nuestra metodología resuelve de forma óptima todas las instancias generadas para los grandes sistemas, la mayoría de las cuales no se resuelven en 10 horas utilizando el SAA tradicional. Además, el número medio de restricciones eliminadas de todas

las instancias con nuestra metodología supera siempre un 95% de las mismas, y la cota inferior del MIP se incrementa notablemente con la inclusión de desigualdades válidas, lo que demuestra los excelentes resultados de la combinación de los métodos desarrollados. La comparación de nuestros resultados con los proporcionados por los métodos aproximados y exactos existentes muestra que nuestro enfoque es computacionalmente muy competitivo para instancias pequeñas y medianas, proporcionando siempre los mejores resultados en términos de coste. Para las instancias grandes abordadas, si bien los métodos aproximados nos superan en términos de tiempo computacional (como era de esperar), nuestra estrategia de solución exacta no sólo proporciona un certificado de optimalidad, sino que además devuelve la solución óptima dentro del límite de tiempo establecido. Por último, somos capaces de acelerar la resolución de la instancia más grande unas cuatro veces incorporando información de la función objetivo durante el preproceso. Esto se consigue mediante el uso de un heurístico propuesto que permite obtener una cota superior del coste óptimo.

- En artículo [48] presentamos un nuevo modelo SOPF. Los enfoques existentes para resolver el SOPF son o bien excesivamente conservadores y caros, o bien dejan el sistema vulnerable a sucesos de baja probabilidad y alto impacto. La nueva formulación del SOPF distingue entre condiciones de operación “normales”, en las que las desviaciones de potencia se equilibran únicamente con el uso de AGC, y condiciones de operación “adversas”, en las que se requieren acciones manuales de redespacho. Como resultado, nuestro enfoque ofrece soluciones más fiables y menos conservadoras que los enfoques existentes en la literatura. Nuestro modelo se formula como un programa con una restricción de probabilidad conjunta que limita la probabilidad de que los operadores ajusten manualmente el nivel de producción de los generadores. En el caso de estudio, los resultados obtenidos demuestran que la metodología propuesta es capaz de producir decisiones de despacho que mantienen niveles de seguridad casi idénticos y siendo un 18% más baratas que los enfoques que persiguen la factibilidad con solo AGC para cualquier realización de la incertidumbre. Como contrapartida, la carga computacional de nuestra propuesta es elevada debido al modelado de las acciones manuales de redespacho. Sin embargo, también sugerimos un heurístico para resolver el modelo propuesto y verificamos que el tiempo computacional se acorta drásticamente sin causar una disminución significativa del rendimiento. Por último, proponemos incorporar información económica en la etapa de preprocesamiento, obteniendo una estimación del coste óptimo mediante el heurístico empleado. Este enfoque conduce a una formulación más ajustada y da lugar a una aceleración del tiempo de cómputo.

## Trabajo Futuro

A continuación, se enumeran las posibles direcciones para futuras investigaciones derivadas del estudio realizado en esta tesis:

1. Aplicación del método de cribado de restricciones basado en costes a formulaciones del UC multiperiodo que incluyen restricciones intertemporales como límites de rampa y tiempos mínimos. En este caso, los retos son dos: i) construir una relajación lo suficientemente ajustada del UC multiperiodo para que el método propuesto tenga un poder de cribado razonable, y ii) diseñar un conjunto adecuado de demandas netas y encontrar una estimación robusta y aproximada del coste de operación del sistema para un horizonte temporal dado.
2. Una prometedora vía de investigación futura de la metodología propuesta para resolver el problema JCC-OPF basado en el SAA consiste en el desarrollo de un conjunto generalizado de desigualdades válidas que combinen variables de pares o subgrupos de líneas y generadores.
3. El novedoso SOPF propuesto en esta tesis tiene el potencial de mejorarse mediante la integración de tecnología puntera, en lugar de depender de los ajustes manuales de los generadores para garantizar el equilibrio y la fiabilidad del sistema en escenarios extremos de baja probabilidad. Entre las opciones más prometedoras para la integración de nuevas tecnologías se incluyen *conexiones de corriente continua de alta tensión* y *transformadores de desplazamiento de fase*. La integración de estas tecnologías añade flexibilidad al funcionamiento de los sistemas eléctricos, lo que se traduce en una reducción significativa de los costes de operación.

## Lista de Publicaciones

- [46] **Á. Porras**, S. Pineda, J. M. Morales and A. Jiménez-Cordero, “Cost-driven screening of network constraints for the unit commitment problem,” *IEEE Transactions on Power Systems*, vol. 38, no. 1, pp. 42-51, Jan. 2023.
- [47] **Á. Porras**, C. Domínguez, J. M. Morales and S. Pineda, “Tight and compact sample average approximation for joint chance-constrained problems with applications to optimal power flow,” *aceptado para su publicación en INFORMS Journal on Computing*, Jun. 2023.
- [48] **Á. Porras**, L. Roald, J. M. Morales and S. Pineda, “Integrating automatic and manual reserves in optimal power flow via chance constraints,” *arXiv preprint arXiv:2303.05412*, 2023.

# Abstract

Power systems are among the most complex and colossal engineering structures in modern society, whose operation implies a challenge due to the coordination of multiple generating units to ensure a safe and dependable energy supply. In the last decades, significant changes have occurred in power systems globally with the purpose of transitioning to sustainable systems. In particular, the integration of renewable energy sources has brought about new challenges in power system operations due to the inherent uncertain nature of these sources and the shift towards a more geographically dispersed power system.

In this context, this thesis tackles two of the most significant problems in power system operations, namely, the *unit commitment* (UC) and the *optimal power flow* (OPF), widely used in electricity markets. Both UC and OPF constitute optimization problems that pose considerable computational challenges. This thesis focuses on two specific challenges within these problems, and given their critical role in electricity markets, improving their algorithms is expected to lead to significant benefits.

Firstly, UC requires the use of binary variables to model the on/off state of generating units, resulting in a combinatorial decision-making process that incurs a significant computational burden. Furthermore, addressing network constraints escalates the complexity of attaining an optimal solution. Leveraging the fact that most of transmission lines are oversized in today's power systems (under a pre-contingency state), this thesis introduces a cost-driven optimization approach aimed at eliminating superfluous network-constraints, what leads to a notable reduction in the computational burden associated with UC.

Secondly, OPF problems often involve the incorporation of stochastic factors like electricity demand and renewable generation, demanding a sophisticated modeling approach to capture their impact on power system operation reliability, namely, *stochastic* OPF. In line with a current trend, we resort to the *joint chance-constrained* OPF model that improves the power systems operation disregarding system's security in low probable, high impact uncertainty realizations. In the absence of a finite, tractable reformulation, we use the *sample average approximation* which produces a data-driven reformulation taking the form of a mixed-integer problem cursed by big-Ms. To solve

it efficiently, in this thesis, we propose a novel methodology based on a tightening-and-screening procedure and valid inequalities.

Most of the existing *joint chance-constrained* OPF models provide a limited vision of power systems operation, since, under extreme circumstances, these approaches may leave the system vulnerable. Otherwise, ensuring the system's security for the whole spectrum of uncertainty realizations would result in excessive operating costs. To circumvent such a caveat, we introduce a novel *stochastic* OPF model that integrates both automatic and manual reserves, thereby yielding economical and highly reliable solutions.



# Contents

<b>1</b>	<b>Introduction</b>	<b>2</b>
1.1	Background and Motivation . . . . .	4
1.2	Contributions . . . . .	8
1.3	Thesis Outline . . . . .	10
1.4	List of Publications . . . . .	11
<b>2</b>	<b>Screening of Network Constraints for the Unit Commitment Problem</b>	<b>13</b>
2.1	Introduction . . . . .	15
2.2	Mathematical Formulation . . . . .	17
2.3	Screening of Network Constraints . . . . .	18
2.3.1	Existing Optimization-based Screening Approaches . . . . .	18
2.3.2	Proposed Cost-driven Constraint Screening . . . . .	20
2.4	Evaluation Procedure . . . . .	24
2.5	Numerical Experiments . . . . .	24
2.5.1	Illustrative Example . . . . .	25
2.5.2	Realistic Case Study . . . . .	28
2.6	Summary and Conclusions . . . . .	33
<b>3</b>	<b>Joint Chance-constrained Optimal Power Flow</b>	<b>34</b>
3.1	Introduction . . . . .	36
3.2	Mathematical Formulation . . . . .	40
3.3	Solution via Sample Average Approximation . . . . .	43
3.3.1	Tightening and Screening . . . . .	44
3.3.2	Valid inequalities . . . . .	45
3.4	Numerical Experiments . . . . .	50
3.4.1	Impact of Tightening Big-Ms . . . . .	51
3.4.2	Impact of Removing Redundant Constraints . . . . .	53
3.4.3	Impact of Valid Inequalities . . . . .	54
3.4.4	Comparison with an Exact Approach . . . . .	55
3.4.5	Comparison with Conservative Approximations . . . . .	56

---

3.4.6	Cost-driven Pre-processing . . . . .	57
3.5	Summary and Conclusions . . . . .	58
<b>4</b>	<b>Integrating Automatic and Manual Reserves in Optimal Power Flow</b>	<b>59</b>
4.1	Introduction . . . . .	61
4.2	Mathematical Formulation . . . . .	63
4.2.1	Extended Joint Chance-constrained Optimal Power Flow . . . . .	63
4.2.2	Balancing Cost and Reliability . . . . .	66
4.3	Solution Methodology . . . . .	67
4.4	Evaluation Procedure . . . . .	70
4.5	Numerical Experiments . . . . .	72
4.5.1	Out-of-sample Performance . . . . .	73
4.5.2	Computational Study . . . . .	75
4.6	Summary and Conclusions . . . . .	76
<b>5</b>	<b>Closure</b>	<b>77</b>
5.1	Summary and Conclusions . . . . .	79
5.2	Limitations of the Conducted Research . . . . .	82
5.3	Outlook . . . . .	83
	<b>References</b>	<b>85</b>

# List of Figures

2.1	Two-node illustrative example . . . . .	20
2.2	1-quantile piecewise linear regression . . . . .	21
2.3	Five-node system . . . . .	26
2.4	Upper-bound Estimation – Illustrative Example . . . . .	28
3.1	In bold, the 5-upper envelope (4-lower envelope, 4-level) of a set $\mathcal{L}_j$ of 8 lines in the plane. In dotted, the lower hull of the 5-upper envelope . . .	47
3.2	Flowchart representation of Algorithm 3.2 . . . . .	48
4.1	Three-node illustrative example . . . . .	65
4.2	Actions planned over the spectrum of uncertainty realizations to mitigate imbalances and ensure the reliability of the power system. A: model (4.1) with $\epsilon = 0$ , B: model (4.1) with $\epsilon > 0$ , C: Proposal. . . . .	67
4.3	Expected cost vs. the average deviation of the %5 scenarios with the largest deviations. . . . .	75

# List of Tables

2.1	Constraint screening approaches . . . . .	25
2.2	Historical data – Illustrative Example . . . . .	25
2.3	Retained capacity constraints in the UC problem at time period $t_4$ – Illustrative Example . . . . .	27
2.4	Results – Fixed load . . . . .	30
2.5	Results – Base Case . . . . .	31
2.6	Results – Worst Case . . . . .	32
3.1	Short Description of Test Power Systems . . . . .	50
3.2	Benchmark approach ( <b>BN</b> ): Results . . . . .	52
3.3	Coefficient tightening approach ( <b>T</b> ): Results . . . . .	52
3.4	Tightening and Screening ( <b>TS</b> ): Results . . . . .	53
3.5	Tightening by valid inequalities ( <b>BN+V</b> ): Results . . . . .	54
3.6	Tightening and screening with valid inequalities ( <b>TS+V</b> ): Results . . . . .	55
3.7	Comparison of the proposed <b>TS+V</b> approach and the BCD approach . . . . .	56
3.8	Comparison of the proposed <b>TS+V</b> approach and existing approximate methods . . . . .	57
3.9	Comparison of <b>TS+V</b> and <b>TS+V+C</b> . . . . .	58
4.1	Results – Illustrative Example . . . . .	65
4.2	Generators with capability to provide reserve. . . . .	73
4.3	Out-of-sample performance comparison. . . . .	73
4.4	Comparison of decisions made by AGC and AMGC. . . . .	74

# Notation

The main notation used throughout this thesis is stated below for quick reference. Other symbols are defined as required in the text.

## Sets

- $\mathcal{G}$  Set of generating units, indexed by  $g$ .
- $\mathcal{L}$  Set of transmission lines, indexed by  $l$ .
- $\mathcal{N}$  Set of nodes, indexed by  $n$ .
- $\mathcal{G}_n$  Set of generating units connected to the node  $n$ .
- $\mathcal{T}$  Set of time periods, indexed by  $t$ .

## Parameters

- $c_g^2/c_g^1/c_g^0$  Quadratic/Linear/Constant coefficient of the operating cost function of generating unit  $g$  [€/MWh].
- $c_g^d/c_g^u$  Downward/Upward reserve capacity cost of generating unit  $g$  [€/MW].
- $c_g^-/c_g^+$  Downward/Upward reserve cost of generating unit  $g$  [€/MWh].
- $B_{ln}$  Power transfer distribution factor (PTDF) of transmission line  $l$  with respect to node  $n$ .
- $d_n$  Forecasted net demand at node  $n$  [MW].
- $\tilde{d}_n$  Actual net demand at node  $n$  [MW].
- $\bar{f}_l$  Maximum capacity of transmission line  $l$  [MW].
- $\underline{p}_g/\bar{p}_g$  Minimum/Maximum output of unit  $g$  [MW].
- $\bar{r}_g^d/\bar{r}_g^u$  Ability of generator  $g$  to provide downward and upward reserves [MW].
- $\omega_n$  Error of the predicted net demand at node  $n$  [MW].

## Variables

$p_g$	Power output dispatch of unit $g$ [MW].
$r_g(\boldsymbol{\omega})$	Reserve deployed by unit $g$ [MW].
$r_g^-(\boldsymbol{\omega})/r_g^+(\boldsymbol{\omega})$	Downward/Upward reserve deployed by unit $g$ [MW].
$r_g^d/r_g^u$	Downward/Upward reserve capacity of unit $g$ [MW].
$r_g^M(\boldsymbol{\omega})$	Manual adjustment of power output dispatch at unit $g$ [MW].
$u_g$	Commitment of generating unit $g$ .
$\beta_g$	Participation factor of unit $g$ .



# Chapter 1

## Introduction



This thesis deals with the operation of today's power systems, with the ultimate goal of providing consumers with cost-effective electricity supply while maintaining the reliability of the grid. The modeling of power system operations has become increasingly complicated in recent years as a result of the transition towards sustainable energy systems. This transition requires the utilization of more sophisticated models that integrate the uncertainty associated with the new system agents. This first chapter describes the motivation for the developed methods and formally states the main contributions of this thesis. The outline of the thesis is provided and the published papers are listed.

## 1.1 Background and Motivation

Power systems are among the most intricate and colossal engineering structures in modern society, necessitating the coordination of multiple generating units to ensure a safe and dependable energy supply. This coordination involves the consideration of various technical aspects of generating units, such as power-output or ramping limits, as well as diverse aspects of power systems, including network constraints.

In the last decades, significant changes have occurred in power systems of numerous regions around the world with the purpose of transitioning to sustainable systems with zero net greenhouse gas emissions. In particular, the integration of renewable energy sources has brought about challenges in power system operations due to the inherent uncertain nature of these sources and the shift towards a more geographically dispersed power system [1]. In addition, the transition towards sustainability implies that the operation of power systems confronts several upcoming questions such as the integration of small distributed energy resources in distribution systems, the development of an end-user centric approach where it is ensured active participation of consumers along with the awareness of the needs of power systems, local energy transactions and the large-scale integration of energy storage systems [2]. This calls for the development of new research avenues to streamline the transition by enhancing the operation of power systems.

In this context, this thesis tackles two of the most significant problems in power system operations, namely, the *unit commitment* (UC) and the *optimal power flow* (OPF). These two problems are mostly considered in electricity markets around the world [3–5].

UC and OPF constitute optimization problems, the solution of which presents a computationally challenging task for numerous reasons. In this thesis, we concentrate on two specific challenges: Firstly, the need in UC for binary variables to model the on/off state of generating units, which renders a combinatorial decision-making process that incurs a significant computational burden. Secondly, mostly in OPF problems, the incorporation of stochastic factors, like electricity demand and renewable generation,

which calls for a sophisticated modeling approach whereby we can capture their impact on the reliability of the power system operation. Furthermore, the solution of both problems is significantly hindered by the modeling of the physical laws that regulate power flow through transmission lines. This is particularly arduous in both their *alternating current* (AC) version, which is non-convex and non-linear, and their *direct current* (DC) version, which is a linear approximation [6].

Given the critical role of these problems in electricity markets, any improvement in their algorithms is expected to have a substantial economic impact, resulting in significant benefits. In this thesis, we present enhancements to the optimization models of both problems in terms of reduced computational burden and improved trade-off between cost-efficiency and system reliability.

Throughout this thesis, all formulations for UC and OPF problems are developed as mixed-integer programs (MIPs), that is, these formulations incorporate binary or integer variables in addition to continuous variables. Efforts in recent literature have been directed towards enhancing the performance of MIP formulations by focusing on two key aspects: **tightness** and **compactness** [7]. The **tightness** of a MIP formulation measures the extension of the search space that the solver needs to explore in order to identify an optimal solution within the integer domain. A tighter formulation implies a smaller search space which results in expediting the solution. Achieving tighter formulations involves modifying constants (bounds) and coefficients (that multiply binary or integer variables), or incorporating additional constraints that reduce the search space, called *valid inequalities*. On the other hand, the **compactness** of a MIP formulation refers to its size, which is influenced by the number of variables, constraints, and non-zero elements. Thus, a formulation is more compact if its size is smaller, resulting in a speedup of the computational time. The most effective approach to achieving compact formulations is through the elimination of superfluous constraints or variables, without which the problem's optimal solution remains unchanged. Therefore, the efforts of this thesis are focused on finding novel, tight, compact optimization models for these problems in order to better represent the operation of power systems, whilst reducing their computational burden.

### Unit Commitment

The solution to the UC problem corresponds to the most economically efficient operating schedule, given by the on/off status and production levels of the generating units. The UC is run one day in advance since some generating units require several hours for start-up. The objective of the UC problem is thus to minimize system operation costs, whereas physics and engineering constraints are satisfied, such as minimum/maximum production levels, ramping limits, minimum up- and down-times or network constraints [8].

Mathematically, the UC problem is typically formulated as a large-scale MIP, which belongs to the class of NP-hard problems, even for a single period [9]. For this reason, the development of strategies to solve this problem to optimality in a computationally efficient manner has been and is still a popular research topic [10].

Given the well-known facts that i) dealing with network-constraints in the UC formulation considerably complicates obtaining and certifying the optimal UC plan, and ii) in many systems most transmission lines are oversized (under a pre-contingency state) and thus are seldom congested, recent research efforts have been put on strategies to get reduced, more compact UC formulations by eliminating superfluous line-flow constraints [11], what results in speeding up the solution. As pointed out in [12], the reduction process rests on identifying redundant and inactive power flow constraints. The former can be eliminated without modifying the feasible region of UC. The latter, despite defining the feasible region, can be eliminated since they are not binding at the optimal solution. Thus, redundant and inactive line-flow constraints can be prudently eliminated from the targeted UC problem without impacting its optimal solution.

Both machine-learning and optimization-based methods have been proposed to reduce the full UC formulation by removing as many superfluous line-flow constraints as possible. While the elimination strategies based on machine learning are fast and typically delete both redundant and inactive constraints, they may be over-optimistic and result in infeasible UC solutions. For their part, optimization-based methods seek to identify redundant constraints in the full UC formulation by exploring the feasibility region of an LP-relaxation.

In this thesis, we propose a procedure to substantially increase the line-flow constraints that are filtered out by optimization-based methods without jeopardizing their appealing ability to preserve feasibility. Our approach is based on tightening the LP-relaxation that the optimization-based method uses with a valid inequality related to the objective function of the UC problem and hence, of an economic nature. The result is that the so strengthened optimization-based method identifies not only redundant line-flow constraints but also inactive ones, thus leading to more reduced UC formulations.

## **Optimal Power Flow**

The OPF problem seeks to determine the least-costly dispatch of thermal generating units to satisfy the system's (net) demand while complying with the technical limits of production and network equipment [27]. This problem often uses as input information the on/off status of the generators that are the result of the UC described above. The OPF is widely applicable, with its solutions sought by system operators at frequencies that range from daily to every five minutes. The utility of the OPF transcends both transmission and distribution networks.

The escalating integration of renewable energy sources into power systems amplifies the variability and uncertainty in power generation and associated power flows, which were already present due to dynamic patterns of electricity demand. Understanding and quantifying the impact of this uncertainty on decision-making problems such as the OPF is crucial to ensure the secure operation of power systems [28].

The OPF problem can be transformed into a stochastic optimization problem to integrate unpredictability in the estimated quantities of demand and renewable generation, and this is known as the *stochastic* OPF (SOPF) problem. The SOPF aims to minimize expected operational cost and avoid constraint violations while considering the uncertainty in its random parameters. Existing works deal with uncertainty in SOPF using different approaches such as multi-stage stochastic programming [29], robust or worst-case optimization [30–32] or chance-constraints [33–40]. The major challenge is to design a model that captures the risk of constraint violations and accurately reflects the operation of power systems while maintaining computational tractability.

A critical aspect in solving the SOPF is to balance between reliability and cost. Ensuring secure and reliable operation of power systems over the entire spectrum of possible uncertainty realizations often leads to a conservative and costly operational planning. Alternatively, a prevalent practice is to model the OPF problem in a cost-effective manner by disregarding the fulfillment of technical constraints under highly improbable and critical circumstances. To achieve this, existing works leverage single and joint chance constraints to address the satisfaction of a singular or a group of constraints with an acceptable level of violation probability [41]. Chance-constrained programming suits applications in areas where decisions have to be made dealing with random parameters. In these situations, it is desirable to ensure feasibility of the system almost surely, but there is hardly any decision which would guarantee it under extreme events or unexpected random circumstances. In this context, the *chance-constrained* OPF (CC-OPF) seeks to minimize the expected operating cost by enforcing technical constraints to be satisfied for a specified (high) probability level. Thus, a larger acceptable violation probability (determined by the system operator) reduces the operating cost while decreasing the system’s preparedness for extreme events.

This variant of SOPF problem has gained more traction in recent years, as it enables the operator to balance security and cost-effectively by incorporating the acceptable violation probability, and is also intuitive in terms of modeling. However, it continues to be a complex problem that necessitates continued research as there exists no finite, tractable reformulation. A diverse array of approaches have been proposed to approximate the feasible region determined by these constraints. Nevertheless, the resulting formulations often suffer from a trade-off between being either tractable or conservative.

In this thesis, we solve the *joint chance-constrained* OPF (JCC-OPF) problem adopting a data-driven deterministic reformulation, namely the *sample average ap-*

*proximation* (SAA), which has been demonstrated to yield better cost performance compared to other approaches in the existing literature. However, this approach poses computational challenges because it requires the use of binary variables, transforming the problem into a MIP by means of big-Ms. We develop a methodology based on a tightening-and-screening procedure and valid inequalities that leads to a tight, compact model that efficiently solves the SAA.

Traditionally, in JCC-OPF models, uncertainty is accommodated by assuming that errors in forecasting electricity demand or renewable generation are balanced by the deployment of generation reserves, and in particular, by systems such as the *automatic generation control* (AGC) [45]. A benefit of modeling system balancing through AGC is that it is naturally represented as an affine control policy, which also simplifies the solution of the optimization problem. Consequently, these models utilize AGC to handle forecast errors while ensuring technical constraints are met with a high probability. However, such operational planning disregards feasibility in unlikely, but highly detrimental scenarios, and, therefore, the system is exposed to potential vulnerabilities. Conversely, guaranteeing the satisfaction of technical constraints for *any* uncertainty realization using AGC implies a higher operating cost.

The application of these approaches is impeded because they provide an insufficient and inaccurate representation of power system operations. Indeed, under severe situations, where AGC could imperil system reliability or entail significant costs, system operators may choose to discontinue AGC and manually set new operating points. To address this issue, in this thesis, we propose a novel SOPF model that explicitly distinguishes between “normal operation”, in which AGC is sufficient to guarantee system security, and “adverse operation”, in which the system operator is required to take additional actions, e.g., manual reserve deployment. This model provides solutions that are more secure than standard JCC-OPF formulations, yet less costly than solutions that guarantee robust feasibility with only AGC.

## 1.2 Contributions

The main contributions of this thesis are:

1. The review of the major modeling challenges of UC problem and methods to speed up its solution removing superfluous line-flow constraints;
2. The development of a cost-driven pre-processing optimization-based method to screen out redundant *and inactive* line-flow constraints from the UC formulation, unlike standard optimization-based methods that only identify redundant constraints. Moreover, the basis of this cost-based technique is used to further

adjust the big-M constants for the OPF formulations implemented throughout this thesis, resulting in more tight, compact models;

3. The proposed cost-driven screening method is solved offline over a diverse set of net demands. This is achieved by modeling the net demand as a convex combination of historical instances, in contrast to the box constraints conventionally utilized in the literature. As a result, this approach enhances the screening capability of the technique, thereby improving its efficacy;
4. The cost-driven screening method is examined in an illustrative example and a realistic power system, including extreme conditions. The findings reveal that the proposed method outperforms conventional optimization-based methods in the removal of constraints, whilst being more reliable than machine learning algorithms. The proposed approach reduces the number of retained constraints and the solution time by 15% and 45%, respectively, compared to conventional constraint-screening methods.
5. A comprehensive review of SOPF problems, chance-constrained programs, SAA reformulation, and CC-OPF problems, and their major modeling challenges;
6. A methodology to efficiently solve the SAA reformulation of the JCC-OPF. Our method results in a tight, compact model that solves the MIP reformulation to optimality. More specifically, this methodology consists of:
  - (a) The adoption of an iterative algorithm that tightens big-M constants. Furthermore, this algorithm is upgraded to screen out redundant constraints;
  - (b) The development of valid inequalities to strengthen the MIP reformulation of the JCC-OPF. In addition, these valid inequalities, combined with the tightening-and-screening procedure, reduce significantly the computational burden;
7. The proposed methodology is tested through extensive computational results using five standard power systems available in the related literature. The combination of the valid inequalities with the tightening of the Big-Ms and the screening procedure allows us to efficiently solve to optimality instances that are not solved with the original MIP formulation, since the combination of both techniques ostensibly reduces their size and difficulty. The proposed methodology is able to achieve speedup factors between 8.5x and 1470x. Our approach is also compared with state-of-the-art approximations, providing the best performance in terms of cost in competitive computational times.
8. A novel formulation of SOPF that integrates various reserve actions employed in actual power systems operations, such as AGC and manual reserve;

9. The use of a joint chance constraint to restrict the probability of manual adjustments occurring, instead of limiting the probability of violation of technical constraints as traditionally done in chance-constrained programs. Hence, it is considered a more realistic setting where the automatic generation control operates under ordinary system conditions and the manual adjustments, which are not automatic, are implemented under adverse scenarios;
10. The novel SOPF model is deeply analyzed using an illustrative example and a standard power system. The proposed approach yields solutions that are more reliable than the conventional JCC-OPF, yet 18% cheaper than those approaches that guarantee robust feasibility.

### 1.3 Thesis Outline

The chapters of this thesis are outlined as follows:

- Chapter 2 describes the UC formulation and delineates standard optimization-based methods for screening out superfluous line-flow constraints. Further, it introduces an enhancement to the traditional optimization-based methods by incorporating information from the objective function via a valid inequality that overestimates the UC cost. By means of two case studies, we explore the viability of the proposed cost-driven method in eliminating superfluous line-flow constraints in contrast to conventional approaches. Additionally, we verify its applicability under unfavorable conditions.
- Chapter 3 begins with the JCC-OPF formulation, along with its SAA reformulation. Subsequently, it delves into the application of an iterative algorithm to tighten the big-M constants and eliminate redundant constraints. Additionally, novel valid inequalities are introduced to strengthen the SAA reformulation by leveraging the structure of the matrix constraint. The chapter concludes with a comprehensive case study, wherein the proposed methodology is tested on five standard power systems, and its performance is benchmarked against existing literature.
- Chapter 4 starts with an extended and realistic formulation of the JCC-OPF, which is subsequently improved by integrating automatic and manual reserves, thus balancing reliability and cost. Ultimately, the efficacy of our proposal in terms of cost and reliability is evaluated on a standard power system.
- Chapter 5 concludes this thesis and provides suggestions for future work.

## 1.4 List of Publications

The work presented in this thesis has been reported by the following publications:

- [46] **Á. Porras**, S. Pineda, J. M. Morales and A. Jiménez-Cordero, “Cost-driven screening of network constraints for the unit commitment problem,” *IEEE Transactions on Power Systems*, vol. 38, no. 1, pp. 42-51, Jan. 2023.
- [47] **Á. Porras**, C. Domínguez, J. M. Morales and S. Pineda, “Tight and compact sample average approximation for joint chance-constrained problems with applications to optimal power flow,” *accepted for publication in INFORMS Journal on Computing*, Jun. 2023.
- [48] **Á. Porras**, L. Roald, J. M. Morales and S. Pineda, “Integrating automatic and manual reserves in optimal power flow via chance constraints,” *arXiv preprint arXiv:2303.05412*, 2023.



## Chapter 2

# Screening of Network Constraints for the Unit Commitment Problem



The *unit commitment* (UC) problem constitutes a fundamental task in the operation of power systems [3]. Its solution corresponds to the most economical operating schedule, as determined by the on/off status and production levels of power generating units. Consequently, UC seeks to minimize operational expenses to meet the electricity (net) demand whilst ensuring the satisfaction of physical and engineering constraints [8].

Notwithstanding the above, due to the inclusion of binary variables pertaining to the on/off status of generating units, this problem is formulated as a *mixed-integer program* (MIP) and classified as an NP-hard problem [49].

As outlined in Chapter 1, while dealing with network constraints makes it difficult to identify and validate an optimal UC plan, the vast majority of transmission lines are oversized (under a pre-contingency state). As a result, research efforts have concentrated on expediting UC solution via the removal of superfluous transmission constraints, specifically those that are redundant and inactive.

This chapter presents a cost-based optimization technique to eliminate redundant and inactive line flow constraints from the UC formulation, thereby yielding a significant reduction in the associated computational burden. The contents of this chapter are based on the publication [46].

## 2.1 Introduction

There is a wealth of literature about constraint screening for operational problems in power systems. For instance, spurred by the recent boom of machine learning and artificial intelligence, a number of data-driven strategies have been proposed to detect redundant and inactive constraints very fast by learning from previously solved problem instances. Different strategies to learn the set of active constraints have been applied to the economic dispatch problem [13], the optimal power flow [14–16] and the unit commitment problem [12, 17]. While computationally inexpensive, the constraint-screening approaches purely based on machine learning carry a risk of constraint misidentification and therefore, may render reduced problems which are not equivalent to the target ones. This means that there exists, by construction, a nonzero probability that the solution to the reduced problem be suboptimal or even infeasible in the original one. These infeasibilities can be removed by combining the machine-learning method with a constraint-generation algorithm, as proposed in [5], at the expense of increasing the computational time.

On the other hand, the technical literature also includes a family of constraint-screening methods that seek to reduce the UC model as much as possible while ensuring the equivalence between the reduced and original UC problems. For this purpose, these methods usually involve, in one way or another, some form of optimization and consequently, are computationally more demanding in general. Perhaps, the most well-known

method within this family is an iterative procedure based on constraint generation, [18]. In this method, the violated constraints from the original UC problem are gradually added to the reduced one until the solution to the latter is feasible in the former. This procedure has been used, for example, in [19,20] to lighten the computational burden of the *security constrained* UC (SCUC) problem by filtering out post-contingency constraints. The main disadvantage of the methods based on constraint generation is that they can become computational costly if the number of iterations that are needed to guarantee solution feasibility is too large.

There is another group of optimization-based methods that concentrates on identifying *redundant* constraints, also referred to as *non-umbrella* constraints in [21]. These are the constraints that, if removed, the feasibility region of the original UC problem remains unchanged. The basic idea behind these methods is thus to check whether the constraints that are candidates to be removed are violated or not over a relaxation of this region. If they are not violated, then they can be safely ruled out. In general, this check requires optimization, as it typically translates into solving a series of bounding problems over the relaxed feasible region and, logically, makes sense provided that these bounding problems are much easier to solve than the target optimization problem. Examples of works that follow this *modus operandi* to solve the UC problem are [22–25]. These bounding-based methods aim to remove as many redundant constraints as possible from the full UC formulation. Nevertheless, even if all the redundant constraints are successfully identified and screened out, there may still remain a number of constraints in the so reduced UC problem that are not needed because they do not oppose to the minimization of the UC cost. In other words, it is the objective function of the UC problem, and not its feasible region, what makes such constraints superfluous. We use the qualifier “inactive” to refer to these constraints. Analogous ideas have been used within the context of the security-constrained DC optimal power flow, see, for instance, [21,26] and references therein.

In this chapter, we propose a strategy to endow bounding-based methods with the ability to detect, and thus discard, not only *redundant* but also *inactive* constraints. On the contrary, the proposed approach retains both *active* and *quasi-active* constraints, as defined in [12]. For this purpose, we build bounding problems that do not only account for technical aspects of the UC problem but also economic ones. To our knowledge, only the recently published paper [50] is in the spirit of our proposal, although they do not follow the trail of bounding-based methods. More specifically, they propose a heuristic algorithm that runs as follows: First, they address the UC without the network, the solution to which they call *cost-based schedule*. Then, they perturb this cost-based schedule by shifting a percentage  $\alpha$  of the total generation output (referred to as the *adjustment coefficient*) to the nodes with the highest or lowest Power Transfer Distribution Factors (PTDFs) for a given line. Finally, they check whether the so

perturbed solution congests that line. If it does not become congested, this line is classified as inactive.

Against this background, we develop a bounding approach with the ability to screen out both redundant and inactive constraints. To this end, in the linear programs that compute bounds on the line power flows, we introduce a valid inequality representing a cost budget, i.e., an upper bound on the UC solution cost. In this way, power dispatches that are implausible because of their high cost are made infeasible in the bounding problems. In addition, we combine the cost-budget constraint with a set of plausible nodal net demands that is a convex combination of historically observed values, so that unlikely nodal allocations of the system net demand are discarded. All this together increases the constraint-screening ability of our approach. Finally, we run a series of numerical experiments where we compare the performance of our proposal and its variants with alternative data-driven procedures and bounding techniques for constraint screening.

This chapter is organized as follows. Section 2.2 presents the mathematical formulation of UC utilized throughout this chapter. Section 2.3 elaborates on the proposed procedure and explains the methodology used to benchmark our approach. Section 2.5 discusses simulation results from an illustrative and a more realistic case study. Finally, conclusions are duly drawn in Section 2.6.

## 2.2 Mathematical Formulation

This section introduces the UC formulation used throughout this chapter. The vast majority of existing papers that propose methods to screen out network constraints consider single-period problems [12–16, 21–24, 26]. We follow suit and focus on the single-period UC problem (with no inter-temporal constraints) where the power system consists of a set of buses (nodes), lines and generators which we denote by  $\mathcal{N}$ ,  $\mathcal{L}$  and  $\mathcal{G}$ , in that order. We use indexes  $n$ ,  $l$  and  $g$  to refer to elements in these sets, respectively. Furthermore,  $\mathcal{G}_n$  represents the set of generators connected to node  $n$ . Besides, we consider nodal *net* demands, i.e., electricity demand *minus* renewable generation, where negative nodal net demands are plausible if renewable generation is greater than the electricity demand. The mathematical formulation of the single-period UC is stated below.

$$\min_{u_g, p_g} \sum_{g \in \mathcal{G}} c_g^1 p_g \quad (2.1a)$$

$$\text{s.t.} \quad \sum_{g \in \mathcal{G}_n} p_g - \sum_{n \in \mathcal{N}} d_n = 0 \quad (2.1b)$$

$$u_g \underline{p}_g \leq p_g \leq u_g \bar{p}_g, \quad \forall g \in \mathcal{G} \quad (2.1c)$$

$$-\bar{f}_l \leq \sum_{n \in \mathcal{N}} B_{ln} \left( \sum_{g \in \mathcal{G}_n} p_g - d_n \right) \leq \bar{f}_l, \quad \forall l \in \mathcal{L} \quad (2.1d)$$

$$u_g \in \{0, 1\}, \quad \forall g \in \mathcal{G}. \quad (2.1e)$$

The objective function (2.1a) minimizes the total production cost. For simplicity, in this work, we consider linear operating costs, but the proposal can be easily extended to quadratic or piecewise linear functions. Constraint (2.1b) corresponds to the power balance. Constraints (2.1c) and (2.1d) enforce the limits on the power output of the generating unit  $g$  and the power flow through the transmission line  $l$ , respectively. Note that the power flows through the transmission network are modeled using a DC approximation, where  $B_{ln}$  in constraint (2.1d) stands for the Power Transfer Distribution Factor (PTDF) of line  $l$  at node  $n$ . Expressions (2.1e) set the binary character of the commitment variables.

## 2.3 Screening of Network Constraints

In this section, we present the proposed methodology and discuss how it compares with existing ones. To this end, first, a general formulation of optimization-based methods to screen out redundant constraints is presented in Section 2.3.1. Subsequently, the proposed approach is introduced in Section 2.3.2, which is based on imposing an upper bound to the operating cost to discard uneconomical dispatches. Moreover, a further improvement is brought forward by considering a range of net demands that is a convex combination of past instances.

### 2.3.1 Existing Optimization-based Screening Approaches

Problem (2.1) can be made significantly easier to solve if those constraints (2.1d) with no effect on the optimal unit-commitment plan are removed [25]. As discussed in the introductory section of this chapter, several optimization-based approaches aim at removing redundant line capacity constraints, in particular, [22, 24]. To do so, these methods check, for each line, whether there is no feasible UC plan under which the line capacity is hit or surpassed. If that is indeed the case, then the corresponding line-flow constraint can be safely screened out because it is essentially redundant. For computational tractability, however, these methods do not work with the feasibility region of the original UC problem, but with that of an LP relaxation that can be swiftly solved using commercially available optimization software. In general, for each transmission line  $l'$ , the following two optimization problems are solved:

$$\max_{u_g, p_g, d_n} / \min_{u_g, p_g, d_n} f_{l'} = \sum_{n \in \mathcal{N}} B_{l'n} \left( \sum_{g \in \mathcal{G}_n} p_g - d_n \right) \quad (2.2a)$$

$$\text{s.t. (2.1b) – (2.1c)} \quad (2.2b)$$

$$0 \leq u_g \leq 1, \quad \forall g \in \mathcal{G} \quad (2.2c)$$

$$-\bar{f}_l \leq \sum_{n \in \mathcal{N}} B_{ln} \left( \sum_{g \in \mathcal{G}_n} p_g - d_n \right) \leq \bar{f}_l, \quad \forall l \in \mathcal{L}, l \neq l', \quad (2.2d)$$

$$\mathbf{d} \in \mathcal{D}. \quad (2.2e)$$

Problem (2.2) seeks to maximize/minimize the power flow through line  $l'$  (denoted as  $f_{l'}$ ) over an LP relaxation of the feasible region of the UC problem (2.1), in which the generated quantities are allowed to take values between zero and the respective generator's capacity  $\bar{p}_g$ . Furthermore, the vector of net nodal demands  $\mathbf{d} = (d_n)_{n \in \mathcal{N}}$  is turned into a vector of decision variables belonging to the set  $\mathcal{D}$ . If the minimum and maximum values of  $f_{l'}$  determined by (2.2) lie between  $-\bar{f}_{l'}$  and  $\bar{f}_{l'}$ , then the corresponding constraints (2.1d) are identified as redundant in problem (2.1) for any  $\mathbf{d} \in \mathcal{D}$ .

Depending on the specific LP relaxation that is used in problem (2.2) and the specific set  $\mathcal{D}$  that is considered, different methods for identifying redundant line-flow constraints can be derived. For instance, if the line-capacity limits (2.2d) are eliminated from (2.2) and the set  $\mathcal{D}$  is reduced to a singleton, namely, the predicted net demand for the hour in question, then we get the screening method proposed in [22]. Of course, enforcing the power flow constraints (2.2d) in (2.2) improves the screening ability of this problem at the expense of increasing its computational burden. Further, if the set  $\mathcal{D}$  is such that the net nodal demands  $d_n$  are not fixed to a given value but vary within a predefined range, i.e.,  $\underline{d}_n \leq d_n \leq \bar{d}_n$ , then we get the method suggested in [24]. The advantage of using a full-dimensional set  $\mathcal{D}$  in (2.2) is that the line-flow constraints that are filtered out by this problem are, in fact, superfluous for a whole range of predicted nodal net demands, i.e., operating conditions. This allows us to reduce the frequency with which we need to solve the set of problems (2.2). For example, if the set  $\mathcal{D}$  covers all the possible realizations of the predicted net nodal demands over the upcoming year, the line-flow constraints that are flagged as redundant by problem (2.2) can be removed from the series of UC problems (2.1) that are to be solved throughout that period of time. The downside of this approach is that, in general, the larger the size of  $\mathcal{D}$ , the lower the number of redundant line-flow constraints that are detected by the collection of problems (2.2). Throughout this chapter, we use the method proposed in [24] as *benchmark* (BN).

A relevant drawback of the LP relaxation (2.2) is that it only accounts for aspects of the UC problem that are purely technical. That is, it completely ignores the economics behind the UC problem, which is embodied in the minimization of the production costs. As a result, the series of problems (2.2) are only able to screen out *redundant* constraints but fail to identify constraints that are *inactive* at the optimum. To illustrate this,

consider the two-node network depicted in Fig. 2.1 with an expensive generator in  $n_1$ , a cheap generator in  $n_2$ , a line with a capacity of 100 MW, and a net load  $d_2$  that varies between 80 MW to 120 MW. Note that line  $l_1$  never becomes congested since  $d_2$  would be first satisfied by the cheaper unit connected to the same node and the maximum production of the expensive unit would be 20 MW without any network congestion. However, if problem (2.2) is solved for  $l_1$  with  $\mathcal{D}$  being the interval  $80 \leq d_2 \leq 120$ , the possible maximum power flow through this line would reach 100 MW by fully dispatching  $g_1$  and therefore, the capacity limit constraint would not be removed. In fact, such a constraint would be kept regardless of the marginal generating cost assigned to each of the two units.

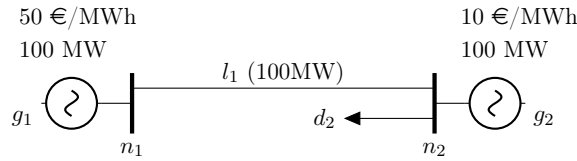


Figure 2.1: Two-node illustrative example

### 2.3.2 Proposed Cost-driven Constraint Screening

To overcome the drawback of existing optimization-based screening approaches and reduce even further the UC problem (2.1), we propose to tighten the LP relaxation used in the set of problems (2.2) by including a valid inequality on the optimal objective function of (2.1). More specifically, we propose to find the maximum power flow through each line  $l'$  by solving (2.3), where constraint (2.3c) imposes an upper bound on the total production cost. Thus, inactive but non-redundant constraints can also be screened out depending on the cost of the unit-commitment plan. This methodology is denoted as UB in this chapter.

$$\max_{u_g, p_g, d_n} / \min_{u_g, p_g, d_n} f_{l'} = \sum_{n \in \mathcal{N}} B_{l'n} \left( \sum_{g \in \mathcal{G}_n} p_g - d_n \right) \quad (2.3a)$$

$$\text{s.t.} \quad (2.2b) - (2.2e) \quad (2.3b)$$

$$\sum_{g \in \mathcal{G}} c_g^1 p_g \leq \bar{C}. \quad (2.3c)$$

Coming back to the illustrative example in Section 2.3.1, if  $d_2$  never exceeds 120 MW, then the maximum generation cost would be equal to €2000. Solving problem (2.3) for  $l_1$ , the range  $80 \leq d_2 \leq 120$ , and constraint (2.3c) formulated as  $50p_{g_1} + 10p_{g_2} \leq 2000$  yields a maximum power flow through that line below its capacity, since  $g_1$  cannot be dispatched above 30 MW. Consequently, the capacity constraint of this line can be

safely removed for these particular values of the units' marginal production costs.

Taken from a more realistic system, Fig. 2.2 displays an example of the total operating cost as a function of the aggregated net demand for 200 past instances of problem (2.1), with  $C^{\max}$  being the highest observed cost. As expected, similar aggregated net demand values may lead to different operating costs due to distinct allocations of such a demand among network buses. Obviously, fixing  $\bar{C} = C^{\max}$  in (2.3) would be a too conservative strategy. Indeed, such an upper bound would be much higher than the actual operating cost for low net demand values and therefore, constraint (2.3c) would be too loose and useless for our purpose. In other words, the constraint-screening ability of problems (2.3) would not be any better than that of (2.2) in this case. Accordingly, to take full advantage of the valid inequality (2.3c), we make  $\bar{C}$  dependent on the net demand vector  $\mathbf{d}$ , i.e.  $\bar{C} = \bar{C}(\mathbf{d})$ . In doing so, tighter upper bounds can be obtained for all net demand levels and a larger number of line capacity constraints can be screened out.

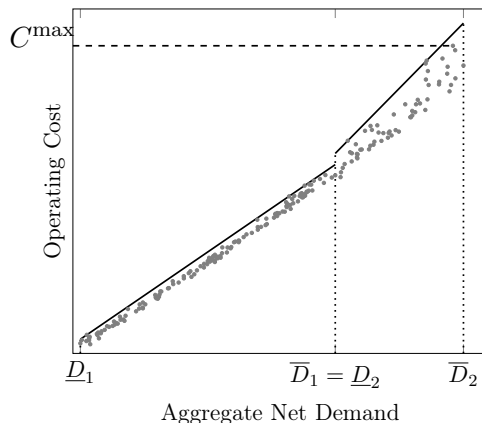


Figure 2.2: 1-quantile piecewise linear regression

We justify next our modeling choices to estimate the function  $\bar{C}(\mathbf{d})$ . First, to reduce model complexity and the risk of overfitting, we make the upper-bound  $\bar{C}$  dependent on the aggregated net demand  $D = \sum_{n \in \mathcal{N}} d_n$  only, as opposed to using all nodal net demands as explanatory variables. Nevertheless, for systems with a high penetration of renewable generation, the operating cost may be better explained by using two explanatory variables, namely, the aggregate demand and the aggregate renewable generation. Second, in order to keep problems (2.3) manageable and computationally tractable, we approximate the relation between the upper-bound  $\bar{C}$  and the aggregate net demand  $D$  through a piecewise linear function. Third, we resort to  $\tau$ -quantile regression, with  $0 \leq \tau \leq 1$ , [51]. More particularly, for each segment, we use 1-quantile regression in order to ensure that the approximated upper bound is higher than the operating cost of all observed instances. The solid line in Fig. 2.2 represents the 1-quantile piecewise linear function for this illustrative data set.

The quantile piecewise linear regression we propose is then characterized by a set of segments  $\mathcal{S}$ , indexed by  $s$ . We can resort to well-established procedures in Statistics to decide on the number of segments. For instance, we can borrow the popular *elbow criterion* from the realm of data clustering to this end. According to this criterion, we compute and plot the quantile loss as a function of the number of segments and the *elbow* of the curve is taken as a good value for the number of pieces to be picked. The idea is to choose the number of segments from which the implied reduction in the quantile loss starts to diminish rapidly. The choice of the number of segments could also be based on even simpler procedures such as the visual inspection of the data scatter plot “net demand vs. cost” (see Fig. 2) and/or more sophisticated tuning techniques based on bootstrapping and cross-validation.

The minimum and maximum aggregate net demand for each segment is denoted by  $\underline{D}_s$  and  $\overline{D}_s$ , and we introduce a binary variable  $y_s$  per segment, which is equal to 1 if  $\underline{D}_s \leq D \leq \overline{D}_s$ , and to 0 otherwise. For illustration, Fig. 2.2 includes  $\underline{D}_s$  and  $\overline{D}_s$  for the two segments considered. The upper bound for an aggregate net demand  $D$  can be thus computed as:

$$\overline{C}(D) = \sum_{s \in \mathcal{S}} y_s (\rho_s + \nu_s D)$$

where  $\rho_s$  and  $\nu_s$  are the intercept and slope of the linear function corresponding to segment  $s$ . Under this approximation, problem (2.3) can be recast as:

$$\max_{u_g, p_g, d_n, y_s, D} / \min_{u_g, p_g, d_n, y_s, D} \quad f' = \sum_{n \in \mathcal{N}} B'_{n'} \left( \sum_{g \in \mathcal{G}_n} p_g - d_n \right) \quad (2.4a)$$

$$\text{s.t.} \quad (2.2b) - (2.2e) \quad (2.4b)$$

$$\sum_{g \in \mathcal{G}} c_g^1 p_g \leq \sum_{s \in \mathcal{S}} y_s (\rho_s + \nu_s D) \quad (2.4c)$$

$$D = \sum_{n \in \mathcal{N}} d_n \quad (2.4d)$$

$$\sum_{s \in \mathcal{S}} y_s \underline{D}_s \leq D \leq \sum_{s \in \mathcal{S}} y_s \overline{D}_s \quad (2.4e)$$

$$\sum_{s \in \mathcal{S}} y_s = 1 \quad (2.4f)$$

$$y_s \in \{0, 1\}, \quad \forall s \in \mathcal{S}. \quad (2.4g)$$

Constraint (2.4c) is identical to (2.3c), except that the constant upper bound is replaced with the piecewise linear function obtained from the 1-quantile regression. Equation (2.4d) computes the aggregate net demand  $D$ . Constraints (2.4e) impose segment-dependent minimum and maximum bounds on the aggregate net demand, in that order. Therefore, if  $y_s = 1$ , then  $\underline{D}_s \leq D \leq \overline{D}_s$ . Expression (2.4f) ensures a one-to-one map-

ping between the aggregate net demand segment and the cost piece. Finally, constraints (2.4g) set the binary character of the decision variables  $y_s$ . The product of binary and continuous variables,  $y_s D$  in (2.4c), can be easily linearized by using integer algebra results [52] so that (2.4) can be formulated as a mixed-integer linear optimization problem and solved using commercial optimization software.

A second drawback of LP relaxation (2.2) relates to the choice of set  $\mathcal{D}$ . For instance, the method proposed in [24] defines  $\mathcal{D}$  as the Cartesian product of the intervals  $[\underline{d}_n, \bar{d}_n]$ . Under this assumption, the solution of problems (2.2) may render an implausible net demand profile  $\mathbf{d} = (d_n)_{n \in \mathcal{N}}$ , which does not conform at all with the observed spatial correlations among the net nodal loads. For this reason, in this chapter, we also explore defining  $\mathcal{D}$  as the set of net demand profiles  $\mathbf{d} = (d_n)_{n \in \mathcal{N}}$  that are a convex combination of the observed ones. This is imposed as follows:

$$d_n = \sum_{t \in \mathcal{T}} \alpha_t \hat{d}_{tn} \quad (2.5a)$$

$$\alpha_t \geq 0, \quad \forall t \in \mathcal{T} \quad (2.5b)$$

$$\sum_{t \in \mathcal{T}} \alpha_t = 1, \quad (2.5c)$$

where  $\hat{d}_{tn}$  denotes the net demand at node  $n$  in past time period  $t$ . We remark that we may allow the sum of the scalars  $\alpha_t$  in (2.5c) to be equal to a number greater than one, if we want to increase the probability of not making a mistake when removing a particular line-flow constraint. However, based on the rationale that demand patterns do not change quickly, our choice of  $\mathcal{D}$  as (2.5) offers a good compromise between risk of mistake and constraint-screening power of the bounding problem (2.2) for UC instances that are to be solved in the near future. Furthermore, the convex hull of past net demand observations we use as  $\mathcal{D}$  can be frequently enriched with new data points as we move forward in time.

Naturally, the performance of the proposed approach requires that the set  $\mathcal{T}$  includes a sufficiently high number of past time periods that characterize the variability of the system operating conditions. Defining  $\mathcal{D}$  through (2.5) instead of as the Cartesian product of the intervals  $[\underline{d}_n, \bar{d}_n]$  results in a more constrained problem (2.2) and a higher number of removed constraints. In this chapter, this modeling choice is denoted as CC (which stands for *convex combination*).

In summary, methods UB and CC shrink the feasible space of generation and net demand variables in problems (2.2), respectively, to leave out unrealistic operating conditions. We also advocate for the synergistic use of UB and CC, that is, for the constraint screening method UB+CC, which exploits an upper-bound function on the total operating cost over a convex combination of the net demand profiles. For clarity, Table 2.1 compiles the optimization problems solved by each of the approaches that are considered

in this chapter.

## 2.4 Evaluation Procedure

The procedure to measure the performance of the approaches described in Section 2.3.2 to screen out line capacity constraints and reduce the computational burden of the UC problem runs as follows:

- 1) Use historical information on past unit commitment instances to adjust some of the parameters of the screening optimization problems. For instance, in BN, this information can be used to adjust the range of each nodal net demand that defines the set  $\mathcal{D}$ , while, in UB, this data is employed to estimate the parameters of the 1-quantile piecewise linear regression. Similarly, imposing the convex combination of net demands in CC requires past net demand profiles. Finally, UB+CC uses historical information to compute both the regression parameters and convex combinations of demands.
- 2) Depending on the approach, solve the optimization problem listed in Table 2.1 for each of the lines of the network and determine the set of line capacity constraints that can be removed from the original UC problem. In particular, if the maximum (minimum) flow of line  $l$  determined by the screening optimization problem is below (above) the limit  $\bar{f}_l$  ( $-\bar{f}_l$ ), then constraint  $f_l \leq \bar{f}_l$  ( $-\bar{f}_l \leq f_l$ ) can be screened out.
- 3) Solve a reduced unit commitment problem similar to (2.1) without including the line capacity constraints (2.1d) that have been filtered out in step 2).
- 4) Fix the binary commitment decisions to those obtained in step 3) and solve the unit commitment problem including all constraints.
- 5) Measure the performance of the screening approach in terms of i) the average number of line capacity constraints that are filtered out in step 2), ii) the average computational time required to solve the reduced UC problem of step 3) with respect to the full UC formulation, and iii) the average optimality loss of the obtained solution with respect to that of the full UC problem.

## 2.5 Numerical Experiments

This section presents numerical results on two power systems. The first one is a small-size system especially designed for illustrative purposes. The second one is based on a

Table 2.1: Constraint screening approaches

Approach	Screening optimization problem
BN	(2.2a) s.t. (2.2b) - (2.2e)
UB	(2.2a) s.t. (2.2b) - (2.2e), (2.4c)-(2.4g)
CC	(2.2a) s.t. (2.2b) - (2.2e), (2.5a)-(2.5c)
UB+CC	(2.2a) s.t. (2.2b) - (2.2e), (2.4c)-(2.4g), (2.5a)-(2.5c)

realistic power system from Texas. All experiments have been carried out on a Linux-based server with CPUs clocking at 2.6 GHz, 1 thread and 16 GB of RAM. The constraint screening approaches presented in Table 2.1 have been modeled using Pyomo 5.7.1 [53] and solved with CPLEX 20.1 [54]. The number of segments of the 1-quantile piecewise linear regression has been set to one in Section 2.5.1 (illustrative example) and to three in Section 2.5.2 (realistic case study). In the latter case, our choice is motivated by the visual inspection of the data scatter plot *net demand vs. cost*. The breakpoints have been found with the Python library PWLF.

### 2.5.1 Illustrative Example

Next we illustrate the most salient features of our approach using the five-node system represented in Figure 2.3. This small system includes three thermal units whose linear operating costs and minimum/maximum power limits are indicated in the figure. For simplicity, the five lines in this small system have the same susceptance of 1 p.u., while their capacity limits are also provided in said figure. Finally, Table 2.2 contains historical unit commitment information including the net demand profile, the optimal operating cost and the congested lines for three times periods.

Due to the capacity limit of line  $l_4$ , which connects nodes  $n_4$  and  $n_5$ , the operating costs may significantly change depending on how the total net demand is distributed among  $d_4$  and  $d_5$ . For instance, in periods  $t_1$  and  $t_2$ , all net demand is located at  $n_4$  and can thus be satisfied by the cheaper units  $g_2$  and  $g_3$  without involving network congestion. Conversely, in period  $t_3$  all net demand is at  $n_5$ , which leads to the congestion of  $l_4$  and a higher operating cost due to the commitment of the expensive unit  $g_1$ .

Table 2.2: Historical data – Illustrative Example

Time period	$d_4$ (MW)	$d_5$ (MW)	Cost (€)	Congested lines
$t_1$	55	0	275.0	-
$t_2$	75	0	575.0	-
$t_3$	0	69	772.5	$l_4$

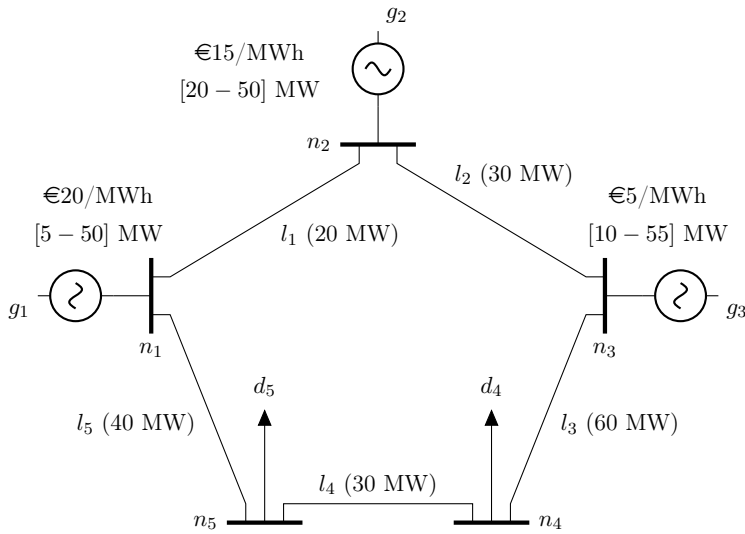


Figure 2.3: Five-node system

Now consider a new time period  $t_4$  with a demand profile of  $(d_4, d_5) = (58, 13.8)$  MW. Solving the complete unit commitment (2.1) for period  $t_4$  yields an operating cost of €611. For such a demand profile, the power flow through  $l_1$  is 7 MW, which is below its limit and thus, the capacity constraint of this line is not binding. However, if such a constraint were removed, the obtained solution would become infeasible since the power flow through  $l_1$  would end up exceeding 20 MW. This type of constraint is referred to as *quasi-active* in [12]. Therefore, to obtain the same solution as the full unit commitment problem, the line capacity constraint of  $l_1$  must be enforced.

Table 2.3 shows the line capacity constraints that are retained in the unit commitment problem for time period  $t_4$  using the different approaches described in Section 2.3. For the BN approach, problems (2.2) are solved for the five lines considering that demands can vary between the minimum and maximum observed values, that is,

$$0 \leq d_4 \leq 75 \quad (2.6a)$$

$$0 \leq d_5 \leq 69 \quad (2.6b)$$

The results obtained by the BN approach indicate that three out of the ten line capacity constraints are redundant and therefore, the reduced unit commitment problem includes seven line capacity constraints.

To illustrate the UB approach, Fig. 2.4 plots the operating cost as a function of the aggregate net demand of time periods  $t_1$ ,  $t_2$  and  $t_3$ . The continuous line represents the 1-quantile regression described in Section 2.3 for a single segment, whose expression is  $\bar{C}(D) = -1679.5 + 35.5D$ . This linear function allows us to estimate an upper bound

Table 2.3: Retained capacity constraints in the UC problem at time period  $t_4$  – Illustrative Example

	BN	UB	CC	UB+CC
$-\bar{f}_{l_1} \leq f_{l_1}$	x			
$f_{l_1} \leq \bar{f}_{l_1}$	x	x	x	x
$-\bar{f}_{l_2} \leq f_{l_2}$				
$f_{l_2} \leq \bar{f}_{l_2}$	x	x	x	
$-\bar{f}_{l_3} \leq f_{l_3}$				
$f_{l_3} \leq \bar{f}_{l_3}$	x	x		
$-\bar{f}_{l_4} \leq f_{l_4}$	x	x	x	x
$f_{l_4} \leq \bar{f}_{l_4}$	x	x	x	x
$-\bar{f}_{l_5} \leq f_{l_5}$	x	x	x	
$f_{l_5} \leq \bar{f}_{l_5}$				
# Retained constraints	7	6	5	3

on the operating cost for new values of the aggregate net demand as follows:

$$20p_{g_1} + 15p_{g_2} + 5p_{g_3} \leq -1679.5 + 35.5(d_4 + d_5) \quad (2.7)$$

The upper bound corresponding to  $t_4$  is equal to €872, which is higher than the actual cost of €611. Considering such an upper bound on the operating cost avoids that the power flow through line  $l_1$  reaches its minimum value and therefore, UB yields a reduced problem that includes six line capacity constraints.

Following the CC approach, the set  $\mathcal{D}$  formulated in (2.6) is replaced by (2.8) so that  $\mathbf{d} = (d_4, d_5)$  is guaranteed to be a convex combination of the data in Table 2.2. In this case, CC retains the five line capacity constraints indicated in Table 2.3.

$$d_4 = \alpha_1 \cdot 55 + \alpha_2 \cdot 75 + \alpha_3 \cdot 0 \quad (2.8a)$$

$$d_5 = \alpha_1 \cdot 0 + \alpha_2 \cdot 0 + \alpha_3 \cdot 69 \quad (2.8b)$$

$$\alpha_1 + \alpha_2 + \alpha_3 = 1 \quad (2.8c)$$

Finally, the UB+CC approach screens out line capacity constraints by considering both the upper bound on the operating cost computed in (2.7) and the convex combination of net demand profiles formulated in (2.8). In doing so, this approach is able to successfully restrict the search space of problems (2.2) so that it takes into account information on

both the feasible region and the objective function of the UC problem. In this way, the UB+CC approach states that only three line capacity limits are to be retained in the unit commitment problem.

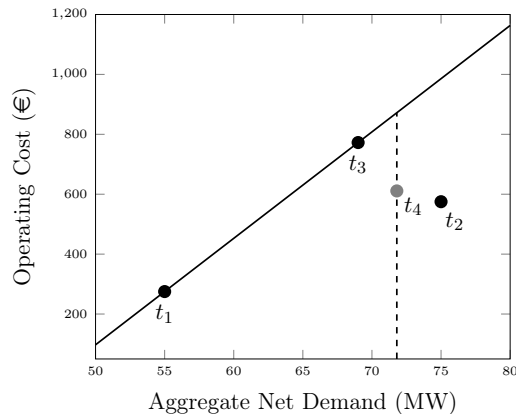


Figure 2.4: Upper-bound Estimation – Illustrative Example

The four approaches compared in this illustrative example correctly retain the maximum capacity limit of line  $l_1$  and hence, all of them obtain the same UC solution as that of the full UC problem. On the other hand, the number of retained constraints significantly vary between the different approaches. The BN method proposed in the literature is the most conservative one and only removes three constraints. The other three approaches screen out a higher number of constraints by solving problems (2.2) with a feasible region that has been tightened using a cost budget and/or a shrunk net demand set  $\mathcal{D}$ . The UB+CC approach screens out the largest number of constraints (seven out of ten), which would result in the highest computational savings.

### 2.5.2 Realistic Case Study

In this section, we consider a realistic power system from Texas, [55]. The network consists of 2000 buses and 3206 lines. Hence, the associated UC problem includes 6412 line capacity constraints. To work with more challenging UC instances, the minimum generating capacity limit,  $\underline{p}_g$ , has been set as the maximum between the nominal value given in [55] and the 10% of the unit's capacity, as done in [12, 24]. In addition, the marginal costs of the generators  $c_g^1$  have been modified so that they vary in the range  $\text{€}[0, 40]/\text{MWh}$ . The line capacities,  $\bar{f}_l$ , are also reduced to have a more congested network. Finally, we synthetically generate the nodal net demands for 8640 time periods as follows. First, a demand value  $L$  for each period is randomly sampled from a uniform distribution in the range  $[50, 70]$  GW. Second, the net demand at node  $n$  is also randomly sampled from a uniform distribution in the range  $[0.95L\xi_n, 1.05L\xi_n]$ , where  $\xi_n$  are the nodal allocation factors of the total system net load taken from [55]. All the data used

in this case study is available for download at [56]. Of the 8640 values of nodal net loads we produce, 7200 are used for training and parameter fitting, and the remaining 1440 for testing and performance comparison. In particular, the training data is employed to conduct the quantile regression on which method UB relies.

Our numerical evaluation consists of four different, but related experiments, which we describe and discuss in the following.

### Experiment 1 – Fixed load

Firstly, we consider the setup in which the demand set  $\mathcal{D}$  in (2.2e) is reduced to a singleton. Specifically, the only element in  $\mathcal{D}$  is the vector of nodal net demands in the hour in question (which is assumed to be known or predicted). In this way, we can compare the bounding-based constraint-screening methods BN and UB with the data-driven method of [12], where the authors propose a *k-nearest neighbors* to identify redundant and inactive constraints, and the heuristic proposed in [50], detailed in Section 2.1. Notice that, when  $\mathcal{D}$  is a singleton, methods CC and UB+CC become correspondingly equivalent to BN and UB. In the case of the data-driven constraint-screening method in [12], here we report results for 50 neighbors only (which is why we have denoted it as DD50). Nevertheless, similar empirical findings are obtained for a number of neighbors equal to 5 and 500. As for the heuristic constraint-screening method introduced in [50], which we denote as H, the tuning parameter on which this method depends has been set to 3% as the authors in [50] suggest.

The main results from this first experiment are collated in Table 2.4. In this table, as in the subsequent ones, we provide the following performance metrics: The average percentage of retained constraints with respect to the full UC formulation (Retained constraints), the number of infeasible or suboptimal instances (#Infeasibilities or #Sub-optimal), the average cost error of the optimal solution with respect to the original UC cost (Cost error), the time needed to solve the screening algorithm (Screening time), the solution time of the reduced UC formulation (Reduced UC time), and the computational burden of each method with respect to the original UC problem (Computational burden). The heuristic method turns out to be the most conservative one, in the sense that it is the one retaining the largest number of line-flow constraints in the reduced UC formulation. Consequently, it leads to the highest solution time. At the other end of the spectrum is the data-driven constraint-screening method DD50, which only keeps 4.8% of the line-flow limits, thus featuring the lowest computational burden by far. However, its remarkable speed comes at a significant cost. Indeed, the daring nature of DD50 results in UC plans that are infeasible in a few instances and suboptimal in many of them, with an average cost error of 0.022%. From among the four methods analyzed in Table 2.4, UB is the one showing a more balanced performance. In fact, the cost-based valid inequality this method utilizes gets to reduce the number of retained constraints

in more than eight percentage points as compared to BN, which, in turn, means a two-times speedup with respect to this one. Most importantly, these improvements come without delivering infeasible or suboptimal UC plans.

Table 2.4: Results – Fixed load

	DD50	BN	UB	H
Retained constraints (%)	4.8	18.5	10.2	23.5
#Infeasibilities	4	0	0	0
#Sub-optimal solutions	540	0	0	0
Cost error (%)	0.022	0.000	0.000	0.000
Screening time (s)	0.05	0.15	0.18	0.02
Reduced UC time (s)	0.39	3.10	1.50	3.34
Total time (s)	0.45	3.25	1.68	3.36
Computational burden (%)	3.9	28.2	14.5	29.1

### Experiment 2 – Base Case

We now consider the alternative setup in which the net demand set  $\mathcal{D}$  is not a singleton, but spans a subset of  $\mathbb{R}^{|\mathcal{N}|}$ . In the case of BN and UB, this subset is given by the Cartesian product of the intervals  $[\underline{d}_n, \bar{d}_n]$ ,  $n \in \mathcal{N}$ , where the bounds  $\underline{d}_n$  and  $\bar{d}_n$  are respectively taken as the minimum and maximum values of net load at node  $n$  that are observed in the training data set. In the case of CC and UB+CC, the set  $\mathcal{D}$  corresponds to the convex combination of the net demand vectors that make up the same training data. This experiment excludes the constraint-screening methods DD50 and H, because these are designed to work with a fixed net load only. In effect, these methods are not intended to filter out line-flow constraints that are superfluous for a (wide) range of net load values. Consequently, unlike BN, UB, CC and UB+CC, methods DD50 and H are to be rerun every hour or every day, that is, every time the predicted vector of nodal net loads is updated.

The first important observation to be made is that the three proposed methods (UB, CC, UB+CC) provide, for the 1440 time periods in the test set, the same optimal UC cost as that obtained by the benchmark approach. Consequently, the performance of these methods, which is summarized in Table 2.5, is assessed and compared in terms of the average percentage of retained constraints and the average computational burden relative to the computational time required to solve the full UC problem. This computational burden does not include the time of the screening procedure, which is assumed to be run offline only once, since the network constraints that are screened out by these approaches can be left out of the UC problem for a wide range of operating conditions. The average computational times of the screening problems to be solved under methods BN, UB, CC and UB+CC amount to 2.9s, 9.7s, 122.4s, and 350.4s, respectively.

Results in Table 2.5 show that method UB involves slight reductions in both the number of retained constraints and the computational burden. Imposing a convex combination of the nodal demand through method CC reduces the retained constraints and computational time by 9% and 29%, respectively. Relevantly, it is the synergistic effect of UB and CC, i.e., the proposed approach UB+CC, which involves the largest improvement. Indeed, this method obtains reduced UC problems with 15% fewer constraints than BN with a computational time 45% lower on average. As pointed out in Section 2.3, these results demonstrate that the estimated cost-budget function  $\bar{C}(D)$  is most effective when combined with a consistent feasible demand set  $\mathcal{D}$ , like the one used in CC.

Table 2.5: Results – Base Case

	BN	UB	CC	UB+CC
Retained constraints (%)	33.8	33.0	24.9	18.9
#Infeasibilities	0	0	0	0
#Sub-optimal solutions	0	0	0	0
Cost error (%)	0.000	0.000	0.000	0.000
Reduced UC time (s)	8.62	8.15	5.28	3.42
Computational burden (%)	74.6	70.5	45.7	29.6

Despite the fact that there are no infeasibilities or suboptimal solutions, these could appear when the cost budget function is underestimated or the unseen net nodal demand vector  $\mathbf{d}$  does not belong to the set  $\mathcal{D}$ , i.e., when not enough data have been used in the screening procedure. Nonetheless, in this experiment, we have not encountered infeasible or suboptimal solutions.

### Experiment 3 – Worst Case

Now we evaluate the performance of the proposed method in an out-of-range situation. To do so, the time periods of the training and test sets are not randomly selected. Instead, we deliberately include the 1440 time periods with the highest aggregate demand values in the test set, and the remaining time periods in the training set. In this manner, we artificially construct an unlikely situation that is, however, very adverse to the methods and, in particular, to UB+CC (which is the one that relies the most on the training data of the four constraint-screening approaches we consider in this experiment).

Similarly to Table 2.5, we provide the results of this out-of-range analysis in Table 2.6. As in the base case, the proposed UB+CC is the method that screens out the largest number of line-flow constraints by far, thus producing reduced UC problems that can be solved in around one fifth of the time that is needed to solve the full UC formulation. However, unlike in the base case, UB+CC leads to UC solutions that are infeasible

or slightly suboptimal in a few instances. Interestingly, both UB and CC are able to deliver feasible and optimal UC plans in all instances of the test set under this very adverse situation. This reinforces the idea that the proposed cost-based valid inequality is only really effective, i.e., it has screening power, when combined with a demand set  $\mathcal{D}$  that does not contain values of the nodal net demands that are too different from the observed ones. This is so because, for a demand value that is too dissimilar from the observations, the upper bound may be too loose or even wrong. Therefore, the design of the set  $\mathcal{D}$  is key to the performance of the proposed UB+CC, as this “worst-case setup” reveals.

Table 2.6: Results – Worst Case

	BN	UB	CC	UB+CC
Retained constraints (%)	34.0	31.9	24.1	12.9
#Infeasibilities	0	0	0	22
#Sub-optimal solutions	0	0	0	55
Cost error (%)	0.000	0.000	0.00	0.008
Reduced UC time (s)	6.48	5.99	4.76	1.86
Computational burden (%)	61.2	57.3	45.5	17.8

#### Experiment 4 – Topological changes

We conclude this case study by assessing the resilience of the proposed constraint-screening approach, i.e., UB-CC, against topological changes. To this end, we have picked 34 corridor lines connecting automatic generation control areas of the 2000-bus system [55] and assumed that *any* of these lines (which are specified in [56]), but only one at the same time, can be out of service. This leads to  $34 + 1$  possible system configurations, where the “+1” corresponds to the base case analyzed and discussed in Experiment 2.

Now, for each of those 35 possible topological configurations, we have run UB-CC following steps 1) and 2) of the procedure described in Section 2.4, with each of these runs delivering a set of superfluous line-flow constraints. We have then computed the intersection set, that is, the set of the line-flow constraints that, according to UB-CC, can be safely removed from the original UC formulation under *any* of those 35 possible configurations (these are the constraints that are detected as dispensable by UB-CC in all the 35 runs of the screening method).

As indicated in Table 2.5, UB-CC identifies that 81.1% of the line-flow constraints are superfluous in the base case with no topological changes. This percentage slightly drops (as should be expected) to 79.5%, which shows that the screening rate of UB-CC remains high even under topological changes. This result suggests that our approach is resilient against this type of changes.

## 2.6 Summary and Conclusions

The computational time of the unit commitment problem can be significantly reduced by screening out line capacity constraints. However, the optimization-based methods proposed in the literature only remove redundant constraints and thus, involve moderate computational savings. This chapter presents a novel constraint screening methodology that removes both redundant and inactive constraints and further reduces the computational burden of this problem.

As existing approaches, the one we propose is based on computing the maximum line power flows on an LP-relaxation of the UC formulation. As a salient feature of our work, we propose to tighten this LP-relaxation to exclude uneconomical operating conditions. In doing so, our methodology is able to filter out a higher number of line capacity constraints. Simulation results using a 2000-bus network show that our proposal reduces the number of retained constraints and the solution time by 15% and 45%, respectively, if compared with existing benchmark methods. Furthermore, the constraint-screening rate of our approach remains quite unaltered when topological changes of the network are considered, which suggests that our approach is resilient against this type of changes. Finally, even though the cost inequality we use to increase the constraint-screening power of our method is data-driven, our numerical analysis reveals that the solution to the reduced UC problem we produce is generally feasible and optimal in the original UC formulation, if enough data are available.

## Chapter 3

# Joint Chance-constrained Optimal Power Flow



The *optimal power flow* (OPF) problem is a routine at the core of important tools for power system operations [27]. This problem seeks to determine the production levels of generating units that satisfy the power (net) demand at minimum cost while complying with some technical constraints imposed by those units and the grid. The demand and renewable generation are factors that increase the uncertainty in power systems operation, and ignoring it can lead to unsafe operating conditions.

As discussed in Chapter 1, the OPF problem can be reformulated as a stochastic optimization problem, to account for the inherent uncertainty associated with demand and renewable generation. Over time, various methodologies have emerged in the literature to tackle this challenging problem. The fundamental focus of these models lies in finding an appropriate trade-off between reliability and cost. A current prevailing practice is to rule out the satisfaction of the technical constraints for improbable and extreme events by using chance constraints. Thus, this approach is designed to reduce the system's operation cost while guaranteeing its security with high probability.

Dealing with chance constraints in optimization problems presents a formidable challenge due to the absence of a finite, tractable reformulation. To cope with this issue, we utilize the *sample average approximation* (SAA) method, which enables us to generate a data-driven deterministic reformulation of the problem. This reformulation has demonstrated superior performance in terms of cost compared to existing approximations documented in the literature. However, SAA is computationally expensive due to the presence of binary variables.

In this chapter, we propose a methodology, based on a tightening-and-screening procedure and valid inequalities, that leads to a tight, compact model that efficiently solves the SAA reformulation of the OPF's probabilistic version. The contents of this chapter rely on the manuscript [47].

### 3.1 Introduction

Chance-constrained programming suits applications in areas where decisions have to be made dealing with random parameters [41]. In these situations, it is desirable to ensure feasibility of the system almost surely, but there is hardly any decision which would guarantee it under extreme events or unexpected random circumstances. In the context of the OPF, chance-constrained programming can be used to minimize the expected operating cost whilst guaranteeing that the system withstands unforeseen peaks of electrical load due to stochastic demand or uncertainty in power generation [33]. The *chance-constrained* OPF (CC-OPF) problem addresses this uncertainty and pursues to ensure the safe operation of a power system with a high level of probability. Under a linear approximation of the power flow equations, the CC-OPF problem can be formulated as the following *chance-constrained problem* (CCP) with joint linear chance

constraints and random RHS and LHS:

$$\min_x f(x) \tag{3.1a}$$

$$\text{s.t. } x \in X \tag{3.1b}$$

$$\mathbb{P} \left\{ a_j(\boldsymbol{\omega})^\top x \leq b_j(\boldsymbol{\omega}), \forall j \in \mathcal{J} \right\} \geq 1 - \epsilon. \tag{3.1c}$$

In (3.1),  $x \in \mathbb{R}^{|\mathcal{I}|}$  is a vector of continuous decision variables,  $X \subseteq \mathbb{R}^{|\mathcal{I}|}$  is a polyhedron that represents a set of deterministic constraints, and  $f : \mathbb{R}^{|\mathcal{I}|} \rightarrow \mathbb{R}$  is a convex function. Uncertainty is represented through the random vector  $\boldsymbol{\omega}$  taking values in  $\mathbb{R}^d$  and giving rise to a technology matrix with random rows  $a_j(\boldsymbol{\omega}) \in \mathbb{R}^{|\mathcal{I}|}$ ,  $j \in \mathcal{J}$  and random  $b_j(\boldsymbol{\omega}) \in \mathbb{R}$ ,  $j \in \mathcal{J}$ .  $\mathbb{P}$  is a probability measure, and  $\epsilon$  is a confidence or risk parameter, typically near zero, so that the set of constraints (3.1c) are satisfied with probability at least  $(1 - \epsilon)$ . Apart from power systems, applications of CCPs include supply chain, location and logistics [57–59], risk control in finance [60, 61], and health-care problems such as operating room planning [62] or vaccine allocation [63], among others.

When the probabilistic constraint corresponds to (3.1c), the CCP has *joint chance constraints* (JCC) and is hence classified as a *joint CCP* (JCCP), in contrast with *single CCPs* (SCCPs), i.e. CCPs with individual or *single chance constraints* (SCC) of the form  $\mathbb{P} \{ a_j(\boldsymbol{\omega})^\top x - b_j(\boldsymbol{\omega}) \leq 0 \} \geq 1 - \epsilon_j, \forall j \in \mathcal{J}$ . JCCPs are suitable for contexts where all constraints need to be simultaneously satisfied with a high probability, and the dependence between random variables makes them clearly harder. Both SCCPs and JCCPs have been extensively studied (see [33, 64] and the references therein).

There are a number of reasons why general CCPs are challenging. The first one is the non-convexity of the feasible set. In general, the feasible region of a CCP is not convex in the original space even when  $x$  is continuous, there is only RHS uncertainty and the constraints inside the probability in (3.1c) result in a polyhedral region [65]. To circumvent this problem, several approaches have been proposed. Some methods (e.g., [66–68]) give convexity results and investigate the conditions under which the feasible region of problem (3.1) is convex. In another line of research, various convex approximation schemes such as quadratic [69] or Bernstein approximation [70], have been proposed in the literature. The CVaR approximation has gained a lot of popularity since its introduction [71, 72], and remains one of the most used methods to deal with stochastic problems. Nonetheless, the solutions to the approximated problems err on the side of over-conservatism. In this context, some iterative schemes such as ALSO-X have been recently proposed to identify tighter inner convex approximations of the CCP at the expense of a higher computational cost [73, 74]. Finally, other works suggest convex approximations for non-linear CCPs. For instance, Hong *et al.* [75] propose to solve the JCCP by a sequence of convex approximations followed by a gradient-based Monte

Carlo method, whereas Peña-Ordieres *et al.* [76] introduce a smooth sampling-based approximation.

The second difficulty of CCPs is that checking the feasibility of a given solution is not, in general, an easy task. For instance, even if the uncertainty follows a known continuous distribution, calculating the joint probability requires a multi-dimensional integration, which becomes increasingly difficult with the dimension of the random vector  $\omega$ . On top of that, in most cases the distribution  $\mathbb{P}$  is not fully known. To cope with these two obstacles at once, in this work we make use of SAA, which in practice boils down to dealing with a finite discrete distribution. The application of SAA may be seen as the result of approximating a general known distribution via the generation of independent Monte Carlo samples of the random vector  $\omega$  [77, 78] or as a data-driven approach that works with observations of  $\omega$  that are available to the decision-maker even if the distribution is unknown.

SAA allows for a deterministic reformulation of the problem, and the resulting model is a *mixed-integer problem* (MIP). For the resolution of CCPs using MIP reformulations, we refer the reader to [65]. When there is only RHS uncertainty (i.e. the technology matrix is fixed), a reformulation of the problem leads to a MIP with a set of constraints that form a *mixing set* and that have been extensively studied, alone or in combination with the knapsack constraint that also appears in the formulation [79–81]. Alternative reformulations like the ones proposed by [82, 83] rely on the concept of  $(1 - \epsilon)$ -efficient points. The case when the technology matrix is random, while the RHS is not, has been studied e.g. in [84]. As for the general case, it has also been addressed in the literature. Specifically, a large line of research has focused on the development of *quantile cuts*, a particular type of valid inequality that can be viewed as a projection of a set of mixing inequalities for the MIP onto the original problem space. These cuts and the associated quantile closure have been recently studied in [85–88] and successfully applied to computational experiments of CCPs in [73, 89], among others.

To address the CC-OPF problem (the interested reader in this topic is referred to the survey paper [90]), several works in the literature, e.g., [42], directly work with SCCs. However, the main drawback of this modeling approach is that, even in those cases where the probability of violating each individual constraint seems more than tolerable, the resulting *joint risk* (that is, the probability that *any* of the technical constraints be violated) may still be excessive and inadmissible. This is the key motivation behind the use of JCCs to tackle the CC-OPF problem (see, e.g., [39]). It is also true that there are ways to guarantee the satisfaction of the joint chance-constraint system by way of SCCs. Unfortunately, the success of this strategy depends on the non-trivial task of how to allocate the joint risk of the system among the single constraints. For example, based on Bonferroni’s inequality, distributing the joint risk evenly across all individual constraints ensures that the joint chance constraint is met. However, this

results in a rather conservative solution in general. To reduce the conservatism of this solution approach, Baker and Bernstein [91] propose a learning algorithm to filter out redundant constraints and, thus, increase the risk of the non-redundant ones, whereas Jia *et al.* [92] devise a non-parametric iterative framework to allocate the joint risk. In contrast to these works, we explicitly model and deal with the joint chance constrained version of the problem.

In this vein, there are several approaches in the literature to solve the *joint* CC-OPF (JCC-OPF) problem. Vrakopoulou *et al.* [34] adopt the scenario approach (SA) to approximate the solution of the JCC-OPF, while Chen *et al.* [43] propose a heuristic data-driven method that involves enforcing the satisfaction of the technical constraints for a box of the uncertainty. This box is inferred using one-class support vector clustering and its size is contingent on the system's desired reliability. Hou and Roald [38] propose an iterative tuning algorithm to solve a robust reformulation of the JCC-OPF problem. Esteban-Pérez and Morales [40] introduce a distributionally robust JCC-OPF model that considers contextual information using an ambiguity set based on probability trimmings. To make their model tractable, they resort to the widely known CVaR-based approximation of the JCC.

The aforementioned SAA method is another effective way to solve JCCPs and has the potential to identify OPF solutions with a better cost performance than that of the more conservative solutions delivered by the previous approaches. However, solving the JCC-OPF problem using SAA is challenging due to the presence of binary variables, the number of scenarios required and the size of the power systems. Lejeune and Dehghanian [44] propose a methodology to solve the SAA of the JCC-OPF without including the power flow equations into the joint chance-constraint system. To the best of our knowledge, we are the first to efficiently solve the JCC-OPF problem by means of the SAA approach, using a MIP reformulation and including the arduous power flow constraints. Furthermore, unlike the sample-based approach introduced in [39], which is based on a smooth nonlinear approximation of the JCC-OPF, ours offers optimality guarantees.

The performance of SAA is, nonetheless, directly contingent on the number of samples available. In particular, we refer the reader to the article by [93], where relations are established between the empirical acceptable probability of violation and the number of samples such that the SAA-based solution be feasible in the JCCP with a predefined confidence level. Statistical considerations apart, the main aim of this work is to prove that the proposed methodology leads to a substantial reduction of the computational burden of JCCPs addressed by a MIP SAA-based reformulation.

The main contribution of our work is the introduction of a new methodology to efficiently solve the SAA reformulation of the JCC-OPF. Our method solves the MIP to optimality, and is based on the combination of a tightening-and-screening procedure

with the development of valid inequalities to obtain a formulation which is compact and tight at a time. We begin with a description of an iterative algorithm to strengthen the Big-Ms present in the mixed-integer reformulation of the JCC-OPF. Interestingly, although the procedure is not new (see [85]), we complement it with a screening procedure that allows us to eliminate an enormous percentage of the line and generator inequalities of the MIP. The screening procedure is possible due to the special features of our model, decisive to speed up the resolution of the instances proposed and, to the best of our knowledge, has not been applied to other CCPs before. Next, we introduce a new set of valid inequalities designed to strengthen the linear relaxation of the model. As for their structure, each valid inequality is developed using quantile information and avoiding the use of Big-M constants, which are known to lead to weak linear relaxation bounds.

Finally, we test our resolution method through extensive computational results using standard power systems available in the related literature. The combination of the valid inequalities with the tightening of the Big-Ms and the screening procedure allows us to effectively solve to optimality instances that are not solved with the initial MIP formulation, since the combination of both techniques ostensibly reduces their size and difficulty. We also compare our resolution approach with state-of-the-art convex inner approximations of CCPs, in particular, the CVaR-based approximation, ALSO-X, and ALSO-X+ [74].

The chapter is organized as follows. In Section 3.2 we introduce the main notation and the formulation of the JCC-OPF, the core problem of this work. Section 3.3 involves the reformulation of the problem into a MIP using the SAA approach and the proposed methodology: Subsection 3.3.1 describes the tightening and screening procedures, whereas Subsection 3.3.2 introduces the valid inequalities and the necessary algorithms to compute them. In Section 3.4 we present a case study, testing our results to solve instances of the OPF available in the literature. Section 3.5 points further research topics and includes some concluding remarks.

## 3.2 Mathematical Formulation

This section presents a standard and well-known formulation of the JCC-OPF problem. To do so, we introduce the following notation and modeling choices:

1. *Power system*: A power system consists of a set of buses (nodes), lines and generators which we denote by  $\mathcal{N}$ ,  $\mathcal{L}$  and  $\mathcal{G}$ , in that order. We use indexes  $n$ ,  $l$  and  $g$  to refer to elements in these sets, respectively. Furthermore,  $\mathcal{G}_n$  represents the set of generators connected to node  $n$ .
2. *Nodal net demands*: The (uncertain) electricity net demand at node  $n$ ,  $\tilde{d}_n$ , is

given by  $\tilde{d}_n = d_n - \omega_n$ , where  $d_n$  is the predicted value and  $\omega_n$  is the forecast error with a change of sign. This error is modeled as a random variable with zero mean which follows an unknown continuous probability distribution.

3. *Generation*: The system-wide aggregate forecast error, which is given by  $\Omega = \sum_{n \in \mathcal{N}} \omega_n$ , is balanced by the dispatchable generators through the deployment of reserve. The reserve deployment follows an affine control policy, modeling the actions of the *automatic generation control* (AGC). According to this policy, the reserve provided by the generator  $g$  is given by  $r_g(\omega) = -\beta_g \Omega$ , where  $\beta_g$  is the participation factor of unit  $g$ ; and, consequently,  $\sum_{g \in \mathcal{G}} \beta_g = 1$ . Thus, the generators' power output is adjusted in the following way:

$$\tilde{p}_g = p_g - \beta_g \Omega, \quad \forall g \in \mathcal{G},$$

where  $p_g$  is the power output dispatch of generating unit  $g$ , respectively (see, e.g., [36, 38–40]). The minimum and maximum power capacity of generator  $g$  is denoted by  $\underline{p}_g$  and  $\bar{p}_g$ , respectively.

4. *Power balance*: Given the affine control policy of the previous point, the power balance equation takes the following form:

$$\sum_{g \in \mathcal{G}} \tilde{p}_g - \sum_{n \in \mathcal{N}} \tilde{d}_n = \sum_{g \in \mathcal{G}} (p_g - \beta_g \Omega) - \sum_{n \in \mathcal{N}} (d_n - \omega_n) = 0.$$

Hence, to ensure the power balance for *any* realization of the forecast errors  $(\omega_n)_{n \in \mathcal{N}}$ , it must hold:

$$\begin{aligned} \sum_{g \in \mathcal{G}} p_g - \sum_{n \in \mathcal{N}} d_n &= 0 \\ \sum_{g \in \mathcal{G}} \beta_g &= 1. \end{aligned}$$

5. *Power flows*: Line flows are modeled using the well-known approximation based on the power transfer distribution factors (PTDFs),  $B_{ln}$ ,  $l \in \mathcal{L}$ ,  $n \in \mathcal{N}$ , which sets a linear relation between the power flow through line  $l$  and the power injected at node  $n$ . The maximum capacity of line  $l$  is denoted by  $\bar{f}_l$ .
6. *Power production cost*: The cost function of each generating unit is assumed to be quadratic and, as a result, the total power production cost is given by

$$\sum_{g \in \mathcal{G}} c_g^2 (p_g - \Omega \beta_g)^2 + c_g^1 (p_g - \Omega \beta_g) + c_g^0,$$

where  $c_g^2$ ,  $c_g^1$ ,  $c_g^0$  are the coefficients defining the quadratic cost function of generating unit  $g$ . On the assumption that  $\omega_n$ , for each  $n \in \mathcal{N}$ , is a random variable with zero mean, we have (see, for instance, [39])

$$\mathbb{E} \left[ \sum_{g \in \mathcal{G}} c_g^2 (p_g - \Omega \beta_g)^2 + c_g^1 (p_g - \Omega \beta_g) + c_g^0 \right] = \sum_{g \in \mathcal{G}} c_g^2 p_g^2 + c_g^1 p_g + c_g^0 + \mathbb{V}(\Omega) c_g^2 \beta_g^2,$$

where  $\mathbb{V}(\Omega)$  denotes the variance of the random variable  $\Omega$ .

With the above ingredients, the JCC-OPF problem that we tackle in this chapter is formulated as follows:

$$\min_{p_g, \beta_g} \sum_{g \in \mathcal{G}} c_g^2 p_g^2 + c_g^1 p_g + c_g^0 + \mathbb{V}(\Omega) c_g^2 \beta_g^2 \quad (3.2a)$$

$$\text{s.t.} \quad \sum_{g \in \mathcal{G}} \beta_g = 1 \quad (3.2b)$$

$$\beta_g \geq 0, \quad \forall g \in \mathcal{G} \quad (3.2c)$$

$$\sum_{g \in \mathcal{G}} p_g - \sum_{n \in \mathcal{N}} d_n = 0 \quad (3.2d)$$

$$\underline{p}_g \leq p_g \leq \bar{p}_g, \quad \forall g \in \mathcal{G} \quad (3.2e)$$

$$-\bar{f}_l \leq \sum_{n \in \mathcal{N}} B_{ln} \left( \sum_{g \in \mathcal{G}_n} p_g - d_n \right) \leq \bar{f}_l, \quad \forall l \in \mathcal{L} \quad (3.2f)$$

$$\mathbb{P} \left( \begin{array}{l} \underline{p}_g \leq p_g - \Omega \beta_g \leq \bar{p}_g, \quad \forall g \in \mathcal{G} \\ -\bar{f}_l \leq \sum_{n \in \mathcal{N}} B_{ln} \left( \sum_{g \in \mathcal{G}_n} (p_g - \Omega \beta_g) + \omega_n - d_n \right) \leq \bar{f}_l, \quad \forall l \in \mathcal{L} \end{array} \right) \geq 1 - \epsilon. \quad (3.2g)$$

The objective (3.2a) is the minimization of the expected total generation cost. The constraints (3.2b), (3.2c) and (3.2d) enforce the power balance in the system, whereas constraints (3.2e) and (3.2f) ensure a feasible power dispatch which corresponds to an error-free scenario, i.e., to a realization of the net-load forecast errors such that  $\omega_n = 0$ ,  $\forall n \in \mathcal{N}$ . Finally, expression (3.2g) constitutes the joint chance-constraint system by which the decision-maker states that the OPF solution must be feasible with a probability greater than or equal to  $1 - \epsilon$ . Accordingly, parameter  $\epsilon$  is the maximum allowed probability of constraint violation set by the user. Formulation (3.2) is quite standard and has been used before by [36, 38, 39], among others.

Problem (3.2) can be written in the form of (3.1), i.e., as a CCP with linear JCC and random RHS and LHS. To see this, define the vector of continuous decision variables  $x$  in (3.1) as  $x := (p_g, \beta_g)_{g \in \mathcal{G}}$ , and group all these variables by means of the set  $\mathcal{I}$  with elements  $i$  running from 1 to  $|\mathcal{I}| = 2|\mathcal{G}|$ . In this way, we have that  $x \in \mathbb{R}_+^{|\mathcal{I}|}$ , the set  $X \subseteq \mathbb{R}^{|\mathcal{I}|}$  represents the polyhedron defined by the deterministic constraints (3.2b)–(3.2f), and  $f : \mathbb{R}^{|\mathcal{I}|} \rightarrow \mathbb{R}$  is the convex function providing the expected total

generation cost (3.2a). Likewise, if we collect all the constraints involved in the joint chance-constraint system (3.2g) into the set  $\mathcal{J}$  (hence  $|\mathcal{J}| = 2|\mathcal{G}| + 2|\mathcal{L}|$ ), this system can be represented by way of a technology matrix with random rows  $a_j(\boldsymbol{\omega}) \in \mathbb{R}^{|\mathcal{I}|}$ ,  $j \in \mathcal{J}$ , and random RHS  $b_j(\boldsymbol{\omega}) \in \mathbb{R}$ ,  $j \in \mathcal{J}$ , where the uncertainty is again represented through the random vector  $\boldsymbol{\omega}$  taking values in  $\mathbb{R}^{|\mathcal{M}|}$ .

### 3.3 Solution via Sample Average Approximation

As discussed in Section 3.1, the CCP (3.2) can be easily reformulated into a MIP using SAA. Thus, we assume that  $\boldsymbol{\omega}$  has a finite discrete support defined by a collection of points  $\{\boldsymbol{\omega}_s \in \mathbb{R}^{|\mathcal{M}|}, s \in \mathcal{S}\}$  and respective probability masses  $\mathbb{P}(\boldsymbol{\omega} = \boldsymbol{\omega}_s) = \frac{1}{|\mathcal{S}|}$ ,  $\forall s \in \mathcal{S} = \{1, \dots, |\mathcal{S}|\}$ . Accordingly,  $\omega_{ns}$  and  $\Omega_s$  are realizations of the respective random variables under scenario  $s$ . We define  $q = \lfloor \epsilon |\mathcal{S}| \rfloor$ , the vector  $y$  of binary variables  $y_s$ ,  $\forall s \in \mathcal{S}$ , and the large enough constants  $M_{gs}^1, M_{gs}^2, M_{ls}^3, M_{ls}^4$ . Thus, the MIP reformulation of problem (3.2) writes as follows:

$$\min_{p_g, \beta_g, y_s} \sum_{g \in \mathcal{G}} c_g^2 p_g^2 + c_g^1 p_g + c_g^0 + \widehat{\mathbb{V}}(\Omega) c_g^2 \beta_g^2 \quad (3.3a)$$

$$\text{s.t.} \quad (3.2b) - (3.2f) \quad (3.3b)$$

$$p_g - \Omega_s \beta_g \geq \underline{p}_g - y_s M_{gs}^1, \quad \forall g \in \mathcal{G}, s \in \mathcal{S} \quad (3.3c)$$

$$p_g - \Omega_s \beta_g \leq \bar{p}_g + y_s M_{gs}^2, \quad \forall g \in \mathcal{G}, s \in \mathcal{S} \quad (3.3d)$$

$$\sum_{n \in \mathcal{N}} B_{ln} \left( \sum_{g \in \mathcal{G}_n} (p_g - \Omega_s \beta_g) - d_n + \omega_{ns} \right) \geq -\bar{f}_l - y_s M_{ls}^3, \quad \forall l \in \mathcal{L}, s \in \mathcal{S} \quad (3.3e)$$

$$\sum_{n \in \mathcal{N}} B_{ln} \left( \sum_{g \in \mathcal{G}_n} (p_g - \Omega_s \beta_g) - d_n + \omega_{ns} \right) \leq \bar{f}_l + y_s M_{ls}^4, \quad \forall l \in \mathcal{L}, s \in \mathcal{S} \quad (3.3f)$$

$$\sum_{s \in \mathcal{S}} y_s \leq q \quad (3.3g)$$

$$y_s \in \{0, 1\}, \quad \forall s \in \mathcal{S}. \quad (3.3h)$$

Constraints (3.3c)-(3.3f) represent the sample-based reformulation of the joint chance constraint (3.2g). For a given scenario  $s \in \mathcal{S}$ , inequalities (3.3c)-(3.3f) guarantee that all the original constraints are satisfied when  $y_s = 0$ . If  $y_s = 1$ , some of the original constraints can be violated for scenario  $s$ . Finally, the inequality (3.3g) ensures that the probability of the JCC is met and the binary character of variables  $y_s$  is declared in (3.3h).

For simplicity and ease of notation, we reformulate model (3.3) as

$$\min_x f(x) \quad (3.4a)$$

$$\text{s.t.} \quad x \in X \quad (3.4b)$$

$$a_{js}^\top x \leq b_{js} + M_{js} y_s, \quad \forall j \in \mathcal{J}, s \in \mathcal{S} \quad (3.4c)$$

$$\sum_{s \in \mathcal{S}} y_s \leq q \quad (3.4d)$$

$$y_s \in \{0, 1\}, \quad \forall s \in \mathcal{S}, \quad (3.4e)$$

where  $x := (p_g, \beta_g)_{g \in \mathcal{G}}$ , the deterministic feasible set  $X$  represents constraints (3.2b)-(3.2f), and constraint (3.4c) is a generalization of constraints (3.3c)-(3.3f). Using the generic formulation (3.4), we present in Subsection 3.3.1 a procedure to properly tune the values of the large constants  $M_{js}$ . We also explain in this subsection how the intermediate results of the tightening procedure can be efficiently used to remove constraints from set (3.4c) that are superfluous, thus making model (3.4) more compact. Finally, we introduce in Subsection 3.3.2 a set of valid inequalities that makes the linear relaxation of (3.4) remarkably tighter.

### 3.3.1 Tightening and Screening

It is well-known that the linear relaxation of a Big-M formulation tends to provide weak lower bounds in general [94]. This is even more so when the Big-Ms are chosen too loose. Constants  $M_{js}$  in (3.4c) should be set large enough for the corresponding constraints to be redundant when the associated binary variables  $y_s$  are equal to 1, and *as small as possible* to tighten the MIP formulation. To this end, Qiu *et al.* [85] provide an algorithm called “Iterative Coefficient Strengthening” that has been successfully applied to other CCPs [89]. A customization of this procedure for the joint chance-constrained formulation (3.4) is detailed in Algorithm 3.1.

---

#### Algorithm 3.1 Iterative Coefficient Strengthening

---

**Input:** The LHS and RHS vectors  $\{a_{js}\}_{j \in \mathcal{J}, s \in \mathcal{S}}$  and coefficients  $\{b_{js}\}_{j \in \mathcal{J}, s \in \mathcal{S}}$ , respectively, parameter  $q$  related to the allowed violation probability, the deterministic feasible set  $X$ , and the total number of iterations  $\kappa$ .

**Output:** The large constants  $M_{js}, \forall j \in \mathcal{J}, s \in \mathcal{S}$ .

Step 1. Initialization,  $k = 0$ ,  $M_{js}^0 = \infty, \forall j \in \mathcal{J}, s \in \mathcal{S}$ .

Step 2. For each  $j \in \mathcal{J}$  and  $s \in \mathcal{S}$  update  $M_{js}^{k+1}$  as follows: If  $M_{js}^k < 0$ , then  $M_{js}^{k+1} = M_{js}^k$ . Otherwise,

$$M_{js}^{k+1} = \max_{x, y_s} a_{js}^\top x - b_{js} \quad (3.5a)$$

$$\text{s.t. } x \in X \quad (3.5b)$$

$$a_{js}^\top x - b_{js} \leq M_{js}^k y_s, \quad \forall j \in \mathcal{J}, s \in \mathcal{S} \quad (3.5c)$$

$$\sum_{s \in \mathcal{S}} y_s \leq q \quad (3.5d)$$

$$0 \leq y_s \leq 1, \quad \forall s \in \mathcal{S}. \quad (3.5e)$$

Step 3. If  $k + 1 < \kappa$ , then  $k = k + 1$  and go to Step 2. Otherwise, stop.

---

The output of Algorithm 3.1 is the tuned Big-Ms that are input to the MIP reformulation (3.4). This algorithm produces Big-Ms whose value either decreases or remains equal at each iteration. There is, in fact, a number of iterations beyond which the resulting Big-Ms converge. To reduce the computational burden of running Algorithm 3.1, all problems (3.5) in Step 2 can be solved in parallel. Hereinafter, we use the short name “ $\mathbf{T}(\kappa)$ ” (from “Tightening”) to refer to the solution of model (3.4) using the Big-M values given by the “Iterative Coefficient Strengthening” algorithm with  $\kappa$  iterations.

Equally important, Algorithm 3.1 can be easily upgraded to delete constraints  $(j, s)$  in (3.4c) that are redundant, and therefore, can be removed from problem (3.4). Indeed, if Algorithm 3.1 delivers a large constant  $M_{js} \leq 0$ , then constraint  $j$  in scenario  $s$  can be deleted from (3.4) without altering its feasible region or its optimal solution. This is so because a non-positive  $M_{js}$  means that there is no  $x$  satisfying (3.5b)–(3.5e) such that the constraint takes on a value strictly greater than zero. Consequently, the constraint is redundant in (3.4), since the feasibility region of (3.5) is a relaxation of (3.4). This upgrade of method  $\mathbf{T}$  not only makes formulation (3.4) tighter through coefficient strengthening, but also more compact by screening out redundant constraints. Naturally, the tightening and screening power of algorithm  $\mathbf{T}$  increases at each iteration. From now on, we use the short name “ $\mathbf{TS}(\kappa)$ ” (from “Tightening and Screening”) to refer to the strategy whereby model (3.4) is solved without the constraints (3.4c) for which the value of  $M_{js}$  provided by Algorithm 3.1 after  $\kappa$  iterations is lower than or equal to 0.

While strengthening the parameters  $M_{js}$  is a common strategy in the technical literature to reduce the computational burden of CCPs, this is the first time, to our knowledge, that intermediate results of Algorithm 3.1 are used to eliminate superfluous constraints from model (3.4). We stress that the screening process itself comes at no cost from Algorithm 3.1, while removing superfluous constraints from (3.4) may substantially facilitate its solution. As we show in Section 3.4, this is particularly true for the JCC-OPF.

Apart from making formulation (3.4) more compact, the screening of superfluous constraints can also be used to accelerate the “Iterative Coefficient Strengthening” process at each iteration. To do so, it suffices to modify Algorithm 3.1 so that (3.5c) only includes the constraints for which  $M_{js}^k > 0$ . Thus, the number of constraints of model (3.5) is significantly reduced and so is its solution time.

### 3.3.2 Valid inequalities

In this section, we propose valid inequalities that apply to JCCPs with a special structure as the OPF problem (3.2). Indeed, each row  $a_j(\boldsymbol{\omega})$  in the technology matrix of (3.1) can be rewritten as  $a_j(\boldsymbol{\omega}) = a_j^0 + \Omega_j(\boldsymbol{\omega})\hat{a}_j$ , with  $a_j^0, \hat{a}_j \in \mathbb{R}^{|\mathcal{I}|}$  and where  $\Omega_j(\boldsymbol{\omega}_s) = \Omega_{js}$

is a real-valued function whose domain includes the support of  $\omega$ . In other words, we derive a set of valid inequalities to make the linear relaxation of problem

$$\min_{x, y_s} f(x) \quad (3.6a)$$

$$\text{s.t. } x \in X \quad (3.6b)$$

$$\Omega_{js} \hat{a}_j^\top x - b_{js} + x^\top a_j^0 \leq M_{js} y_s, \quad \forall j \in \mathcal{J}, s \in \mathcal{S} \quad (3.6c)$$

$$\sum_{s \in \mathcal{S}} y_s \leq q \quad (3.6d)$$

$$y_s \in \{0, 1\}, \quad \forall s \in \mathcal{S} \quad (3.6e)$$

tighter. Note that we do not make any assumptions on the sign of  $\hat{a}_j^\top$ ,  $b_{js}$  and  $a_j^0$ . Furthermore, these valid inequalities can also be added to the constraint set (3.5) of Algorithm 3.1, thus dramatically increasing the tightening and screening power of **TS**. To facilitate the comparative analysis carried out in Section 3.4, the so upgraded algorithm is named “**TS+V**( $\kappa$ )” (from “Tightening and Screening with Valid inequalities”).

To derive the set of valid inequalities for problem (3.6), we define the real variables  $z_j \in \mathbb{R}$  as  $z_j := \hat{a}_j^\top x$ , and let  $z_j^d = \inf_{x \in X} \hat{a}_j^\top x$ ,  $z_j^u = \sup_{x \in X} \hat{a}_j^\top x$  denote the lower and upper bounds on  $z$  induced by the polyhedral feasibility set (3.6b). Let us also define the function  $L_{js} : f_{js}(z_j) = \Omega_{js} z_j - b_{js}$  for  $z_j \in [z_j^d, z_j^u]$  and the set of functions  $\mathcal{L}_j := \{L_{js}, \forall s \in \mathcal{S}\}$ . The valid inequalities we propose are heavily supported by the concepts of *k-lower* and *k-upper envelopes*, which we define in the following.

**Definition 3.1.** For a given line  $L_{js}$ , we say that the point  $(\tilde{z}, \tilde{t}) \in \mathbb{R}^2$  lies below, on or above function  $L_{js}$  depending on whether  $\tilde{t} < \Omega_{js} \tilde{z} - b_{js}$ ,  $\tilde{t} = \Omega_{js} \tilde{z} - b_{js}$  or  $\tilde{t} > \Omega_{js} \tilde{z} - b_{js}$ , respectively. Naturally, we also say that function  $L_{js}$  lies above, contains, or lies below point  $(\tilde{z}, \tilde{t})$  in these cases. We also say that a point  $(\tilde{z}, \tilde{t})$  belongs to the set of lines  $\mathcal{L}_j$  if there exists a line  $L_{js} \in \mathcal{L}_j$  that contains the point  $(\tilde{z}, \tilde{t})$ .

**Definition 3.2.** For a set of lines  $\mathcal{L}_j$ , the lower (resp. upper) score of a point is the number of lines in  $\mathcal{L}_j$  that lie below (resp. above) that point. The *k-lower* (resp. *k-upper*) envelope of a set of lines  $\mathcal{L}_j$  is the closure of the set of points that belong to  $\mathcal{L}_j$  and that have lower (resp. upper) score equal to  $k - 1$ . The *k-lower envelope* is also known as *k-level*.

For the sake of illustration, Figure 3.1 shows in bold the 5-upper envelope of a set of 8 lines. Clearly, the *k-envelopes* of sets  $\mathcal{L}_j$  can be seen as piece-wise linear functions on  $z_j$ .

**Proposition 3.1.** For a fixed  $j \in \mathcal{J}$ , let  $U_j^{q+1}(\cdot)$  be the  $(q+1)$ -upper envelope of the set of lines  $\mathcal{L}_j$ , with  $q = \lfloor \epsilon |\mathcal{S}| \rfloor$ . Then the inequality

$$U_j^{q+1}(\hat{a}_j^\top x) + x^\top a_j^0 \leq 0, \quad x \in X \quad (3.7)$$

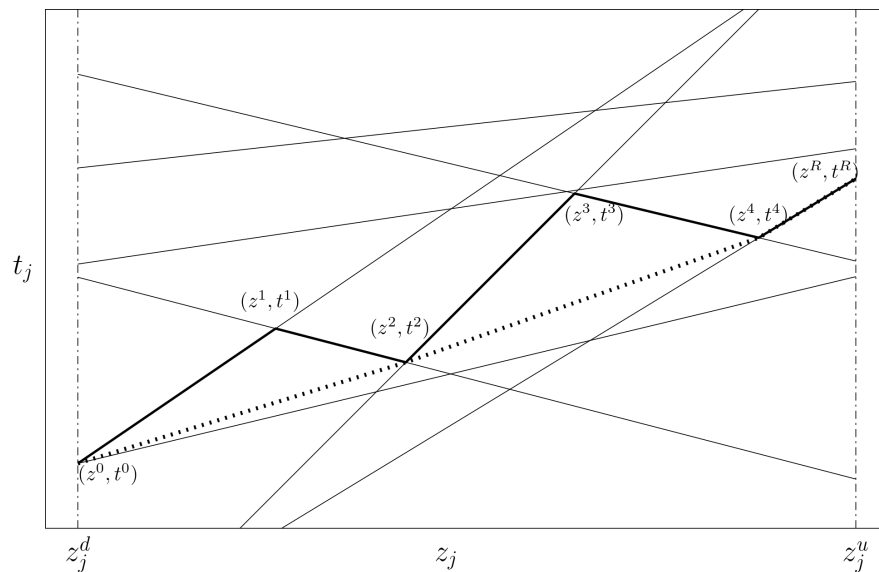


Figure 3.1: In bold, the 5-upper envelope (4-lower envelope, 4-level) of a set  $\mathcal{L}_j$  of 8 lines in the plane. In dotted, the lower hull of the 5-upper envelope

is valid for problem (3.6).

**Proof 3.1.** Let  $\bar{x}, \bar{y}$  be any feasible solution of problem (3.6) with  $\bar{z}_j = \hat{a}_j^\top \bar{x} \in [z_j^d, z_j^u]$ , and suppose that  $U_j^{q+1}(\bar{z}_j) + \bar{x}^\top a_j^0 > 0$ . By definition of  $k$ -upper envelope, there exist  $q + 1$  lines in  $\mathcal{L}_j$ ,  $L_{js_i} : f_{js_i}(z_j) = \Omega_{js_i} z_j - b_{js_i} \forall i \in \{1, \dots, q + 1\}$  such that  $f_{js_i}(\bar{z}_j) = \Omega_{js_i} \bar{z}_j - b_{js_i} \geq U_j^{q+1}(\bar{z}_j)$ . Then for  $i \in \{1, \dots, q + 1\}$  it holds that  $\Omega_{js_i} \bar{z}_j - b_{js_i} + \bar{x}^\top a_j^0 > 0$ . Substituting in constraint (3.6c), we obtain that  $\bar{y}_{s_i} M_{s_i} > 0 \Rightarrow \bar{y}_{s_i} = 1$ , for  $i \in \{1, \dots, q + 1\}$ . But then constraint (3.6d) is not satisfied, since  $\sum_{s \in \mathcal{S}} \bar{y}_s \geq \sum_{i=1}^{q+1} \bar{y}_{s_i} = q + 1 > q$ . This is, however, in contradiction with our initial statement that  $\bar{x}, \bar{y}$  is a feasible solution of problem (3.6).

The technical literature already includes references that propose methodologies to determine the  $k$ -envelope of a set of linear functions. For instance, the authors of [95] give a basic algorithm for constructing  $k$ -envelopes called the Rider Algorithm. Essentially, this algorithm is based on the fact that the  $k$ -envelope is an unbounded polygonal chain that can be described by a sequence of vertices, which are intersections of lines of the set. In fact, every point in the  $k$ -envelope is contained in a given line. In this chapter, we adapt the algorithm proposed in [95] to the particular case in which  $z_j^d, z_j^u$  are finite. Algorithm 3.2 describes our procedure in detail for a general set of the type  $\mathcal{L}_j$ . To facilitate its comprehension, Fig. 3.2 offers, by means of a flowchart, a more intuitive explanation of how Algorithm 3.2 works.

The LHSs of the valid inequalities (3.7) are piece-wise linear functions not necessarily convex. Therefore, the inclusion of these inequalities into model (3.6) would require a significant amount of additional binary variables, which, in turn, is expected to increase

---

**Algorithm 3.2** Rider Algorithm to construct the  $k$ -upper envelope of  $\mathcal{L}_j$  (adapted to the bounded case)

---

To describe the  $k$ -upper envelope of a set of lines  $\mathcal{L}_j$ , we derive the sequence of vertices of the polygonal chain (intersections of lines in  $\mathcal{L}_j$ )  $((z^0, t^0), \dots, (z^R, t^R))$  with  $(z^d = z^0 < \dots < z^R = z^u)$ .

- Step 1. Set  $r = 0$ . Let  $\{(z_j^d, \Omega_{j_s} z_j^d - b_{j_s}), \forall s \in \mathcal{S}\}$ , be the intersections of the lines  $L_{j_s} \in \mathcal{L}_j$  with the vertical line  $z = z_j^d$ , and assume w.l.o.g. that all the points have different upper scores. Let  $s_0 \in \mathcal{S}$  be such that the intersection  $(z_j^d, \Omega_{j_{s_0}} z_j^d - b_{j_{s_0}})$  has upper score equal to  $k - 1$ . Then  $(z^0, t^0) = (z_j^d, \Omega_{j_{s_0}} z_j^d - b_{j_{s_0}})$ .
- Step 2. Compute the value of  $z_j$  for which the line  $L_{j_{s_r}}$  intersects the rest of the lines  $L_{j_s} \in \mathcal{L}_j$  as  $\text{int}_z(s, s_r) = \frac{b_{j_s} - b_{j_{s_r}}}{\Omega_{j_s} - \Omega_{j_{s_r}}}$ . If  $\exists s' : z^r < \text{int}_z(s', s_r) < z^u$ , go to Step 3. Otherwise, go to Step 4.
- Step 3. Find the line that intersects  $L_{j_{s_r}}$  at the leftmost point to the right of  $z^r$ , that is, find  $s_{r+1} = \arg \min_s \{\text{int}_z(s, s_r) : \text{int}_z(s, s_r) > z^r\}$ . Set  $(z^{r+1}, t^{r+1}) = (\text{int}_z(s_{r+1}, s_r), \Omega_{j_{s_r}} \text{int}_z(s_{r+1}, s_r) - b_{j_{s_r}})$ , update  $r = r + 1$  and go to Step 2.
- Step 4. Set  $(z^R, t^R) = (z_j^u, \Omega_{j_{s_r}} z_j^u - b_{j_{s_r}})$ .
- 

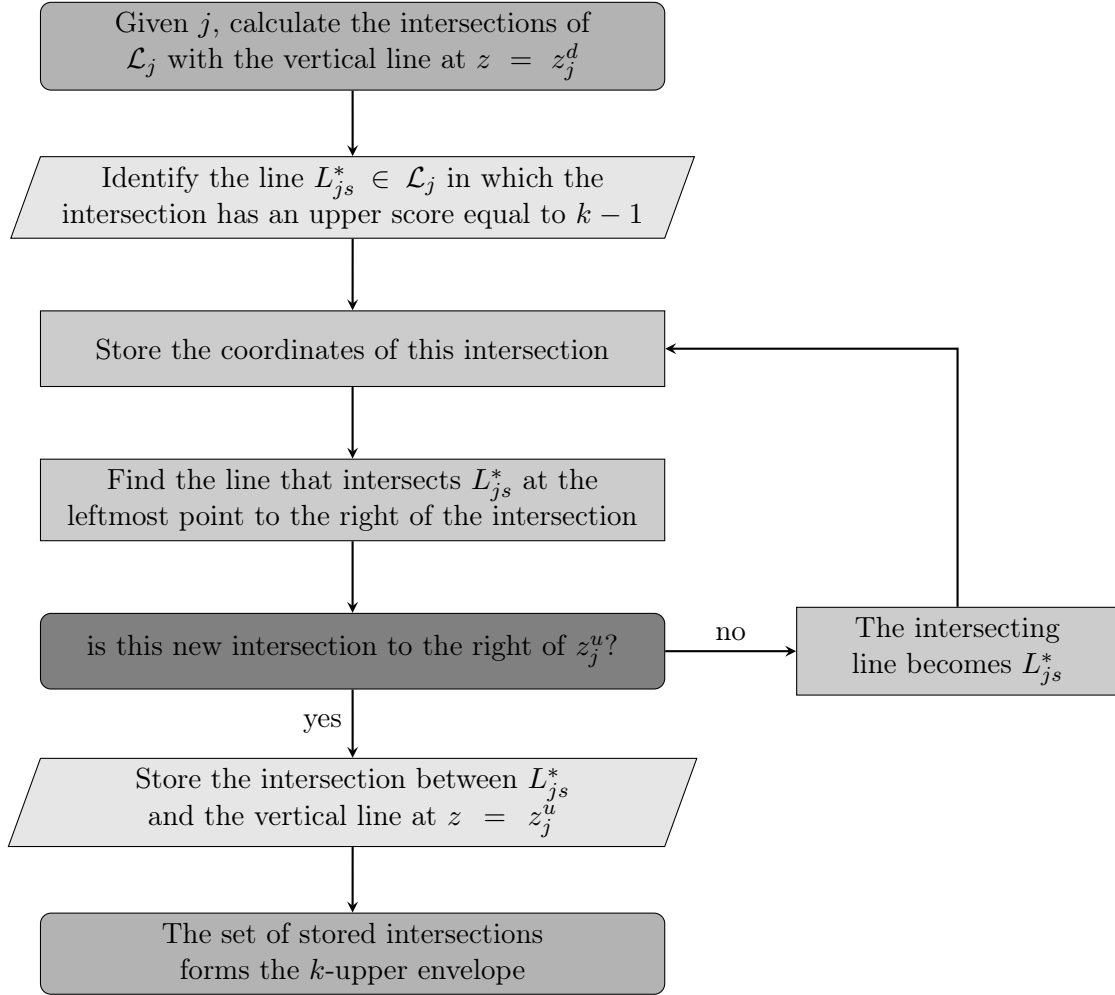


Figure 3.2: Flowchart representation of Algorithm 3.2

the computational burden of this problem even further. Alternatively, we compute the lower hull of the  $k$ -upper envelope of  $\mathcal{L}_j$ , which takes the form of a convex piece-wise linear function. From this lower hull, we can extract a set of linear valid inequalities (the linear extensions of the pieces) that can be seamlessly inserted into model (3.6) without the need of any extra binary variables. In doing so, we are able to tighten model (3.6), which can thus be solved more efficiently by available optimization software. Before presenting the set of valid inequalities, the following definition is required.

**Definition 3.3.** *Let  $Z$  be the convex hull of a set of points  $P$ . The upper (resp. lower) hull of  $P$  is the set of edges of  $Z$  that lie on or above (resp. on or below) every point in  $P$ .*

Corollary 3.1 presents the set of linear valid inequalities (3.8) given by the lower hull of the  $k$ -upper envelope of  $\mathcal{L}_j$ .

**Corollary 3.1.** *Let  $\{(z^r, t^r)\}$ ,  $r \in \{0, \dots, R\}$ , be the ordered set of vertices obtained by applying Algorithm 3.2 to set  $\mathcal{L}_j$ , and let  $\{(z^{r'}, t^{r'})\}$ ,  $r' \in \{0, \dots, R'\} \subseteq \{0, \dots, R\}$ , be the ordered subset of vertices such that the associated polygonal chain is the lower hull. Then the following linear inequalities*

$$\frac{t^{r'+1} - t^{r'}}{z^{r'+1} - z^{r'}}(\hat{a}_j^\top x - z^{r'}) + t^{r'} \leq -x^\top a_j^0, \quad x \in X, r' \in \{0, \dots, R' - 1\} \quad (3.8)$$

are valid for problem (3.6).

**Proof 3.2.** *The proof is straightforward, since for each  $x \in X$  it holds  $\frac{t^{r'+1} - t^{r'}}{z^{r'+1} - z^{r'}}(\hat{a}_j^\top x - z^{r'}) + t^{r'} \leq U_j^{q+1}(\hat{a}_j^\top x) \leq -x^\top a_j^0$ , by hypothesis and using (3.7).*

There exist plenty of algorithms of convexification of a set of points in the plane. Two of the most well-known are the *Jarvis march* and the *Graham scan* [96]. Here, we give a simplified version of the former where we make use of special features of our set of points and only compute the lower hull. In particular, we assume that we have a set of presorted points  $\{(z^r, t^r)\}$ ,  $r \in \{0, \dots, R\}$  whose first and last points always belong to the hull. To speed up the process, we can find the point  $(z^{\bar{r}}, t^{\bar{r}})$  from the previous set with the lowest  $t$ -coordinate (which always belongs to the lower hull), and then apply the algorithm to the subsets  $\{(z^0, t^0), \dots, (z^{\bar{r}}, t^{\bar{r}})\}$  and  $\{(z^{\bar{r}}, t^{\bar{r}}), \dots, (z^R, t^R)\}$ . Algorithm 3.3 describes in detail the proposed convexification procedure.

Algorithm 3.2 constructs the  $k$ -upper envelope of  $\mathcal{L}$  in  $O(n_k \log^2 |\mathcal{L}|)$  time and  $O(n_k |\mathcal{L}| + |\mathcal{L}|)$  space, where  $n_k$  denotes the maximum number of edges of the  $k$ -upper envelope of any set with  $|\mathcal{L}|$  lines (see [97]). An upper bound on  $n_k = O(|\mathcal{L}| k^{\frac{1}{2}})$  can be found in [98]. Authors of [99–101] have subsequently improved the upper bound of the complexity of this problem by studying a closely related problem, the  $k$ -set problem, in the two-dimensional case. As for the Jarvis March Algorithm, in the two-dimensional case presented here it has running time  $O((R + 2)(R' + 1))$  [96].

---

**Algorithm 3.3** Jarvis March Algorithm to obtain the lower hull of a set of presorted points  $P$

---

Let  $P = \{(z^r, t^r)\}$ ,  $r \in \{0, \dots, R\}$  be a set of points with  $z^0 < \dots < z^R$ . The algorithm derives a subset  $P' = \{(z^{r'}, t^{r'})\}$ ,  $r' \in \{0, \dots, R'\} \subseteq \{0, \dots, R\}$ , which constitutes the lower hull of the first set.

Step 1. Initially, set  $P' = \{(z^0, t^0)\}$ .

Step 2. Assume  $(z^{r'}, t^{r'})$  is the last point included in  $P'$ . If  $r' = R$ , the lower hull of  $P$  is given by the set of points  $P'$ . Otherwise, let  $r' + 1 := \arg \min_r \left\{ \frac{t^r - t^{r'}}{z^r - z^{r'}} : (z^r, t^r) \in P \text{ with } z^r > z^{r'} \right\}$ . Update  $P' = P' \cup \{(z^{r'+1}, t^{r'+1})\}$ . Repeat Step 2.

---

Valid inequalities (3.7) and Algorithms 3.2 and 3.3 can be generalized to work with finite discrete distributions with unequal probabilities. Observe that the definition of the  $(q+1)$ -lower (resp.  $(q+1)$ -upper) envelope is based on satisfying constraint (3.6d). In this extension, constraint (3.6d) is replaced with  $\sum_{s \in \mathcal{S}} \gamma_s y_s \leq \epsilon$ , where  $\gamma_s$  is the probability of scenario  $s$ . Hence, it suffices to redefine the lower (resp. upper) score of a point as the *probability of the lines* that lie below (resp. above) that point, and modify the definition of  $k$ -lower (resp. upper) envelope and Step 3 of Algorithm 3.2 accordingly, so that this more general constraint is satisfied.

### 3.4 Numerical Experiments

This section discusses a series of numerical experiments with which we evaluate the different approaches presented in Section 3.3 to solve the SAA-based MIP reformulation of the JCC-OPF. In particular, we compare the performance of approaches **T**, **TS** and **TS+V** using five standard power systems widely employed in the technical literature on the topic, namely the IEEE-RTS-24, IEEE-57, IEEE-RTS-73, IEEE-118, and IEEE-300 test systems. All data pertaining to these systems are publicly available in the repository [102] under version 21 and their main features are listed in Table 3.1. All optimization problems have been solved using GUROBI 9.1.2 [103] on a Linux-based server with CPUs clocking at 2.6 GHz, 6 threads and 32 GB of RAM. In all cases, the optimality GAP has been set to  $10^{-9}$  and the time limit to 10 hours.

Table 3.1: Short Description of Test Power Systems

	IEEE-RTS-24	IEEE-57	IEEE-RTS-73	IEEE-118	IEEE-300
# Nodes	24	57	73	118	300
# Generators	32	4	96	19	57
# Lines	38	41	120	186	411

Similarly to [39], we assume that the error of net loads is normally distributed, i.e.,  $\omega \sim N(\mathbf{0}, \Sigma)$ , where  $\mathbf{0}$  and  $\Sigma$  represent, respectively, the zero vector and the covariance

matrix. We also assume that the standard deviation of  $\omega_n$  at node  $n$  is proportional to the net nodal demand  $d_n$  according to a parameter  $\zeta$  between 0 and 1. Thus, this parameter controls the magnitude of net demand fluctuations. Under these assumptions, the procedure to model uncertainty proposed in [39] runs as follows. First, we compute the positive definite matrix  $C = \widehat{C}\widehat{C}^\top$  where each element of matrix  $\widehat{C}$  is a sample randomly drawn from a uniform distribution with support in  $[-1, 1]$ . Then, to obtain a positive definite matrix  $\Sigma$  in which the diagonal elements are equal to  $(\zeta d_n)^2$ , we define each of its entries  $(\sigma_{nn'})$  as follows:

$$\sigma_{nn'} = \zeta^2 \frac{c_{nn'}}{\sqrt{c_{nn}c_{n'n'}}} d_n d_{n'}, \quad \forall n, n' \in \mathcal{N}.$$

where  $c_{nn'}$  denotes the element of matrix  $C$  in row  $n$  and column  $n'$ . To avoid generating infeasible instances of the JCC-OPF problem, the parameter  $\zeta$  has been set to 0.15 for the four smallest systems and to 0.05 for the IEEE-300 system. To characterize the net demand uncertainty, we consider 1000 scenarios and a tolerable probability of violation of the joint chance constraint of 5% (i.e.,  $\epsilon = 0.05$  and  $q = 50$ ). Finally, each solution strategy is run for ten different sets of randomly generated samples. Accordingly, in this section we provide tables with figures averaged over these ten instances.

Table 3.2 includes the results of solving the mixed-integer quadratic optimization model (3.3) if the large constants  $M_{gs}^1$ ,  $M_{gs}^2$ ,  $M_{ls}^3$  and  $M_{ls}^4$  are set to a high enough arbitrary value, specifically  $10^4$ . Despite being remarkably computationally expensive, this approach has been used in the technical literature (e.g., [104]), and thus we refer to it as *benchmark approach* (**BN**). Table 3.2 includes the number of constraints in the model (**#CON**), the linear relaxation gap (**LR-GAP**) calculated using the optimal solution of each instance, the optimality gap given by the difference between the best lower bound and the best integer solution found by the MIP solver (**MIP-GAP**), the number of instances solved to global optimality in less than 10 hours (**#OPT**) and the solution time in seconds (**Time**). As expected, the computational time needed to solve the OPF with the Big-M model (3.3) increases significantly with the size of the instances. While the 10 instances from systems IEEE-RTS-24, IEEE-57 and IEEE-37 are solved in less than 10 hours, none of the instances for systems IEEE-118 and IEEE 300 are solved to global optimality within that time limit, and the average MIP-GAP after 10 hours amounts to 0.29% and 0.27%, respectively. Interestingly, despite the fact that the LR-GAP is relatively low for the IEEE-RTS-73 system, the average computational time required to solve this case is particularly high compared to the two smaller systems.

### 3.4.1 Impact of Tightening Big-Ms

As discussed in the technical literature, a proper tuning of the Big-Ms makes model (3.3) tighter and generally easier to solve [85] by the MIP routine. Therefore, we evaluate

Table 3.2: Benchmark approach (**BN**): Results

	IEEE-RTS-24	IEEE-57	IEEE-RTS-73	IEEE-118	IEEE-300
#CON	140143	168171	432435	410413	936939
LR-GAP	1.756%	0.623%	0.061%	0.956%	1.114%
MIP-GAP (#OPT)	0.00% (10)	0.00% (10)	0.00% (10)	0.29% (0)	0.27% (0)
Time (s)	1121.3	103.2	11161.2	36000.0	36000.0

the computational performance of the “Iterative Coefficient Strengthening” Algorithm and provide the corresponding results in Table 3.3. In particular, **T**(1), **T**(2) and **T**(3) represent the results obtained by solving model (3.3) with the Big-M values provided by Algorithm 3.1 with  $\kappa = 1, 2$  and  $3$ , respectively. Table 3.3 includes the average values of LR-GAP and MIP-GAP, the number of instances solved to optimality in less than 10 hours (#OPT), and the speedup factor with respect to the benchmark approach in those systems where all instances are solved in less than 10 hours. Note that the speedup factor considered is conservative since the IEEE-118 and IEEE-300 systems would spend more than 10 hours to be solved. To determine this factor, we have considered that the total computational time of approach **T** is given as the sum of the time required to run Algorithm 3.1  $\kappa$  times to determine the Big-Ms plus the time it takes to solve problem (3.3).

Table 3.3: Coefficient tightening approach (**T**): Results

		IEEE-RTS-24	IEEE-57	IEEE-RTS-73	IEEE-118	IEEE-300
LR-GAP	<b>T</b> (1)	1.755%	0.510%	0.061%	0.711%	0.472%
	<b>T</b> (2)	1.662%	0.330%	0.055%	0.522%	0.324%
	<b>T</b> (3)	1.386%	0.255%	0.029%	0.434%	0.264%
MIP-GAP (#OPT)	<b>T</b> (1)	0.00% (10)	0.00% (10)	0.00% (10)	0.27% (0)	0.16% (0)
	<b>T</b> (2)	0.00% (10)	0.00% (10)	0.03% (2)	0.16% (0)	0.09% (0)
	<b>T</b> (3)	0.00% (10)	0.00% (10)	0.00% (10)	0.12% (0)	0.07% (0)
Speedup factor	<b>T</b> (1)	0.22x	0.07x	0.61x	-	-
	<b>T</b> (2)	0.17x	0.13x	-	-	-
	<b>T</b> (3)	0.48x	0.24x	0.66x	-	-

Since reducing the Big-M values makes model (3.3) tighter, the results in Table 3.3 show lower values of LR-GAP with respect to **BN**. Furthermore, this effect grows with the number of iterations since Algorithm 3.1 ensures that the Big-Ms never increase between iterations. Although decreasing the values of the Big-Ms leads to tighter MIPs for all the test systems, the numerical results in Table 3.3 clearly indicate that computational savings are not guaranteed in all cases. Indeed, while the ten instances are solved by **BN** in less than 10 hours for the IEEE-RTS-73 system, **T**(2) only provides the optimal solution for two instances. On top of that, the speedup factors for the three smaller systems are always lower than 1, which means that the computational times ac-

tually increase in these cases. On the contrary, the average MIP-GAP of the two largest systems is significantly decreased with respect to **BN**. Therefore, we conclude that, due to the heuristics implemented in current commercial MIP solvers, the computational advantages that one could expect a priori from “Iterative Coefficient Strengthening” are not always guaranteed and are contingent on the structure and data of the problem.

### 3.4.2 Impact of Removing Redundant Constraints

Next, in Table 3.4 we provide the computational results related to the **TS** method, in which Algorithm 3.1 is extended to remove redundant constraints from model (3.3). Here, #CON is provided as the percentage of the number of constraints of the reference model **BN** (indicated in Table 3.2) that are retained by **TS** in each iteration. Table 3.4 also includes the average MIP-GAP, the number of instances solved to optimality and the average speedup factor in relation to **BN** when all instances are solved in less than 10 hours.

Table 3.4: Tightening and Screening (**TS**): Results

		IEEE-RTS-24	IEEE-57	IEEE-RTS-73	IEEE-118	IEEE-300
#CON	<b>TS</b> (1)	23.9%	2.8%	26.0%	8.9%	12.7%
	<b>TS</b> (2)	23.3%	2.2%	23.8%	6.3%	9.1%
	<b>TS</b> (3)	23.1%	2.1%	23.0%	5.6%	8.0%
MIP-GAP (#OPT)	<b>TS</b> (1)	0.00% (10)	0.00% (10)	0.00% (10)	0.15% (0)	0.08% (0)
	<b>TS</b> (2)	0.00% (10)	0.00% (10)	0.00% (10)	0.03% (2)	0.04% (0)
	<b>TS</b> (3)	0.00% (10)	0.00% (10)	0.00% (10)	0.01% (6)	0.01% (4)
Speedup factor	<b>TS</b> (1)	1.5x	1.8x	4.7x	-	-
	<b>TS</b> (2)	1.5x	3.8x	2.6x	-	-
	<b>TS</b> (3)	3.8x	4.4x	15.1x	-	-

Table 3.4 shows that the upgraded Algorithm 3.1 screens out a huge percentage of the constraints in model (3.3), only retaining between 2% and 26% of them. The results in this table demonstrate that combining the tightening of the Big-Ms and the elimination of superfluous constraints leads to significant computational savings. For instance, the speedup factor for the three smallest systems ranges now between 1.5x and 15.1x. In addition, **TS**(3) is able to solve six and four instances to optimality for systems IEEE-118 and IEEE-300, respectively, in less than 10 hours, and the average MIP-GAP is reduced to 0.01% in these two largest power systems. Therefore, the computational performance of model (3.3) has been drastically improved by combining the strengthening of the Big-Ms (making model (3.3) tighter) and the removal of redundant constraints (making model (3.3) more compact). Equally important, the elimination of superfluous constraints largely reduces the need of the MIP solver for RAM memory, which decreases from around 100 GB in **T** to 32 GB in **TS**.

### 3.4.3 Impact of Valid Inequalities

We continue the numerical experiments by evaluating the impact of including the valid inequalities derived in Section 3.3.2 into model (3.3). The so obtained results are collated in Table 3.5. In what follows, this approach is called **BN+V** for short. The results in Table 3.5 comprise, in order and following the previous notation, the average number of constraints, the average values of LR-GAP and MIP-GAP, the number of instances solved to optimality, and the average speedup factor with respect to the **BN** approach of Table 3.2 for those systems where all instances are solved before the time limit is reached.

Table 3.5: Tightening by valid inequalities (**BN+V**): Results

	IEEE-RTS-24	IEEE-57	IEEE-RTS-73	IEEE-118	IEEE-300
#CON	101.0%	101.2%	101.2%	101.6%	101.5%
LR-GAP	0.3374%	0.2038%	0.0001%	0.4784%	0.3192%
MIP-GAP (#OPT)	0.00% (10)	0.00% (10)	0.00% (10)	0.03% (1)	0.08% (0)
Speedup factor	46.4x	13.8x	65.2x	-	-

As can be seen, our valid inequalities only increase the total number of constraints by 1.0-1.6%. However, the LR-GAP is significantly reduced compared to that obtained by **BN**. This effect is particularly noticeable for the IEEE-RTS-73 system with an average value of the linear relaxation gap equal to 0.0001%, meaning that the linear relaxation of problem (3.3) with the proposed valid inequalities is very tight and its solution very close to the actual solution of that problem. Furthermore, the inclusion of the valid inequalities lead to average speedup factors that range between 13.8x and 65.2x for the three smallest systems. For the two largest systems, the time limit is reached in most instances, but the average MIP-GAP is reduced to 0.03% and 0.08%, respectively.

Finally, we present similar simulation results for the setup in which the valid inequalities are also used to boost the tightening and screening power of Algorithm 3.1 (that is, the valid inequalities are also included in problem (3.5)), leading to method **TS+V**. Table 3.6 provides the average number of constraints, the average values of LR-GAP and MIP-GAP, and the average speedup factor of **TS+V** with respect to **BN** in Table 3.2. Since increasing the number of iterations of Algorithm 3.1 barely affects the performance of **TS+V**, all the data shown in Table 3.6 correspond to  $\kappa = 1$ .

The comparison of the results in Tables 3.4, 3.5 and 3.6 yields the following observations. First, including the valid inequalities in Algorithm 3.1 strengthens the Big-Ms even further, which in turn remarkably reduces the linear relaxation gap and increases the number of constraints identified as redundant in model (3.3). Indeed, the total number of constraints eventually retained by **TS+V** ranges between 1.61% and 3.84% if compared with **BN**. Second, **TS+V** can solve the 10 instances to global optimality in

Table 3.6: Tightening and screening with valid inequalities (**TS+V**): Results

	IEEE-RTS-24	IEEE-57	IEEE-RTS-73	IEEE-118	IEEE-300
#CON	3.49%	1.61%	3.84%	2.68%	3.30%
LR-GAP	0.3365%	0.1519%	0.0001%	0.2821%	0.1603%
MIP-GAP (#OPT)	0.00% (10)	0.00% (10)	0.00% (10)	0.00% (10)	0.00% (10)
Speedup factor	706.8x	35.3x	1470.0x	23.1x	8.5x

less than 10 hours for the five test systems considered in these numerical experiments. In fact, the optimal solutions obtained by **TS+V** are the ones we use to compute the values of the linear relaxation gap throughout these simulations. Third, **TS+V** is able to achieve speedup factors between 8.5x and 1470.0x depending on the test system. All in all, **TS+V** features the best computational performance in terms of resolution time and MIP-GAP among all the methods tested so far.

#### 3.4.4 Comparison with an Exact Approach

In this section, we compare our solution approach with the one proposed in [105]. This author presents an exact approach to solve the SAA reformulation of CCPs based on the addition of quantile cuts in a so-called *lazy fashion* to a relaxation of the problem (3.3) that only includes the deterministic constraints. In this way, at each node of the branching tree we seek for a violated constraint from a scenario  $s$  with  $y_s = 0$ . Using the coefficients of this violated constraint, a valid inequality is derived by means of the resolution of  $|\mathcal{S}|$  linear separation subproblems. These strengthened cuts contain binary variables associated to several scenarios and are obtained by applying the *star inequalities* of [106].

We have implemented the procedure including, at each iteration, both the initial or *base* violated inequality and the strengthened one, since this approach delivered the best results. The comparison between our approach and the one proposed in [105] (which we name BCD for short, from *branch-and-cut decomposition*) is shown in Table 3.7. As can be seen, a similar number of constraints are generated in the BCD approach (that includes the deterministic constraints and the cuts generated dynamically). Furthermore, our procedure clearly outperforms the BCD approach in terms of computational time. One possible explanation, already pointed out in the paper, is that the generation of the cuts requires solving 1000 subproblems at each iteration. In the particular application presented in [105], however, this potential bottleneck is overcome by leveraging the specific structure of the subproblem to develop a closed-form expression of its solution, thus avoiding the need to optimize over all the scenario sets. With that said, we remark that the times provided in Table 3.7 under the acronym BCD-P correspond to a *parallel* implementation of the BCD algorithm, in which only the time required to solve

the most time-consuming subproblem out of the 1000 to be solved at each iteration is added to the final solution time reported. For completeness and because the *parallel* implementation of BCD using off-the-shelf optimization solvers is not trivial at all, we also report in Table 3.7 the speedup factor that is attained by a *serial* implementation of BCD, termed BCD-S in the table. As can be seen, this implementation is, however, far from being competitive in all cases.

Table 3.7: Comparison of the proposed **TS+V** approach and the BCD approach

		IEEE-RTS-24	IEEE-57	IEEE-RTS-73	IEEE-118	IEEE-300
#CONS	<b>TS+V</b>	3.49%	1.61%	3.84%	2.68%	3.30%
	BCD	11.37%	2.69%	3.58%	2.46%	1.53%
Speedup factor	<b>TS+V</b>	706.8x	35.3x	1470.0x	23.1x	8.5x
	BCD-P	10.12x	2.05x	69.00x	9.24x	4.74x
	BCD-S	0.12x	0.04x	0.30x	1.45x	0.42x

### 3.4.5 Comparison with Conservative Approximations

Next, in Table 3.8 the results of **TS+V** are contrasted with those provided by state-of-the-art approximations of joint chance-constraints available in the literature. In particular, we consider the CVaR-based and ALSO-X conservative approximations, including the improved version ALSO-X+, all described in [74]. Furthermore, inspired by ALSO-X, we propose a heuristic which works with the tighter and compacter formulation that **TS+V** produces and which is able to quickly identify good feasible solutions of problem (3.3). As ALSO-X, our heuristic works iteratively: It first relaxes the integrality of  $\mathbf{y}$  and then enters a loop whose core step is to perform a bisection search over parameter  $q$ . A pseudocode of this heuristic is provided in Algorithm 3.4.

---

#### Algorithm 3.4 Iterative heuristic

---

Input: Stopping tolerance parameter  $\delta$

**Require:** Relax the integrality of  $\mathbf{y}$  in (3.3)

$q \leftarrow 0, \bar{q} \leftarrow \lfloor \epsilon |\mathcal{S}| \rfloor$

**while**  $\bar{q} - q \geq \delta$  **do**

Set  $q = (q + \bar{q})/2$  and compute an optimal solution  $\mathbf{y}^*$  to (3.3).

Set  $\underline{q} = q$  if  $\mathbb{P}(\mathbf{y}^* = 0) \geq 1 - \epsilon$ ; otherwise,  $\bar{q} = q$

**end while**

Output: A feasible solution of model (3.3).

---

Table 3.8 provides the average cost increase in percentage with respect to the optimal cost and the speedup factor with regard to **BN** for the different methodologies compared. As expected, the CVaR-based approximation leads to conservative results and involves average cost increases that range between 0.49% and 2.88%. Interestingly,

**TS+V** computes the optimal solution and involves a higher speedup factor than the CVaR-based approach for two of the five systems. Compared with the two ALSO-X approximations, **TS+V** obtains the global optimal solution in all cases with speedup factors that are still tantamount to those of these approximate methods. Finally, the heuristic method achieves solutions that are close to the two ALSO-X approximations while significantly outperforming them in terms of speed.

Table 3.8: Comparison of the proposed **TS+V** approach and existing approximate methods

		IEEE-RTS-24	IEEE-57	IEEE-RTS-73	IEEE-118	IEEE-300
Average cost increase	<b>TS+V</b>	0.00%	0.00%	0.00%	0.00%	0.00%
	CVaR	2.88%	0.53%	1.71%	0.57%	0.49%
	ALSO-X	0.80%	0.08%	0.41%	0.08%	0.05%
	ALSO-X+	0.53%	0.07%	0.12%	0.05%	0.04%
	Heuristic	0.68%	0.10%	0.13%	0.09%	0.05%
Speedup factor	<b>TS+V</b>	706.8x	35.3x	1470.0x	23.1x	8.5x
	CVaR	387.1x	117.0x	265.1x	4045.5x	779.7x
	ALSO-X	17.2x	1.2x	19.7x	143.1x	11.0x
	ALSO-X+	7.7x	0.7x	6.4x	48.7x	3.6x
	Heuristic	15.7x	454.2x	187.5x	6569.2x	484.2x

### 3.4.6 Cost-driven Pre-processing

Based on the results obtained in Chapter 2 of this thesis, in this section, we propose to add economic information from the objective function (3.3a) to Algorithm 3.1 in addition to the valid inequalities of Section 3.3.2. To do so, we need to estimate an upper bound on the optimal objective function value of problem (3.3). This can be done, for instance, by way of the heuristic proposed in the previous section. We refer to this approach as **TS+V+C**, since we are adding cost information to **TS+V**. For illustration, we run this experiment for the IEEE-300 system, which is the largest system and the most expensive in computational terms. Table 3.9 collects the results of this experiment as a comparison with **TS+V**. Note that the speedup factor of **TS+V+C** accounts for the computational time of running the heuristic described in the previous section, of running Algorithm 3.1 with the upper-bound cost inequality and of solving problem (3.3).

While the strengthening of Algorithm 3.1 with the cost-based inequality slightly improves the LR-GAP, the number of retained constraints is reduced since both redundant *and* inactive constraints are removed thanks to the upper bound on the cost. Although these improvements may be small, the impact on the speedup factor is more significant, becoming almost four times higher.

Table 3.9: Comparison of **TS+V** and **TS+V+C**

	Method	IEEE-300
#CON	TS+V	3.30%
	TS+V-C	2.40%
LR-GAP	TS+V	0.1603%
	TS+V-C	0.1596%
Speedup factor	TS+V	8.5x
	TS+V-C	31.7x

### 3.5 Summary and Conclusions

In this chapter, we propose a novel exact resolution technique for a MIP SAA-based reformulation of the JCC-OPF problem. Our methodology includes a screening method to eliminate superfluous constraints based on an iterative procedure to repeatedly tighten the Big-Ms present in the MIP. These procedures are combined with the addition of valid inequalities based on the special structure of the model. Said inequalities strengthen its linear relaxation and allow for additional screening of constraints. The resultant model is thus compact and tight.

In the case study, we show that, in comparison with the benchmark model, our methodology provides remarkable results in terms of the linear relaxation bounds, the RAM memory needed to solve the instances, and the total computational time. Specifically, our method **TS+V** solves to optimality all of the instances generated for the IEEE-RTS-118 and the IEEE-RTS-300 test systems, the majority of which are not solved within 10 hours of computational time using the benchmark approach. Furthermore, the average number of constraints eliminated from all instances with **TS+V** always exceeds 95% of them, and the lower bound is markedly increased by the inclusion of the valid inequalities, showing the outstanding results of the combination of the methods developed. We remark that the inclusion of valid inequalities makes the model tighter, but less compact. However, this a-priori potential loss of model compactness is clearly counterbalanced by augmenting the screening rate of superfluous constraints within the tightening-and-screening procedure.

The comparison of our results with those provided by existing approximate and exact methods shows that our approach is computationally very competitive for small and medium-sized instances, always providing the best results in terms of cost. For the large instances addressed, while outperformed by the approximate methods in terms of computational time (as expected), our exact solution strategy not only provides a certificate of optimality but also returns the optimal solution within the set time limit. Finally, we are able to speed up the resolution of the largest instances about four times by incorporating information from the objective function during the pre-processing step. This is achieved through the use of a heuristic that delivers a good upper bound on the optimal OPF cost.

## Chapter 4

# Integrating Automatic and Manual Reserves in Optimal Power Flow



Typically in joint chance-constrained OPF (JCC-OPF) problems, it is common to assume that forecast errors in demand and renewable generation are balanced by the deployment of generation reserves, and in particular, by systems such as the *automatic generation control* (AGC) [45], as it is done in Chapter 3. Modeling power balancing through AGC offers the advantage of being expressed as an affine control policy, which eases the solution of the optimization problem.

Through the utilization of AGC, JCC-OPF problems can effectively manage forecast errors and ensure system security with a high probability. However, it proves inadequate for low probable, high-impact scenarios, leaving the system susceptible to potential vulnerabilities. Conversely, ensuring robust feasibility exclusively through AGC is excessively expensive.

The issues encountered with these models are attributed to their incomplete representation of the operator’s actions in adverse scenarios. For instance, in the event of a scenario where the AGC may jeopardize the reliability of the system or incur significant costs, the operator may elect to discontinue its operation and instead manually adjust the production level of the units. To circumvent such a caveat, in this chapter, we propose a novel *stochastic* OPF model that differentiates between two distinct operating scenarios: “normal operation”, where AGC ensures system security, and “adverse operation”, where the system operator must undertake extra measures, such as manual reserve deployment. The contents of this chapter are based on the article [48].

## 4.1 Introduction

The common AGC models implemented in the literature typically assume that all generators contribute reserve power according to an affine policy, even for large uncertainty deviations. In reality, generator output will saturate (or stop increasing/decreasing as the deviation grows larger) when they hit their lower or upper generation limit. Furthermore, operators generally take additional actions to manage both balancing and congestion in situations with very large deviations. For example, the *North American Reliability Corporation* (NERC) [107] standard for regulating the use of AGC, BAL-005, states that if the AGC becomes inoperative or may impair the reliability of the interconnection, the system operator must use manual controls to adjust generation in order to guarantee balance.

While a limited number of studies have shown that modeling generation saturation [108] or accounting for manual reserve activation during large deviations [109] leads to better operating conditions, these models are often computationally expensive. Thus, a more common approach is to apply the affine control policy, but explicitly disregard constraint satisfaction in a fraction of the most severe operating conditions. This is typically done by introducing chance constraints, as it is shown in Chapter 3, which allow violations in a (typically small) percentage of scenarios [33,34,36–41], or by

solving robust optimization formulations where the uncertainty set has been designed to contain a certain probability mass [110]. Unfortunately, by failing to model the impact of the worst scenarios (those for which the constraint satisfaction is discarded), a chance-constrained formulation may leave the system vulnerable to large disruptions that include generator and line outages, or load shed. As discussed in [36], there could be instances where the combination of generators and renewable outputs collude to produce power flows that significantly exceed the nominal line ratings, even in the absence of a large total power deviation. When the maximum rating of a line is exceeded, this line becomes more likely to trip, leaving the network vulnerable to cascading failures and associated load shed.

To address this issue, in this work we propose a new SOPF formulation where, in the worst-case scenarios, operators account for additional reserve to reduce their impact. The proposed formulation distinguishes between two different operating regimes: *normal operation* and *adverse operation*. In *normal operation*, AGC is sufficient to maintain the system balance, while in *adverse operation*, the system operator may need to implement additional actions, such as manual adjustments, to preserve system security.

Unlike the standard *joint chance-constrained* OPF (JCC-OPF), which limits the joint probability of violation of technical constraints, our formulation uses a joint chance-constraint to *control* the probability of utilizing different reserve actions. Thus, we can impose that AGC alone is to be sufficient with a high probability, while additional corrective actions are only to be implemented for the most adverse scenarios. In doing so, we reduce the need for frequent manual intervention by operators (computational expensive), while also guaranteeing that additional resources are available to handle adverse operating conditions, e.g., by scheduling more reserve capacity for manual deployment.

To demonstrate the suitability of our proposed formulation, we conduct a computational experiment that compared it to two state-of-the-art approaches. The former is the standard JCC-OPF, whose drawback is to leave the power system vulnerable to severe events, e.g., by dispatching insufficient generation capacity or giving up on alleviating congestion. The second approach guarantees robust feasibility using AGC only, which results in conservative solutions with increased operating costs, for instance, due to inefficient and oversized generation capacity. Our novel formulation results in decisions that are more reliable than the former approach and more cost-efficient than the latter.

This chapter is organized as follows. Section 4.2 describes the proposed SOPF formulation, which is derived from two traditional approaches in the literature. Section 4.3 describes the reformulation and algorithm used to make our proposal tractable and computationally efficient. Section 4.4 explains the methodology we use to benchmark our approach, while Section 4.5 discusses experimental results from a case study. Finally, conclusions are duly drawn in Section 4.6.

## 4.2 Mathematical Formulation

We start this section by extending the formulation of the JCC-OPF problem (3.2). This extended formulation will serve us as a basis to construct and motivate our proposal immediately after.

### 4.2.1 Extended Joint Chance-constrained Optimal Power Flow

This extended formulation distinguishes between *upward* or *positive* reserve,  $r_g^+(\boldsymbol{\omega})$ , and *downward* or *negative* reserve,  $r_g^-(\boldsymbol{\omega})$ , with  $r_g(\boldsymbol{\omega}) = r_g^+(\boldsymbol{\omega}) - r_g^-(\boldsymbol{\omega})$ , whose costs in the objective function are  $c_g^+$  and  $c_g^-$ , respectively. Furthermore, we explicitly model the upward and downward reserve *capacity* provided by the dispatchable generator  $g$  and respectively represented by  $r_g^u$  and  $r_g^d$ , with costs  $c_g^u$  and  $c_g^d$  in that order. This reserve capacity is procured by the system operator before the forecast errors  $\boldsymbol{\omega}$  are known.

With this notation in place and the notation described in Section 3.2, the *joint chance-constrained DC-OPF problem* used in this chapter can be formulated as follows:

$$\min_{\Xi} \sum_{g \in \mathcal{G}} c_g^1 p_g + c_g^u r_g^u + c_g^d r_g^d + \mathbb{E} [c_g^+ r_g^+(\boldsymbol{\omega}) - c_g^- r_g^-(\boldsymbol{\omega})] \quad (4.1a)$$

$$\text{s.t.} \quad \sum_{g \in \mathcal{G}} \beta_g = 1 \quad (4.1b)$$

$$\sum_{g \in \mathcal{G}} p_g - \sum_{n \in \mathcal{N}} d_n = 0 \quad (4.1c)$$

$$\underline{p}_g + r_g^d \leq p_g \leq \bar{p}_g - r_g^u, \quad \forall g \in \mathcal{G} \quad (4.1d)$$

$$-\bar{f}_l \leq \sum_{n \in \mathcal{N}} B_{ln} \left( \sum_{g \in \mathcal{G}_n} p_g - d_n \right) \leq \bar{f}_l, \quad \forall l \in \mathcal{L} \quad (4.1e)$$

$$0 \leq r_g^d \leq \bar{r}_g^d, \quad \forall g \in \mathcal{G} \quad (4.1f)$$

$$0 \leq r_g^u \leq \bar{r}_g^u, \quad \forall g \in \mathcal{G} \quad (4.1g)$$

$$r_g^+(\boldsymbol{\omega}) - r_g^-(\boldsymbol{\omega}) = -\Omega \beta_g, \quad \forall g \in \mathcal{G} \quad (4.1h)$$

$$\mathbb{P} \left( \begin{array}{l} -r_g^d \leq -\Omega \beta_g \leq r_g^u, \quad \forall g \in \mathcal{G} \\ -\bar{f}_l \leq \sum_{n \in \mathcal{N}} B_{ln} \left( \sum_{g \in \mathcal{G}_n} (p_g - \Omega \beta_g) - d_n + \omega_n \right) \leq \bar{f}_l, \quad \forall l \in \mathcal{L} \end{array} \right) \geq 1 - \epsilon \quad (4.1i)$$

$$\beta_g, r_g^+(\boldsymbol{\omega}), r_g^-(\boldsymbol{\omega}) \geq 0, \quad \forall g \in \mathcal{G}, \quad (4.1j)$$

where  $\Xi = (p_g, r_g^+(\boldsymbol{\omega}), r_g^-(\boldsymbol{\omega}), r_g^d, r_g^u, \beta_g)$  is the set of decision variables.

The three terms of the objective function (4.1a) to be minimized correspond to the power dispatch cost, the cost of procuring reserve capacity, and the expected cost related to the actual deployment of that capacity, respectively. For ease of explanation, we consider linear cost functions, but it can be easily extended to quadratic or piecewise linear functions. The power balance in the system is guaranteed for *all* possible

realizations of  $\omega$  through equations (4.1b) and (4.1c). Note that, by requiring  $\beta_g \geq 0$  in (4.1j), we enforce that reserve is deployed only to counterbalance the forecast errors and not to redispatch generators to counter congestion too. Constraints (4.1d) ensure that the power produced by dispatchable generators is within their minimum and maximum power output limits, i.e.,  $\underline{p}_g$  and  $\bar{p}_g$ , respectively, considering the reserve capacity the system operator procures from them. Expressions (4.1e) ensure a feasible power flow under the error-free scenario. Constraints (4.1f) and (4.1g) set a limit on the maximum reserve capacity each generator is willing or able to provide. Equation (4.1h) models the affine control policy for reserve deployment (AGC) we discussed in Section 3.2. Expression (4.1i) constitutes the joint chance-constraint system by which the system operator states that the reserves deployed and the line flows must be within their bounds with a probability greater than or equal to  $1 - \epsilon$ . Accordingly, parameter  $\epsilon$  is the maximum allowed probability of constraint violation set by the operator. Finally, (4.1j) imposes the positive character of decision variables  $\beta_g$  and random functions  $r_g^+(\omega)$  and  $r_g^-(\omega)$  for all  $g$ . Note that the probability in (4.1i) is computed over the probability space of  $\omega$  and that the equality (4.1h) and the inequality (4.1j) must hold for almost all  $\omega$ .

The popularity of the joint chance-constrained formulation (4.1) stems from its ability to reduce the expected system operating cost substantially by allowing the violation of reserve capacity constraints and/or line flow limits under a small  $\epsilon$ -percentage of realizations of  $\omega$ . These realizations, or scenarios, are thus the most detrimental to the system in terms of cost. Parameter  $\epsilon$  in (4.1) controls the level of risk aversion of the system operator (the lower, the more risk averse), to the point that if  $\epsilon$  is set to 0, formulation (4.1) becomes *robustly feasible*, meaning that all the constraints and variable limits are to be satisfied with probability one.

Nonetheless, the critical nature of power systems practically forces operators to guarantee robust feasibility. In this regard, formulation (4.1), even if  $\epsilon = 0$ , offers an incomplete picture of how power systems are actually operated. Indeed, in those very few  $\omega$ -scenarios for which AGC is unable or too costly to ensure the system's integrity, the operators can still take over the affine control policy and *manually* set new operating points for some generators in the system, those needed to guarantee the satisfaction of the system's constraints ideally at the minimum cost. The fact that formulation (4.1) ignores the possibility of a manual control taking over AGC (albeit with a low occurrence) causes it to underestimate the operating cost when  $\epsilon > 0$  or overestimate it when robust feasibility is pursued ( $\epsilon = 0$ ). The ultimate result is that formulation (4.1) may produce uneconomical or suboptimal affine control policies.

To illustrate our point, we use an example based on the small power system depicted in Fig. 4.1. The system includes two thermal generating units with the linear production costs, reserve capacity costs and maximum power limits indicated in the figure. For simplicity, the susceptances of all lines are assumed to be 1 p.u. and the capacity of

each line is also specified in the figure. A single net demand of 60 MW is located at node  $n_3$ . We assume that the associated (random) forecast error can take on three different values only, namely, 20, 10, and  $-20$  MW, corresponding to three equally probable realizations or scenarios 1, 2 and 3, in that order. The costs of deploying upward and downward reserve, i.e.,  $c_n^+$  and  $c_n^-$ , are 1.2 and 0.8 times the generator's linear operating cost, respectively.

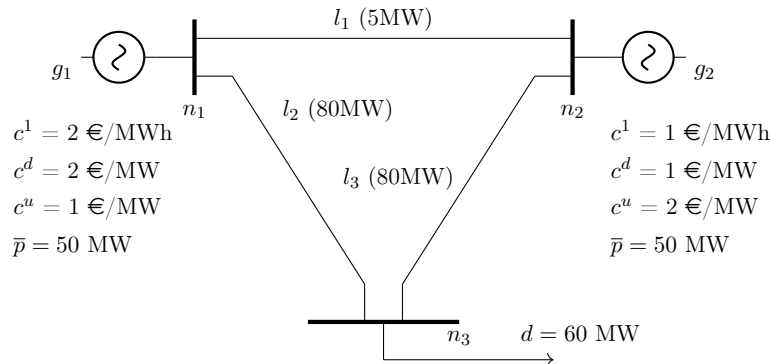


Figure 4.1: Three-node illustrative example

Results from problem (4.1) when  $\epsilon = 1/3$  and  $\epsilon = 0$  are collated in the first two rows of Table 4.1. These results include the optimal power dispatch, participation factors and procured reserve capacities, together with the optimal expected operating cost. Unsurprisingly, the results are quite sensitive to  $\epsilon$ . For example, when this is set to zero (to achieve robust feasibility), much more reserve capacity is to be procured than when we allow the system's constraints to be violated under one of the scenarios, in particular, scenario 3. Accordingly, the cost increases from €95 to €137.5, when  $\epsilon$  goes from  $1/3$  to 0. In contrast, if we take the solution delivered for  $\epsilon = 1/3$  and scenario 3 actually occurs, meaning that the net demand forecast error takes on the value  $-20$  MW, the AGC requires generator  $g_2$  to increase its production up to 65 MW, that is, above its maximum output limit, while exceeding the maximum capacity of line  $l_1$  too. But what is more important from a practical point of view is that, under such a scenario, the solution to problem (4.1) when  $\epsilon = 1/3$  does *not* allow for any *manual re-dispatch* that can restore system feasibility immediately after, because no upward reserve capacity has been procured beforehand.

Table 4.1: Results – Illustrative Example

Method	$p_1$	$p_2$	$\beta_1$	$\beta_2$	$r_1^u$	$r_2^u$	$r_1^d$	$r_2^d$	Cost (€)
model (4.1) ( $\epsilon = 1/3$ )	15	45	0	1	0	0	0	20	95
model (4.1) ( $\epsilon = 0$ )	12.5	47.5	0.625	0.375	12.5	7.5	12.5	7.5	137.5
model (4.3) ( $\epsilon = 1/3$ )	15	45	0	1	20	0	0	20	123

### 4.2.2 Balancing Cost and Reliability

The previous example illustrates that formulation (4.1) may be too risky or too costly. Instead, we propose next a novel joint chance-constrained formulation of the DC-OPF problem that does account for the possibility of resorting to a manual re-dispatch in this  $\epsilon$ -percentage of events in which the implementation of AGC is too expensive or even infeasible. To provide a more technical description of our proposal, Fig. 4.2 illustrates how the mentioned approaches respond to an uncertain scenario. Our approach involves the use of manual adjustments to balance and ensure reliability under extreme conditions, while model (4.1) with  $\epsilon = 0$  only employs AGC and model (4.1) with  $\epsilon > 0$  does not consider any corrective measures for adverse scenarios. To obtain our formulation, we replace the set of constraints (4.1h)–(4.1i) in (4.1) with the following ones:

$$\sum_{g \in \mathcal{G}} r_g^M(\omega) = 0 \quad (4.2a)$$

$$r_g^+(\omega) - r_g^-(\omega) = -\Omega\beta_g + r_g^M(\omega), \quad \forall g \in \mathcal{G} \quad (4.2b)$$

$$-r_g^d \leq -\Omega\beta_g + r_g^M(\omega) \leq r_g^u, \quad \forall g \in \mathcal{G} \quad (4.2c)$$

$$-\bar{f}_l \leq \sum_{n \in \mathcal{N}} B_{ln} \left( \sum_{g \in \mathcal{G}_n} (p_g - \Omega\beta_g + r_g^M(\omega)) - d_n + \omega_n \right) \leq \bar{f}_l, \quad \forall l \in \mathcal{L} \quad (4.2d)$$

$$\mathbb{P}(r_g^M(\omega) = 0, \quad \forall g \in \mathcal{G}) \geq 1 - \epsilon, \quad (4.2e)$$

where  $r_g^M(\omega)$  is a random variable that represents the manual adjustment of the power output of the generator  $g$ .

Equation (4.2a) is required for the implemented power adjustments to preserve the power balance. Equation (4.2b) is analogous to (4.1h), but including the manual adjustment requested by the system operator. Inequalities (4.2c) and (4.2d) enforce that the use of AGC in combination with manual re-dispatch guarantees that the system's constraints are satisfied under any realization of  $\omega$ . Finally, in our proposal, chance-constrained programming is employed for a different purpose than that in (4.1) whereby the violation probability of system's constraints is limited. Specifically, the joint chance-constraint (4.2e) seeks to characterize the use of manual control as an *occasional* recourse action, thus ensuring that AGC is the standard control policy. Thereby, the system operator is capable to guarantee robust feasibility, that is, system's security. Again, constraints (4.2a)–(4.2d) are to be satisfied for almost all  $\omega$ . The underlying concept behind the performance of this set of constraints can be explained as follows: AGC is employed to mitigate system imbalances, and if a technical constraint, be it (4.2c) or (4.2d), is violated or enforcement entails significant costs (with a probability less than  $\epsilon$ ), variable  $r_g^M(\omega)$  assumes a non-zero value for any generator  $g$  to ensure feasibility or to reduce the expensive operating cost associated with the restrictive nature

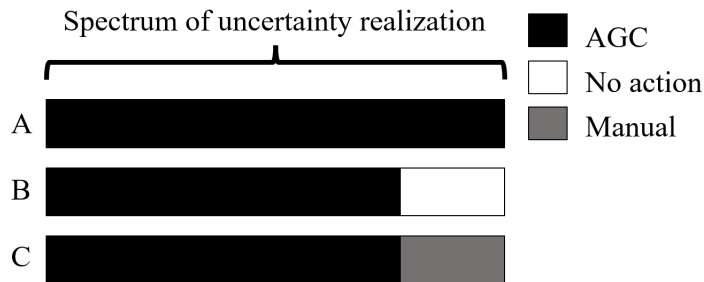


Figure 4.2: Actions planned over the spectrum of uncertainty realizations to mitigate imbalances and ensure the reliability of the power system. A: model (4.1) with  $\epsilon = 0$ , B: model (4.1) with  $\epsilon > 0$ , C: Proposal.

of this affine control policy.

Our proposal can thus be formulated as follows:

$$\min_{\Xi} \sum_{g \in \mathcal{G}} c_g^1 p_g + c_g^u r_g^u + c_g^d r_g^d + \mathbb{E} [c_g^+ r_g^+(\boldsymbol{\omega}) - c_g^- r_g^-(\boldsymbol{\omega})] \quad (4.3a)$$

$$\text{s.t.} \quad (4.1b) - (4.1g), (4.2a) - (4.2e), (4.1j). \quad (4.3b)$$

Coming back to our example, results from (4.3) are also included in the last row of Table 4.1. Observe that the system operating cost is significantly reduced with respect to that of formulation (4.1) with  $\epsilon = 0$ . Furthermore, as in the case of formulation (4.1) with  $\epsilon = 1/3$ , our proposal also renders a solution for which, if scenario 3 occurs, the implementation of AGC violates the maximum output limit of generator  $g_2$  and the capacity of line  $l_1$ . However, unlike the solution to (4.1), the one delivered by our proposal procures 20 MW of upward reserve capacity from generator  $g_1$  so that the system operator can release this generator from AGC and manually dispatch it at 20 MW under scenario 3.

In the following section, we discuss how we solve formulations (4.1) and (4.3).

### 4.3 Solution Methodology

Chance-constrained programs such as (4.1) and (4.3) belong to the class of NP-hard problems. In general, there is no finite, tractable reformulation of the chance-constraint (4.1i) or (4.2e). As a result, a wide variety of different approaches have been proposed to approximate the feasible region determined by these constraints, namely, *distributionally robust optimization* (DRO) [111], the *scenario approach* (SA) [78], *sample average approximation* (SAA) [93], and the inner convex approximations based on the *conditional value-at-risk* (CVaR) [70] or ALSO-X [74].

In this chapter, we resort to SAA boosted with the bounding, tightening and valid inequalities proposed in Chapter 3. To do that, as in Chapter 3, we assume that  $\boldsymbol{\omega}$

has a finite discrete support defined by a collection of atoms  $\{\boldsymbol{\omega}_s \in \mathbb{R}^{|\mathcal{M}|}, s \in \mathcal{S}\}$  and respective probability masses  $\mathbb{P}(\boldsymbol{\omega} = \boldsymbol{\omega}_s) = \frac{1}{|\mathcal{S}|}, \forall s \in \mathcal{S} = \{1, \dots, |\mathcal{S}|\}$ . Accordingly,  $\omega_{ns}$  and  $\Omega_s$  are realizations of the respective random variables under scenario  $s$ , and the decisions  $r_{gs}^M, r_{gs}^+$  and  $r_{gs}^-$  for the dispatchable unit  $g$  may vary for each scenario  $s$ . We define  $q = \lfloor \epsilon |\mathcal{S}| \rfloor$ , the vector  $\mathbf{y}$  of binary variables  $y_s, \forall s \in \mathcal{S}$  and the large enough constants  $\underline{M}_{gs}, \overline{M}_{gs}$ . Thus, the MIP reformulation of problem (4.3) writes as follows:

$$\min_{\Theta} \sum_{g \in \mathcal{G}} c_g^1 p_g + c_g^u r_g^u + c_g^d r_g^d + \frac{1}{|\mathcal{S}|} \sum_{s \in \mathcal{S}} c_g^+ r_{gs}^+ - c_n^- r_{gs}^- \quad (4.4a)$$

$$\text{s.t. (4.1b) – (4.1g)} \quad (4.4b)$$

$$\sum_{g \in \mathcal{G}} r_{gs}^M = 0, \quad \forall s \in \mathcal{S} \quad (4.4c)$$

$$r_{gs}^+ - r_{gs}^- = -\Omega_s \beta_g + r_{gs}^M, \quad \forall g \in \mathcal{G}, s \in \mathcal{S} \quad (4.4d)$$

$$-r_g^d \leq -\Omega_s \beta_g + r_{gs}^M \leq r_g^u, \quad \forall g \in \mathcal{G}, s \in \mathcal{S} \quad (4.4e)$$

$$-\bar{f}_l \leq \sum_{n \in \mathcal{N}} B_{ln} \left( \sum_{g \in \mathcal{G}_n} (p_g - \Omega_s \beta_g + r_{gs}^M) - d_n + \omega_{ns} \right) \leq \bar{f}_l, \quad \forall l \in \mathcal{L}, s \in \mathcal{S} \quad (4.4f)$$

$$-y_s \underline{M}_{gs} \leq r_{gs}^M \leq y_s \overline{M}_{gs}, \quad \forall g \in \mathcal{G}, s \in \mathcal{S} \quad (4.4g)$$

$$\beta_g, r_{gs}^+, r_{gs}^- \geq 0, \quad \forall g \in \mathcal{G}, s \in \mathcal{S} \quad (4.4h)$$

$$\sum_{s \in \mathcal{S}} y_s \leq q \quad (4.4i)$$

$$y_s \in \{0, 1\}, \quad \forall s \in \mathcal{S}, \quad (4.4j)$$

where the set of decision variables is  $\Theta = (p_g, r_{gs}^-, r_{gs}^+, r_g^d, r_g^u, y_s, r_{gs}^M, \beta_g)$ .

Constraints (4.4g)–(4.4j) represent the sample-based MIP reformulation of the joint chance-constraint (4.2e). For a given scenario  $s \in \mathcal{S}$ , the inequalities (4.4g) establish that a manual adjustment to the production of the dispatchable unit  $g$  in scenario  $s$  can only be done when  $y_s = 1$ . Otherwise, if  $y_s = 0$ , the power forecast error must be handled by the AGC. Expression (4.4i) ensures that the probability of the joint chance-constraint is met and (4.4j) enforces the binary character of variables  $y_s$ . A MIP reformulation for the sample average approximation of (4.1) can be found in Section 3.3. Note that (4.1) is an extension of (3.2), but the procedure to reformulate the joint chance constraint is equivalent.

Chapter 3 demonstrates the importance of setting the values of  $\underline{M}_{gs}$  and  $\overline{M}_{gs}$  as small as possible in order to tighten problem (4.4) and speed up its solution. To do so, we adapt Algorithm 3.1 from Section 3.3.1 to tune these constants. The adaptation can be found in Algorithm 4.1.

The output of Algorithm 4.1 are the tuned big-Ms, which are input for the MIP reformulation of (4.3). Note that, at each iteration, the big-M values decrease or remain equal. In our experience, one iteration is enough to get a tight formulation of problem (4.4). To reduce the computational burden of Algorithm 4.1, Step 2 is solved in par-

**Algorithm 4.1** Iterative Tuning of  $\underline{M}_{gs}$  and  $\overline{M}_{gs}$ 

**Input:** Constraints (4.4b)-(4.4f), (4.4h)-(4.4i), parameter  $q$  related to the allowed violation probability and the total number of iterations  $\kappa$ .

**Output:** The large constants  $\underline{M}_{gs}^k, \overline{M}_{gs}^k, \forall g \in \mathcal{G}, s \in \mathcal{S}$ .

Step 1. Initialization,  $k = 0, \underline{M}_{gs}^0 = \bar{r}_g^d, \overline{M}_{gs}^0 = \bar{r}_g^u, \forall g \in \mathcal{G}, s \in \mathcal{S}$ .

Step 2. For each  $g \in \mathcal{G}$  and  $s \in \mathcal{S}$  update  $\underline{M}_{gs}^{k+1}$  and  $\overline{M}_{gs}^{k+1}$  as follows: If  $\underline{M}_{gs}^k < 0$ , then  $\underline{M}_{gs}^{k+1} = \underline{M}_{gs}^k$ , likewise for  $\overline{M}_{gs}^{k+1}$ . Otherwise,

$$-\underline{M}_{gs}^{k+1} / \overline{M}_{gs}^{k+1} = \min_{\Theta} / \max_{\Theta} r_{gs}^M \quad (4.5a)$$

$$(4.4b) - (4.4f), (4.4h) - (4.4i) \quad (4.5b)$$

$$-y_s \underline{M}_{gs}^k \leq r_{gs}^M \leq y_s \overline{M}_{gs}^k, \quad \forall g \in \mathcal{G}, s \in \mathcal{S} \quad (4.5c)$$

$$0 \leq y_s \leq 1, \quad \forall s \in \mathcal{S}. \quad (4.5d)$$

Step 3. If  $k + 1 < \kappa$ , then  $k = k + 1$  and go to Step 2. Otherwise, stop.

allel. Furthermore, as outlined in Section 3.3.1, if the computed big-M value in Step 2 is strictly lower than zero, then the corresponding constraint of (4.4g) can be safely removed in problem (4.4), since the feasibility region of (4.5) is a relaxation of that in (4.4). In addition, this improvement can be implemented in Algorithm 4.1, speeding it up if the identified redundant constraint of (4.5c) is removed at the next iteration.

Moreover, we introduce the valid inequalities developed in Section 3.3.2 to tighten the relaxed LP formulation of (4.4). These inequalities ensure that constraints (4.4e) and (4.4f) are individually satisfied by the deployment of AGC in at least  $(1 - \epsilon)$ -percentage of scenarios. Thus, they are also valid in problem (4.4). To further tighten the large constants  $\underline{M}_{gs}$  and  $\overline{M}_{gs}$ , we include these valid inequalities to the constraint set (4.5) of Algorithm 4.1.

As seen in Chapter 2 and, indirectly, in Chapter 3, line constraints can significantly increase the computational burden of problem (4.4). To mitigate this issue, we propose to eliminate redundant line constraints (4.4f) from (4.4). To do so, we compute the minimum and maximum power flow for each line and scenario using two optimization problems. Mathematically, these optimization problems can be expressed as follows:

$$\min_{\Theta} / \max_{\Theta} f_{ls} = \sum_{n \in \mathcal{N}} B_{ln} \left( \sum_{g \in \mathcal{G}_n} (p_g - \Omega_s \beta_g + r_{gs}^M) - d_n + \omega_{ns} \right), \quad \forall l \in \mathcal{L}, s \in \mathcal{S} \quad (4.6a)$$

$$\text{s.t.} \quad (4.4b) - (4.4i) \quad (4.6b)$$

$$0 \leq y_s \leq 1, \quad \forall s \in \mathcal{S}. \quad (4.6c)$$

Note that problem (4.6) is built on a relaxation of problem (4.4). Then, if the computed power flow,  $f_{ls}$ , is strictly smaller (greater) than the line capacity  $\bar{f}_l$  ( $-\bar{f}_l$ ), the  $\leq$ -constraint ( $\geq$ ) in (4.4f) can be safely removed. Additionally, we remark that the

identified redundant line constraints (4.4f) can be also removed from problem (4.5) to expedite Algorithm 4.1.

Alternatively, we implement a heuristic (see Algorithm 4.2) based on Algorithm 3.4 of Section 3.4.5. This heuristic identifies good, feasible solutions of problem (4.4) with a low computational burden.

---

**Algorithm 4.2** Iterative heuristic

---

Input: Stopping tolerance parameter  $\delta$

**Require:** Relax the integrality of  $\mathbf{y}$  in (4.4)

$\underline{q} \leftarrow 0, \bar{q} \leftarrow \lfloor \epsilon |\mathcal{S}| \rfloor$

**while**  $\bar{q} - \underline{q} \geq \delta$  **do**

    Set  $q = (\underline{q} + \bar{q})/2$  and compute an optimal solution  $\mathbf{y}^*$  to (4.4).

    Set  $q = \bar{q}$  if  $\mathbb{P}(\mathbf{y}^* = 0) \geq 1 - \epsilon$ ; otherwise,  $\bar{q} = q$

**end while**

Output: A feasible solution of model (4.4).

---

To illustrate the procedure we have described throughout this section, we summarize each step in Algorithm 4.3 below.

---

**Algorithm 4.3** Procedure to efficiently solve (4.4)

---

This algorithm demonstrates the steps carried out to solve the tight and compact version of problem (4.4)

Step 1. Solve problem (4.6),  $\forall l \in \mathcal{L}, s \in \mathcal{S}$ , to identify redundant line flow constraints (4.4f) in problem (4.4), which can be safely removed, resulting in a more compact model (4.4).

Step 2. Run Algorithm 4.1 including the valid inequalities proposed in Section 3.3.2 and removing the redundant line constraints identified in previous step to strengthen problem (4.4) tightening its big-M constants, i.e.,  $\underline{M}_{gs}$  and  $\overline{M}_{gs}$ . In this chapter, parameter  $\kappa$  is set to 1 as we have experienced similar results for greater values.

Step 3. Solve the resulting tight and compact mixed-integer model of problem (4.4). This can be done in two ways:

- (a) Directly solve the resulting mixed-integer program using off-the-shelf solvers.
  - (b) Use the heuristic proposed in Algorithm 4.2.
- 

If we run Algorithm 4.3 choosing Step 3b, we can obtain an initial estimate of the optimal cost of problem (4.4) with hardly any computational resources. This estimate can then be included as an upper-bound constraint of the operating cost in Step 1 and/or Step 2, as discussed in Chapters 2 and 3, to tighten and simplify the formulation (4.4), thus efficiently solving it in Step 3a.

## 4.4 Evaluation Procedure

In this section, we outline the procedure for evaluating the performance of the two approaches compared in this chapter, namely:

- The joint chance-constrained problem with automatic generation control only formulated in (4.1) and denoted as AGC- $\epsilon$  hereinafter. For  $\epsilon = 0$ , the constraints must be satisfied for all scenarios and model (4.1) is formulated as a linear program. For  $\epsilon \neq 0$ , model (4.1) is reformulated as a MIP problem and efficiently solved using the procedure described in Chapter 3.
- The joint chance-constrained problem with both automatic and manual generation control formulated in (4.3) and denoted as AMGC- $\epsilon$ . Notice that for  $\epsilon = 0$ , the results obtained by AGC-0 and AMGC-0 are the same. For  $\epsilon \neq 0$ , model (4.3) is reformulated as the MIP model (4.4) and solved using the procedure described in Section 4.3, i.e., running Algorithm 4.3 choosing Step 3a. The approach that solves model (4.4) using Step 3b in Algorithm 4.3 is denoted as AMGC-H- $\epsilon$ .

First, let  $(p_g^*, r_g^{d,*}, r_g^{u,*}, \beta_g^*)$  denote the optimal dispatch and reserve capacity decisions delivered by AGC- $\epsilon$ , AMGC- $\epsilon$  or AMGC-H- $\epsilon$  with the in-sample scenario set  $\mathcal{S}$ . We evaluate the performance of these decisions on an out-of-sample scenario set denoted by  $\mathcal{S}'$  and indexed by  $s'$ , with  $|\mathcal{S}| \ll |\mathcal{S}'|$ . Each out-of-sample scenario  $s'$  is characterized by the realization of the forecast errors  $\omega_{ns'}$  and the system-wise aggregate forecast error  $\Omega_{s'}$ , with  $\Omega_{s'} = \sum_{n \in \mathcal{N}} \omega_{ns'}$ . For each scenario  $s'$ , we formulate the following real-time operation problem:

$$\min_{\Psi} \sum_{g \in \mathcal{G}} c_g^1 p_g^* + c_g^u r_g^{u,*} + c_g^d r_g^{d,*} + c_g^+ r_{gs'}^+ - c_g^- r_{gs'}^- + P \sum_{n \in \mathcal{N}} (\Delta_{ns'}^+ + \Delta_{ns'}^-) \quad (4.7a)$$

$$\text{s.t.} \quad \sum_{g \in \mathcal{G}} r_{gs'}^M + \sum_{n \in \mathcal{N}} \Delta_{ns'}^+ - \Delta_{ns'}^- = 0, \quad (4.7b)$$

$$r_{gs'}^+ - r_{gs'}^- = -\Omega_{s'} \beta_g^* + r_{gs'}^M, \quad \forall g \in \mathcal{G} \quad (4.7c)$$

$$-r_g^{d,*} \leq -\Omega_{s'} \beta_g^* + r_{gs'}^M \leq r_g^{u,*}, \quad \forall g \in \mathcal{G} \quad (4.7d)$$

$$-\bar{f}_l \leq \sum_{n \in \mathcal{N}} B_{ln} \left( \sum_{g \in \mathcal{G}_n} (p_g^* - \Omega_{s'} \beta_g^* + r_{gs'}^M) - d_n + \omega_{ns'} + \Delta_{ns'}^+ - \Delta_{ns'}^- \right) \leq \bar{f}_l, \quad \forall l \in \mathcal{L} \quad (4.7e)$$

$$r_{gs'}^+, r_{gs'}^- \geq 0, \quad \forall g \in \mathcal{G} \quad (4.7f)$$

$$\Delta_{ns'}^+, \Delta_{ns'}^- \geq 0, \quad \forall n \in \mathcal{N}. \quad (4.7g)$$

Note that  $\Psi = (r_{gs'}^+, r_{gs'}^-, r_{gs'}^M, \Delta_{ns'}^+, \Delta_{ns'}^-)$  where  $\Delta_{ns'}^+$  and  $\Delta_{ns'}^-$  are two slack variables that quantify the positive and negative power deviations at each node  $n$ , respectively. These deviations are penalized in the objective function through parameter  $P$ , which is to be set large enough so that scenario  $s'$  is counted as *infeasible* if any of the corresponding slack variables takes on a strictly positive value. For each scenario  $s'$ , model (4.7) determines the reserve deployments to keep the network balanced at the minimum

cost. Note that constraints (4.7b)-(4.7g) are equivalent to constraints (4.4c)-(4.4h) but with the addition of the slack variables  $\Delta_{ns'}^+, \Delta_{ns'}^-$ , which guarantee the feasibility of model (4.7) for any scenario realization.

Using the solution to model (4.7), we split the out-of-sample scenario set  $\mathcal{S}'$  into three subsets as follows. First, we solve model (4.7) with variables  $r_{gs'}^M, \Delta_{ns'}^+$  and  $\Delta_{ns'}^-$  fixed to 0, that is, enforcing that forecast errors can only be handled by AGC. If the problem is feasible, the scenario  $s'$  belongs to subset  $\mathcal{S}'_A$  and the real-time operation cost is denoted by  $C_{s'}$ . If this problem is infeasible, we solve model (4.7) without fixing any variable. If  $\max(\Delta_{ns'}^+, \Delta_{ns'}^-) = 0$ , then the forecast errors can be offset using automatic and manual reserves, and scenario  $s'$  is included in subset  $\mathcal{S}'_M$ . Finally, if  $\max(\Delta_{ns'}^+, \Delta_{ns'}^-) > 0$ , then automatic and manual reserves are not enough to maintain the power balance and power deviations occur during the real-time operation. In that case, scenario  $s'$  belongs to the subset  $\mathcal{S}'_D$ . In the next section, we evaluate the performance of the different approaches by comparing the percentage of scenarios that belong to each subset as well as the expected cost of the real-time operation.

## 4.5 Numerical Experiments

In this section, we compare the performance of the different approaches presented in Section 4.2 using a modified version of the IEEE-118 test system widely employed in the technical literature on the topic. The IEEE-118 test system has 118 nodes, 19 generators and 186 transmission lines, and the original data pertaining to this system are publicly available in the repository [102]. We assume that six generators can provide reserves, and their corresponding data is collated in Table 4.2. Notice that units 2, 11 and 19 have a much higher production cost than units 7, 10 and 17. For these six units, the reserve deployment costs are computed as  $c_g^- = 0.8 c_g^1$  and  $c_g^+ = 1.2 c_g^1$ , and the reserve capacity costs are  $c_g^d = c_g^u = 0.2 c_g^1$ . Besides, we add 25 wind power plants throughout the system as suggested in [112]. Given that the variability in the load is relatively small compared to that of wind power, we only consider forecast errors in the latter. We consider that the wind power forecast error is normally distributed, i.e.,  $\boldsymbol{\omega} \sim N(\mathbf{0}, \Sigma)$ , where  $\mathbf{0}$  and  $\Sigma$  represent, respectively, the zero vector and the covariance matrix. We also assume that the standard deviation of  $\omega_n$  at node  $n$  is a 15% of the wind power forecast. The uncertainty pertaining to the renewable generation of the wind farms is characterized using 1000 scenarios, that is,  $|\mathcal{S}| = 1000$ . Finally, the penalty cost  $P$  due to deviations is twice the production cost of the most expensive generator. All data of this modified 118-bus system is available at [113].

To provide meaningful statistics, each method is run for ten different sets of randomly generated scenarios. Accordingly, we report results averaged over these ten instances. All optimization problems have been solved using GUROBI 9.1.2 [103] on a

Table 4.2: Generators with capability to provide reserve.

$g$	$c_g^1$	$c_g^-$	$c_g^+$	$c_g^d/c_g^u$	$\bar{r}_g^d/\bar{r}_g^u$
2	124.6	99.7	149.5	24.9	85
7	16.7	13.3	20.0	3.3	223
10	16.1	12.8	19.3	3.2	195
11	100.0	80.0	120.0	20.0	441
17	12.6	10.1	15.1	2.5	653
19	110.0	88.0	132.0	22.0	79

Linux-based server with CPUs clocking at 2.6 GHz, 6 threads and 16 GB of RAM. In all cases, the optimality GAP has been set to  $10^{-4}$  and the time limit to 10 hours.

#### 4.5.1 Out-of-sample Performance

We compare the different approaches following the out-of-sample evaluation procedure described in Section 4.4 with 100 000 different scenarios drawn from the same distribution, that is,  $|\mathcal{S}'| = 100\,000$ . Table 4.3 collates the results of four different approaches, namely: i) AGC-0, which corresponds to model (4.1) with  $\epsilon = 0\%$  (i.e., all scenarios must be satisfied); ii) AGC-5, which is model (4.1) with  $\epsilon = 5\%$  (that is, 50 scenarios may have violated constraints); iii) the proposed AMGC-5 approach, which is model (4.3) with  $\epsilon = 5\%$  (50 scenarios may use manual adjustments to re-dispatch generators), and iv) AMGC-H-5, which corresponds to a heuristic procedure to solve AMGC-5. These results include the percentage of (i) the number of scenarios in which the forecast errors are handled using automatic generation control only  $|\mathcal{S}'_A|$ , (ii) the number of scenarios in which manual re-dispatch is required to keep power balance throughout the network  $|\mathcal{S}'_M|$ , (iii) the number of scenarios in which automatic and manual reserves are not enough to offset power imbalances and therefore, power deviations are inevitable and the system security is compromised  $|\mathcal{S}'_D|$ , and (iv) the total expected cost.

Table 4.3: Out-of-sample performance comparison.

	$ \mathcal{S}'_A $	$ \mathcal{S}'_M $	$ \mathcal{S}'_D $	$\mathbb{E}[C_{s'}]$ (k€)
<b>AGC-0</b>	99.56%	0.16%	0.28%	73.65
<b>AGC-5</b>	94.12%	0.17%	5.71%	53.04
<b>AMGC-5</b>	94.30%	5.41%	0.29%	60.15
<b>AMGC-H-5</b>	94.77%	4.98%	0.25%	61.05

As expected, AGC-0 gives very conservative and expensive solutions in which power imbalances are handled using AGC in 99.56% of the scenarios. Conversely, AGC-5 obtains OPF solutions that are 28% cheaper on average than those of AGC-0. However, these solutions are not able to offset power imbalances with both types of reserves

in 5.71% of the scenarios, thus compromising the safety of the system. The proposed AMGC-5 approach is able to compute dispatch solutions taking into account both automatic and manual reserves. Indeed, imbalances are compensated with AGC in 94.30% of the scenarios, and manual reserves are only required in 5.41% of them. Note that these percentages are very close to the desired values of 95% and 5%. Although deviations still exist in 0.29% of the scenarios, the proposed methodology reduces the expected cost by 18% with respect to AGC-0 for similar reliability levels. Finally, the results of AMGC-H-5 are slightly more conservative and expensive than those of AMGC-5, but certainly these results confirm that Algorithm 4.2 is able to provide a good feasible solution to the proposed formulation (4.4).

Table 4.4: Comparison of decisions made by AGC and AMGC.

	Cheap Generators			Expensive Generators		
	$\beta$	$r^d$	$r^u$	$\beta$	$r^d$	$r^u$
<b>AGC-0</b>	0.77	533.6	538.5	0.23	160.1	162.5
<b>AGC-5</b>	1.00	509.4	364.5	0.00	0.0	0.0
<b>AMGC-5</b>	0.99	684.7	386.3	0.01	7.9	314.7
<b>AMGC-H-5</b>	0.96	675.7	395.3	0.04	16.9	305.6

To give more details on the out-of-sample performance of the different approaches, Table 4.4 gathers a summary of the OPF decisions  $\beta_g^*$ ,  $r_g^{d,*}$  and  $r_g^{u,*}$ . For conciseness, we aggregate the units providing reserves into cheap and expensive generators. Interestingly, AGC-0 yields more conservative OPF decisions since both cheap and expensive generators are dispatched to provide AGC. Conversely, the other methods mainly allocate AGC to cheap generators only. Notice that in the case of AGC-5, the values of  $\beta$ ,  $r^d$  and  $r^u$  are 0 for expensive generators, which means that these units will not be available for manual reserve during the real-time operation of the power system and therefore, the probability of incurring dangerous power deviations increases. Conversely, both AMGC-5 and AMGC-H-5 procure more reserve capacities so that cheap and expensive generators can be effectively and efficiently redispatched to minimize the real-time operation cost while reducing power deviations.

To further illustrate the differences between the methods compared in this section, we compute for each out-of-sample scenario  $s'$  the total deviation  $\Delta_{s'}$  as follows:

$$\Delta_{s'} = \sum_{n \in \mathcal{N}} (\Delta_{ns'}^+ + \Delta_{ns'}^-)$$

Figure 4.3 plots the average value of  $\Delta_{s'}$  for the 5% scenarios with largest deviations ( $\bar{\Delta}^{5\%}$ ) versus the expected cost for each of the 10 independent samples. As observed, AGC-0 involves very low deviation levels but the highest expected cost. Under AGC-5, the expected cost is decreased at the expense of increasing the system deviations.

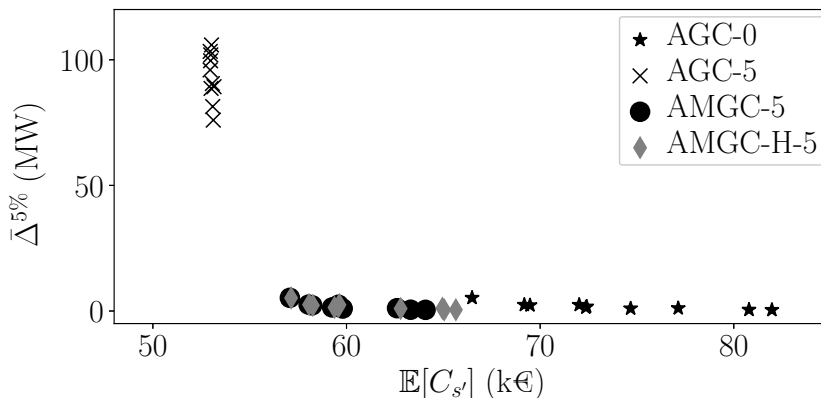


Figure 4.3: Expected cost vs. the average deviation of the %5 scenarios with the largest deviations.

Finally, the two methods proposed in this chapter manage to maintain the low levels of deviations featured by AGC-0 at a significantly lower cost.

#### 4.5.2 Computational Study

To conclude this case study, we assess the computational performance of the different approaches. AGC-0 is formulated as a linear programming problem and takes an average of 6.1s to be solved. With the efficient solution procedure proposed in Chapter 3, AGC-5 can be solved in 14.3s. However, the proposed AMGC-5 requires extra variables to properly model the deployment of manual reserves, which increases its average computational time to 3288.5s. Nevertheless, the heuristic procedure described in Section 4.3, i.e., running Algorithm 4.3 choosing Step 3b, can reduce this time to 73.6s with a very slight impact on the performance of AMGC-5. Note that all computational times include the pre-processing step, which can be parallelized (we take the maximum time of all optimization problems), if necessary.

Since AMGC-H-5 is 44.7 times faster than AMGC-5, we suggest to use the former to include an upper-bound cost constraint in the Step 1 and/or Step 2 of Algorithm 4.3, in the spirit of what we have proposed and discussed in the previous chapters of this thesis. This upper-bound cost constraint can be exploited in both the screening of line constraints of Section 4.3, i.e., Step 1 of Algorithm 4.3, and in the application of Algorithm 4.1 to tune the big-M constants, i.e., Step 2 of Algorithm 4.3, replicating what is done in Section 3.4.6. It is important to note that  $\underline{M}_{gs}$  and  $\overline{M}_{gs}$  are related to the deployment of manual reserves, which affects the cost. Therefore, by imposing a maximum cost, these constants can be further tightened. For that reason, in this chapter we only use the cost-based inequality to obtain tighter big-Ms, that is Step 2 of Algorithm 4.3, and not to further screen out superfluous line constraints, although the latter is possible. By incorporating the cost-based inequality into Algorithm 4.1,

the cost of the root relaxation of problem (4.4) increases on average from €59370 to €59619, although without eliminating any superfluous constraints, i.e., the resulting  $\underline{M}_{gs}$  and  $\overline{M}_{gs}$  are always greater than zero. This slight improvement results in an average reduction of the computational time by up to 2000s approximately. Note that the time of executing the heuristic is included in the total solution time. Hence, this fact demonstrates once again the potential of adding cost information in the pre-processing step.

## 4.6 Summary and Conclusions

Existing approaches to solving the stochastic OPF are either overly conservative and expensive, or leave the system vulnerable to low-probability, high-impact events. To address this issue, we present a novel stochastic optimal power flow formulation that distinguishes between “normal” operation conditions in which power deviations are balanced with AGC only, and “adverse” operation under which manual re-dispatch actions are required. As a result, our approach yields solutions that are more reliable and less conservative than existing approaches in the literature.

Our model is formulated as a joint chance-constraint program that limits the probability that operators manually adjust the power output of the generators. To assess the contributions of our proposal, we compare it with existing approaches using an illustrative 3-bus network and a more realistic 118-bus system. The obtained results for the larger system demonstrate that the proposed methodology is able to yield dispatch decisions that maintain almost identical security levels, but are 18% cheaper than approaches that pursue feasibility with AGC actions only under any uncertainty realization. As a counterpart, the computational burden of the proposed approach increases due to the modeling of the manual re-dispatch actions. However, we also suggest a heuristic algorithm to solve the proposed model and verify that the computational time is drastically shortened without causing a significant decline in performance. Finally, we propose incorporating economic information into the big-M tightening algorithm by first solving a heuristic. This approach leads to a tighter formulation and results in a significant computational speedup.

## Chapter 5

# Closure



In this closing chapter, the thesis is summarized, conclusions are drawn and directions for future research are given.

## 5.1 Summary and Conclusions

The *unit commitment* (UC) and *optimal power flow* (OPF) are fundamental tools at the core of power systems operation and are widely used in electricity markets. The UC and OPF are optimization problems that translate into computationally challenging tasks for several reasons and, given their critical role in electricity markets, any enhancement of them may result in significant benefits. In this thesis, we focus on addressing the following challenges:

1. **Computational burden of the UC problem.** The on/off status of generating units are modeled as binary variables which render a combinatorial decision-making process incurring a significant computational time.
2. **Incorporating uncertainty of electricity demand and renewable generation in the OPF problem.** Accurately quantifying the impact of uncertainty is essential in OPF to ensure the secure operation of power systems. Consequently, stochastic OPF (SOPF) models emerge, but they present the difficulties of trading-off between reliability and cost, and being tractable.

To cope with these issues, several topics and tools have been studied in this thesis:

- **Compacting UC formulation.** It is well-known that network-constraints complicate the solution to the UC problem. In today's power systems, most transmission lines are oversized (under a pre-contingency state), making their constraints superfluous. In this thesis, we delve into methods that speed up the solution of UC by removing superfluous transmission constraints.
- **Joint chance-constrained OPF (JCC-OPF).** This model reduces the expected cost of operation by ruling out the satisfaction of technical constraints for a specified percentage of uncertainty realizations, ensuring the security of the system for the rest. The adaptability and practicality of the model is noteworthy, as the system operator can adjust the proportion of scenarios violated, thus, influencing both system reliability and operating costs. As a drawback, this optimization problem lacks a finite, tractable reformulation. Among the existing approximations, this thesis focuses on investigating the *sample average approximation* (SAA), which yields the least conservative performance in terms of cost. The shortcoming of the SAA reformulation is that it takes significant computational time due to the presence of binary variables, thus leading to a *mixed-integer program* (MIP).

- **Integration of various reserve actions.** In SOPF models, in particular JCC-OPF problems, it is common to assume that the forecast errors of electricity demand and renewable generation are balanced by the deployment of reserve, such as *automatic generation control* (AGC). The AGC is modeled as an affine control policy, thus its implementation simplifies the solution of the SOPF. However, under extreme scenarios, AGC can jeopardize the system reliability or incurs significant costs. In practice, in those cases, system operators may resort to additional resources, e.g., manual reserve. For that reason, we study the integration of AGC and manual reserve as a tool to balance reliability and cost in SOPF problems.

In this thesis, we have developed several tight and compact optimization models for UC and OPF problems that contribute to these research challenges. The contents of this thesis are included in the published papers [46, 47], and the preprint [48]:

- In our paper [46], we present a methodology to reduce the computational time of the UC by screening out superfluous line capacity constraints. The optimization-based methods proposed in the literature only remove redundant constraints and thus, involve moderate computational savings. This paper presents a novel constraint screening methodology that removes both redundant *and inactive* constraints and further reduces the computational burden of this problem. As existing approaches, the one we propose is based on computing the maximum line power flows on an LP-relaxation of the UC formulation. As a salient feature of our work, we propose to tighten this LP-relaxation to exclude uneconomical operating conditions. In doing so, our methodology is able to filter out a higher number of line capacity constraints. Simulation results using a 2000-bus network show that our proposal reduces the number of retained constraints and the solution time by 15% and 45%, respectively, if compared with existing benchmark methods. Furthermore, the constraint-screening rate of our approach remains quite unaltered when topological changes of the network are considered, which suggests that our approach is resilient against this type of changes. Finally, even though the cost inequality we use to increase the constraint-screening power of our method is data-driven, our numerical analysis reveals that the solution to the reduced UC problem we produce is generally feasible and optimal in the original UC formulation, if enough data are available.
- In the work [47], we propose a novel exact resolution technique for a MIP SAA-based reformulation of the JCC-OPF problem. Our methodology includes a screening method to eliminate superfluous constraints based on an iterative procedure to repeatedly tighten the Big-Ms present in the MIP. These procedures are

combined with the addition of valid inequalities based on the special structure of the model. Said inequalities strengthen its linear relaxation and allow for additional screening of constraints. The resultant model is thus compact and tight. In the case study, we show that, in comparison with the benchmark model, our methodology provides remarkable results in terms of the linear relaxation bounds, the RAM memory needed to solve the instances, and the total computational time. Specifically, our method **TS+V** solves to optimality all of the instances generated for the IEEE-RTS-118 and the IEEE-RTS-300 test systems, the majority of which are not solved within 10 hours of computational time using the benchmark approach. Furthermore, the average number of constraints eliminated from all instances with **TS+V** always exceeds 95% of them, and the lower bound is markedly increased by the inclusion of the valid inequalities, showing the outstanding results of the combination of the methods developed. It is worth noting that the addition of the valid inequalities enhances the tightness of the model but compromises its compactness, albeit this trade-off is counterbalanced by augmenting the filtering rate of constraints within the tightening-and-screening procedure. The comparison of our results with those provided by existing approximate and exact methods shows that our approach is computationally very competitive for small and medium-sized instances, always providing the best results in terms of cost. For the large instances addressed, while outperformed by the approximate methods in terms of computational time (as expected), our exact solution strategy not only provides a certificate of optimality but also returns the optimal solution within the set time limit. Finally, we are able to speed up the resolution of the largest instances about four times by incorporating information from the objective function during the pre-processing step. This is achieved through the use of a heuristic that delivers a good upper bound on the optimal OPF cost.

- In the preprint [48], we present a novel SOPF model. Existing approaches to solving the SOPF are either overly conservative and expensive, or leave the system vulnerable to low-probability, high-impact events. The novel SOPF formulation distinguishes between “normal” operation conditions in which power deviations are balanced with AGC only, and “adverse” operation under which manual re-dispatch actions are required. As a result, our approach yields solutions that are more reliable and less conservative than existing approaches in the literature. Our model is formulated as a joint chance-constraint program that limits the probability that operators manually adjust the power output of the generators. In the case study, the obtained results demonstrate that the proposed methodology is able to yield dispatch decisions that maintain almost identical security levels, but are 18% cheaper than approaches that pursue feasibility with AGC actions only under any uncertainty realization. As a counterpart, the computational burden

of the proposed approach increases due to the modeling of the manual re-dispatch actions. However, we also suggest a heuristic algorithm to solve the proposed model and verify that the computational time is drastically shortened without causing a significant decline in performance. Finally, we propose incorporating economic information into the Big-M tightening by first solving a heuristic. This approach leads to a tighter formulation and results in a significant computational speedup.

## 5.2 Limitations of the Conducted Research

The findings garnered from the research subject of this thesis provide noteworthy contributions within the realm of power system operation. Nonetheless, this study encompasses certain limitations that necessitate further investigation to bolster the contributions raised in this thesis. The following are the delineated limitations:

1. The cost-driven screening method is based on a single-period version of the UC. This poses a practical limitation, as the UC problem entails a 24-hour time horizon including supplementary ramping limits and minimum down- and up-time constraints. An extended formulation of the UC brings about additional challenges to be addressed in the screening method, such as deriving a tight multi-period UC relaxation, and defining a proper net demand set as well as estimating a system operating cost that accurately represents an upper bound of the optimal one within the specified time horizon.

Furthermore, the cost-driven screening relies on imposing an upper bound on the operating cost, thus discarding uneconomical operating conditions and increasing the screening power. This upper bound cost is estimated through statistical regression where pairs of historical data on optimal UC cost and aggregate net demand are needed. Similarly to other machine learning techniques, in cases where an ample amount of data is accessible, the likelihood of misidentifying redundant or inactive constraints is minimal, as we demonstrate through the numerical experiments carried out in this thesis. Nonetheless, our data-driven approach does not provide performance guarantees, thus implying the possibility of erroneously identifying superfluous constraints that may result in suboptimal or infeasible solutions.

2. The proposed methodology for solving the SAA-based JCC-OPF, which is based on deriving strong valid inequalities, exhibits the limitation of being tailored towards a particular form of the matrix constraint. Specifically, the derived valid inequalities in this thesis are built on linear constraints and rely on a two-dimensional  $k$ -envelope framework, which becomes impractical when extended to

higher-dimensional cases.

Moreover, the valid inequalities are individually derived for each constraint in the joint-chance constraint system. In doing so, these valid inequalities do not capture potential dependencies among the constraints. For example, certain constraints may dominate others, such that the satisfaction of those constraints that are dominant inherently guarantees the satisfaction of the remaining constraints. If such an approach were undertaken, it would yield stronger valid inequalities. This issue can be remedied by formulating valid inequalities that merge variables from subgroups of constraints within the joint-chance constraint system. However, it is worth noting that as the degree of combination increases, so does the associated computational cost.

3. The novel SOPF introduced in this work, which integrates both automatic and manual reserves, regards thermal generating units as the sole recourse for addressing deviations from the predicted net demand. However, while this approach expands the repertoire of actions available to system operators traditionally used in the literature, it could be further enhanced by incorporating cutting-edge technologies already deployed in corrective control mechanisms.

Viable options of cutting-edge technology are *high voltage direct current connections* (HVDC) and *phase shifting transformers* (PST). These technologies are typically managed by the system operator and offer cost-efficient solutions, as it extends the range of potential solutions. In contrast, resorting to generation re-dispatching, which interferes with the market operation and entails substantial expenses, can be avoided. These technologies are already considered in some works, as [114], where they are implemented to effectively address system contingencies and respond to uncertainty.

### 5.3 Outlook

Directions for future research resulting from the study carried out in this thesis are listed below:

1. Application of the cost-driven screening method to multi-period unit commitment formulations that include inter-temporal constraints such as ramping limits and minimum times. In this case, the challenges are twofold, namely, i) building a sufficiently tight relaxation of the multi-period UC to produce an algorithm with a reasonable screening power, and ii) designing a proper set of net demands and finding a tight upper bound on the system operating cost for a given time horizon.

2. A promising future research avenue for the proposed methodology to solve the SAA-based JCC-OPF problem consists of the development of a generalized set of valid inequalities that combine variables from pairs or subgroups of lines and generators.
3. The novel SOPF proposed in this thesis has the potential to be enhanced through the integration of cutting-edge technology, rather than relying on manual adjustments of generators to ensure system balance and reliability for extreme, low probable scenarios. Promising options for new technology integration include HVDC and PST. The integration of such technologies enables greater flexibility in the operation of power systems, leading to significant reductions in operating costs.

# References

- [1] J. M. Morales, A. J. Conejo, H. Madsen, P. Pinson, and M. Zugno, *Integrating Renewables in Electricity Markets: Operational Problems*, vol. 205. Springer Science & Business Media, 2013.
- [2] J. A. P. Lopes, A. G. Madureira, M. Matos, R. J. Bessa, V. Monteiro, J. L. Afonso, S. F. Santos, J. P. Catalão, C. H. Antunes, and P. Magalhães, “The future of power systems: Challenges, trends, and upcoming paradigms,” *Wiley Interdisciplinary Reviews: Energy and Environment*, vol. 9, no. 3, p. e368, 2020.
- [3] M. Shahidehpour, H. Yamin, and Z. Li, *Market Operations in Electric Power Systems: Forecasting, Scheduling, and Risk Management*. John Wiley & Sons, 2003.
- [4] Federal Energy Regulatory Commission and others, “Energy primer: A handbook of energy market basics.” [Online]. Available: <https://www.ferc.gov/market-oversight/guide/energy-primer.pdf>, 2015.
- [5] A. J. Conejo and L. Baringo, *Power System Operations*, vol. 11. Springer, 2018.
- [6] A. Gómez-Expósito, A. J. Conejo, and C. Cañizares, *Electric Energy Systems: Analysis and Operation*. CRC press, 2018.
- [7] D. A. Tejada-Arango, S. Lumbreras, P. Sánchez-Martín, and A. Ramos, “Which unit-commitment formulation is best? a comparison framework,” *IEEE Transactions on Power Systems*, vol. 35, no. 4, pp. 2926–2936, 2020.
- [8] B. Knueven, J. Ostrowski, and J.-P. Watson, “On mixed-integer programming formulations for the unit commitment problem,” *INFORMS Journal on Computing*, vol. 32, no. 4, pp. 857–876, 2020.
- [9] P. Bendotti, P. Fouilhoux, and C. Rottner, “On the complexity of the unit commitment problem,” *Annals of Operations Research*, vol. 274, no. 1, pp. 119–130, 2019.

- 
- [10] N. P. Padhy, "Unit commitment-a bibliographical survey," *IEEE Transactions on Power Systems*, vol. 19, no. 2, pp. 1196–1205, 2004.
- [11] Y. Yang and L. Wu, "Machine learning approaches to the unit commitment problem: Current trends, emerging challenges, and new strategies," *The Electricity Journal*, vol. 34, no. 1, p. 106889, 2021.
- [12] S. Pineda, J. M. Morales, and A. Jiménez-Cordero, "Data-driven screening of network constraints for unit commitment," *IEEE Transactions on Power Systems*, vol. 35, no. 5, pp. 3695–3705, 2020.
- [13] Y. Yang, Z. Yang, J. Yu, K. Xie, and L. Jin, "Fast economic dispatch in smart grids using deep learning: An active constraint screening approach," *IEEE Internet of Things Journal*, vol. 7, no. 11, pp. 11030–11040, 2020.
- [14] S. Misra, L. Roald, and Y. Ng, "Learning for constrained optimization: Identifying optimal active constraint sets," *INFORMS Journal on Computing*, vol. 34, no. 1, pp. 463–480, 2022.
- [15] D. Deka and S. Misra, "Learning for DC-OPF: Classifying active sets using neural nets," in *2019 IEEE Milan PowerTech*, pp. 1–6, 2019.
- [16] F. Hasan, A. Kargarian, and J. Mohammadi, "Hybrid learning aided inactive constraints filtering algorithm to enhance AC OPF solution time," *IEEE Transactions on Industrial Applications*, vol. 57, no. 2, pp. 1325–1334, 2021.
- [17] A. S. Xavier, F. Qiu, and S. Ahmed, "Learning to solve large-scale security-constrained unit commitment problems," *INFORMS Journal on Computing*, vol. 33, no. 2, pp. 739–756, 2021.
- [18] W. Ben-Ameur and J. Neto, "A constraint generation algorithm for large scale linear programs using multiple-points separation," *Mathematical Programming*, vol. 107, no. 3, pp. 517–537, 2006.
- [19] A. S. Xavier, F. Qiu, F. Wang, and P. R. Thimmapuram, "Transmission constraint filtering in large-scale security-constrained unit commitment," *IEEE Transactions on Power Systems*, vol. 34, no. 3, pp. 2457–2460, 2019.
- [20] D. A. Tejada-Arango, P. Sánchez-Martín, and A. Ramos, "Security constrained unit commitment using line outage distribution factors," *IEEE Transactions on Power Systems*, vol. 33, no. 1, pp. 329–337, 2018.
- [21] A. J. Ardakani and F. Bouffard, "Identification of umbrella constraints in DC-based security-constrained optimal power flow," *IEEE Transactions on Power Systems*, vol. 28, no. 4, pp. 3924–3934, 2013.

- 
- [22] Q. Zhai, X. Guan, J. Cheng, and H. Wu, "Fast identification of inactive security constraints in SCUC problems," *IEEE Transactions on Power Systems*, vol. 25, no. 4, pp. 1946–1954, 2010.
- [23] R. Madani, J. Lavaei, and R. Baldick, "Constraint screening for security analysis of power networks," *IEEE Transactions on Power Systems*, vol. 32, no. 3, pp. 1828–1838, 2017.
- [24] L. A. Roald and D. K. Molzahn, "Implied constraint satisfaction in power system optimization: The impacts of load variations," in *2019 57th Annual Allerton Conference on Communication, Control, and Computing (Allerton)*, pp. 308–315, 2019.
- [25] S. Zhang, H. Ye, F. Wang, Y. Chen, S. Rose, and Y. Ma, "Data-aided offline and online screening for security constraint," *IEEE Transactions on Power Systems*, vol. 36, no. 3, pp. 2614–2622, 2021.
- [26] R. Weinhold and R. Mieth, "Fast security-constrained optimal power flow through low-impact and redundancy screening," *IEEE Transactions on Power Systems*, vol. 35, no. 6, pp. 4574–4584, 2020.
- [27] S. Frank, I. Steponavice, and S. Rebennack, "Optimal power flow: A bibliographic survey I," *Energy Systems*, vol. 3, no. 3, pp. 221–258, 2012.
- [28] L. Xie, P. M. Carvalho, L. A. Ferreira, J. Liu, B. H. Krogh, N. Popli, and M. D. Ilić, "Wind integration in power systems: Operational challenges and possible solutions," *Proceedings of the IEEE*, vol. 99, no. 1, pp. 214–232, 2010.
- [29] J. M. Morales, A. J. Conejo, and J. Pérez-Ruiz, "Economic valuation of reserves in power systems with high penetration of wind power," *IEEE Transactions on Power Systems*, vol. 24, no. 2, pp. 900–910, 2009.
- [30] R. A. Jabr, S. Karaki, and J. A. Korbane, "Robust multi-period OPF with storage and renewables," *IEEE Transactions on Power Systems*, vol. 30, no. 5, pp. 2790–2799, 2015.
- [31] J. Warrington, P. Goulart, S. Mariéthoz, and M. Morari, "Policy-based reserves for power systems," *IEEE Transactions on Power Systems*, vol. 28, no. 4, pp. 4427–4437, 2013.
- [32] A. Lorca and X. A. Sun, "The adaptive robust multi-period alternating current optimal power flow problem," *IEEE Transactions on Power Systems*, vol. 33, no. 2, pp. 1993–2003, 2018.

- 
- [33] W. Van Ackooij, R. Zorgati, R. Henrion, and A. Möller, “Chance constrained programming and its applications to energy management,” *Stochastic Optimization-Seeing the Optimal for the Uncertain*, pp. 291–320, 2011.
- [34] M. Vrakopoulou, K. Margellos, J. Lygeros, and G. Andersson, “Probabilistic guarantees for the N-1 security of systems with wind power generation,” in *Reliability and Risk Evaluation of Wind Integrated Power Systems*, pp. 59–73, Springer, 2013.
- [35] L. Roald, F. Oldewurtel, T. Krause, and G. Andersson, “Analytical reformulation of security constrained optimal power flow with probabilistic constraints,” in *2013 IEEE Grenoble Conference*, pp. 1–6, IEEE, 2013.
- [36] D. Bienstock, M. Chertkov, and S. Harnett, “Chance-constrained optimal power flow: Risk-aware network control under uncertainty,” *SIAM Review*, vol. 56, no. 3, pp. 461–495, 2014.
- [37] M. Lubin, Y. Dvorkin, and S. Backhaus, “A robust approach to chance constrained optimal power flow with renewable generation,” *IEEE Transactions on Power Systems*, vol. 31, no. 5, pp. 3840–3849, 2015.
- [38] A. M. Hou and L. A. Roald, “Chance constraint tuning for optimal power flow,” in *2020 International Conference on Probabilistic Methods Applied to Power Systems (PMAPS)*, pp. 1–6, 2020.
- [39] A. Peña-Ordieres, D. K. Molzahn, L. A. Roald, and A. Wächter, “DC optimal power flow with joint chance constraints,” *IEEE Transactions on Power Systems*, vol. 36, no. 1, pp. 147–158, 2021.
- [40] A. Esteban-Pérez and J. M. Morales, “Distributionally robust optimal power flow with contextual information,” *European Journal of Operational Research*, vol. 306, no. 3, pp. 1047–1058, 2023.
- [41] B. L. Miller and H. M. Wagner, “Chance constrained programming with joint constraints,” *Operations Research*, vol. 13, no. 6, pp. 930–945, 1965.
- [42] L. Roald and G. Andersson, “Chance-constrained AC optimal power flow: Reformulations and efficient algorithms,” *IEEE Transactions on Power Systems*, vol. 33, no. 3, pp. 2906–2918, 2018.
- [43] G. Chen, H. Zhang, H. Hui, and Y. Song, “Time-efficient joint chance-constrained optimal power flow with a learning-based robust approximation,” *arXiv preprint arXiv:2112.09827*, 2021.

- [44] M. A. Lejeune and P. Dehghanian, “Optimal power flow models with probabilistic guarantees: A boolean approach,” *IEEE Transactions on Power Systems*, vol. 35, no. 6, pp. 4932–4935, 2020.
- [45] J. Warrington, P. J. Goulart, S. Mariéthoz, and M. Morari, “Robust reserve operation in power systems using affine policies,” in *2012 IEEE 51st IEEE Conference on Decision and Control (CDC)*, pp. 1111–1117, 2012.
- [46] Á. Porras, S. Pineda, J. M. Morales, and A. Jiménez-Cordero, “Cost-driven screening of network constraints for the unit commitment problem,” *IEEE Transactions on Power Systems*, vol. 38, no. 1, pp. 42–51, 2022.
- [47] Á. Porras, C. Domínguez, J. M. Morales, and S. Pineda, “Tight and compact sample average approximation for joint chance constrained optimal power flow,” *arXiv preprint arXiv:2205.03370*, 2022.
- [48] Á. Porras, L. Roald, J. M. Morales, and S. Pineda, “Integrating automatic and manual reserves in optimal power flow via chance constraints,” *arXiv preprint arXiv:2303.05412*, 2023.
- [49] G. C. Calafiore, “Random convex programs,” *SIAM Journal on Optimization*, vol. 20, no. 6, pp. 3427–3464, 2010.
- [50] Z. Ma, H. Zhong, T. Cheng, J. Pi, and F. Meng, “Redundant and nonbinding transmission constraints identification method combining physical and economic insights of unit commitment,” *IEEE Transactions on Power Systems*, vol. 36, no. 4, pp. 3487–3495, 2021.
- [51] R. Koenker and K. F. Hallock, “Quantile regression,” *Journal on Economic Perspectives*, vol. 15, no. 4, pp. 143–156, 2001.
- [52] C. A. Floudas, *Nonlinear and Mixed-integer Optimization: Fundamentals and Applications*. Oxford University Press, 1995.
- [53] M. L. Bynum, G. A. Hackebeil, W. E. Hart, C. D. Laird, B. L. Nicholson, J. D. Siirola, J.-P. Watson, and D. L. Woodruff, *Pyomo - Optimization Modeling in Python*, vol. 67. Springer Nature, 2021.
- [54] “CPLEX Optimizer.” IBM, 2021. Available (online): <https://www.ibm.com/analytics/cplex-optimizer>.
- [55] A. B. Birchfield, T. Xu, K. M. Gegner, K. S. Shetye, and T. J. Overbye, “Grid structural characteristics as validation criteria for synthetic networks,” *IEEE Transactions on Power Systems*, vol. 32, no. 4, pp. 3258–3265, 2017.

- [56] OASYS, “Data of 5-node and 2000-node Power Systems,” *GitHub repository* ([https://github.com/groupoasys/Cost-driven\\_Screening\\_Method\\_Data](https://github.com/groupoasys/Cost-driven_Screening_Method_Data)), 2021.
- [57] A. A. Taleizadeh, S. T. A. Niaki, and A. Makui, “Multiproduct multiple-buyer single-vendor supply chain problem with stochastic demand, variable lead-time, and multi-chance constraint,” *Expert Systems with Applications*, vol. 39, no. 5, pp. 5338–5348, 2012.
- [58] K. Shaw, M. Irfan, R. Shankar, and S. S. Yadav, “Low carbon chance constrained supply chain network design problem: A Benders decomposition based approach,” *Computers & Industrial Engineering*, vol. 98, pp. 483–497, 2016.
- [59] Ö. Elçi, N. Noyan, and K. Bülbül, “Chance-constrained stochastic programming under variable reliability levels with an application to humanitarian relief network design,” *Computers & Operations Research*, vol. 96, pp. 91–107, 2018.
- [60] J. Daniélsson, B. N. Jorgensen, C. G. de Vries, and X. Yang, “Optimal portfolio allocation under the probabilistic VaR constraint and incentives for financial innovation,” *Annals of Finance*, vol. 4, no. 3, pp. 345–367, 2008.
- [61] K. Natarajan, D. Pachamanova, and M. Sim, “Incorporating asymmetric distributional information in robust value-at-risk optimization,” *Management Science*, vol. 54, no. 3, pp. 573–585, 2008.
- [62] A. Najjarbashi and G. J. Lim, “A decomposition algorithm for the two-stage chance-constrained operating room scheduling problem,” *IEEE Access*, vol. 8, pp. 80160–80172, 2020.
- [63] M. W. Tanner, L. Sattenspiel, and L. Ntaimo, “Finding optimal vaccination strategies under parameter uncertainty using stochastic programming,” *Mathematical Biosciences*, vol. 215, pp. 144–151, Oct. 2008.
- [64] A. Prékopa, “Probabilistic programming,” *Handbooks in Operations Research and Management Science*, vol. 10, pp. 267–351, 2003.
- [65] S. Küçükyavuz and R. Jiang, “Chance-constrained optimization under limited distributional information: A review of reformulations based on sampling and distributional robustness,” *EURO Journal on Computational Optimization*, vol. 10, p. 100030, 2022.
- [66] C. M. Lagoa, X. Li, and M. Sznaier, “Probabilistically constrained linear programs and risk-adjusted controller design,” *SIAM Journal on Optimization*, vol. 15, no. 3, pp. 938–951, 2005.

- [67] R. Henrion, “Structural properties of linear probabilistic constraints,” *Optimization*, vol. 56, no. 4, pp. 425–440, 2007.
- [68] R. Henrion and C. Strugarek, “Convexity of chance constraints with dependent random variables: The use of copulae,” in *Stochastic Optimization Methods in Finance and Energy*, pp. 427–439, Springer, 2011.
- [69] A. Ben-Tal and A. Nemirovski, “Robust solutions of linear programming problems contaminated with uncertain data,” *Mathematical Programming*, vol. 88, no. 3, pp. 411–424, 2000.
- [70] A. Nemirovski and A. Shapiro, “Convex approximations of chance constrained programs,” *SIAM Journal on Optimization*, vol. 17, no. 4, pp. 969–996, 2007.
- [71] R. T. Rockafellar and S. Uryasev, “Optimization of conditional value-at-risk,” *The Journal of Risk*, vol. 2, no. 3, pp. 21–41, 2000.
- [72] H. Sun, H. Xu, and Y. Wang, “Asymptotic analysis of sample average approximation for stochastic optimization problems with joint chance constraints via conditional value at risk and difference of convex functions,” *Journal of Optimization Theory and Applications*, vol. 161, pp. 257–284, Apr. 2014.
- [73] S. Ahmed, J. Luedtke, Y. Song, and W. Xie, “Nonanticipative duality, relaxations, and formulations for chance-constrained stochastic programs,” *Mathematical Programming*, vol. 162, no. 1, pp. 51–81, 2017.
- [74] N. Jiang and W. Xie, “ALSO-X and ALSO-X+: Better convex approximations for chance constrained programs,” *Operations Research*, vol. 70, no. 6, pp. 3581–3600, 2022.
- [75] L. J. Hong, Y. Yang, and L. Zhang, “Sequential convex approximations to joint chance constrained programs: A Monte Carlo approach,” *Operations Research*, vol. 59, no. 3, pp. 617–630, 2011.
- [76] A. Peña-Ordieres, J. R. Luedtke, and A. Wächter, “Solving chance-constrained problems via a smooth sample-based nonlinear approximation,” *SIAM Journal on Optimization*, vol. 30, no. 3, pp. 2221–2250, 2020.
- [77] A. Shapiro, “Monte Carlo sampling methods,” *Handbooks in Operations Research and Management Science*, vol. 10, pp. 353–425, 2003.
- [78] A. Nemirovski and A. Shapiro, “Scenario approximations of chance constraints,” *Probabilistic and Randomized Methods for Design under Uncertainty*, pp. 3–47, 2006.

- [79] O. Günlük and Y. Pochet, “Mixing mixed-integer inequalities,” *Mathematical Programming*, vol. 90, no. 3, pp. 429–457, 2001.
- [80] J. Luedtke, S. Ahmed, and G. L. Nemhauser, “An integer programming approach for linear programs with probabilistic constraints,” *Mathematical Programming*, vol. 122, no. 2, pp. 247–272, 2010.
- [81] A. Abdi and R. Fukasawa, “On the mixing set with a knapsack constraint,” *Mathematical Programming*, vol. 157, no. 1, pp. 191–217, 2016.
- [82] D. Dentcheva, A. Prékopa, and A. Ruszczyński, “Concavity and efficient points of discrete distributions in probabilistic programming,” *Mathematical Programming*, vol. 89, no. 1, pp. 55–77, 2000.
- [83] R. Nair and E. Miller-Hooks, “Fleet management for vehicle sharing operations,” *Transportation Science*, vol. 45, no. 4, pp. 524–540, 2011.
- [84] S. R. Tayur, R. R. Thomas, and N. R. Natraj, “An algebraic geometry algorithm for scheduling in presence of setups and correlated demands,” *Mathematical Programming*, vol. 69, no. 1, pp. 369–401, 1995.
- [85] F. Qiu, S. Ahmed, S. S. Dey, and L. A. Wolsey, “Covering linear programming with violations,” *INFORMS Journal on Computing*, vol. 26, pp. 531–546, Apr. 2014.
- [86] W. Xie and S. Ahmed, “On the quantile cut closure of chance-constrained problems,” in *International Conference on Integer Programming and Combinatorial Optimization*, pp. 398–409, Springer, 2016.
- [87] W. Xie and S. Ahmed, “On quantile cuts and their closure for chance constrained optimization problems,” *Mathematical Programming*, vol. 172, no. 1, pp. 621–646, 2018.
- [88] S. Ahmed and W. Xie, “Relaxations and approximations of chance constraints under finite distributions,” *Mathematical Programming*, vol. 170, no. 1, pp. 43–65, 2018.
- [89] Y. Song, J. R. Luedtke, and S. Küçükyavuz, “Chance-constrained binary packing problems,” *INFORMS Journal on Computing*, vol. 26, no. 4, pp. 735–747, 2014.
- [90] L. A. Roald, D. Pozo, A. Papavasiliou, D. K. Molzahn, J. Kazempour, and A. Conejo, “Power systems optimization under uncertainty: A review of methods and applications,” *Electric Power Systems Research*, vol. 214, p. 108725, 2023.

- [91] K. Baker and A. Bernstein, “Joint chance constraints in AC optimal power flow: Improving bounds through learning,” *IEEE Transactions on Smart Grid*, vol. 10, no. 6, pp. 6376–6385, 2019.
- [92] M. Jia, G. Hug, and C. Shen, “Iterative decomposition of joint chance constraints in OPF,” *IEEE Transactions on Power Systems*, vol. 36, no. 5, pp. 4836–4839, 2021.
- [93] J. Luedtke and S. Ahmed, “A sample approximation approach for optimization with probabilistic constraints,” *SIAM Journal on Optimization*, vol. 19, no. 2, pp. 674–699, 2008.
- [94] M. Conforti, G. Cornuéjols, and G. Zambelli, *Integer Programming*, vol. 271. Springer, 2014.
- [95] M. Cheema, Z. Shen, X. Lin, and W. Zhang, “A unified framework for efficiently processing ranking related queries,” 2014.
- [96] C. D. Tóth, J. O’Rourke, and J. E. Goodman, *Handbook of Discrete and Computational Geometry*. CRC press, 2017.
- [97] H. Edelsbrunner and E. Welzl, “Constructing belts in two-dimensional arrangements with applications,” *SIAM Journal on Computing*, vol. 15, no. 1, 1986.
- [98] H. Edelsbrunner and E. Welzl, “On the number of line separations of a finite set in the plane,” *Journal of Combinatorial Theory, Series A*, vol. 38, no. 1, pp. 15–29, 1985.
- [99] T. K. Dey, “Improved bounds for planar k-sets and related problems,” *Discrete & Computational Geometry*, vol. 19, no. 3, pp. 373–382, 1998.
- [100] G. Tóth, “Point sets with many k-sets,” in *Proceedings of the Sixteenth Annual Symposium on Computational Geometry*, pp. 37–42, 2000.
- [101] G. Nivasch, “An improved, simple construction of many halving edges,” *Contemporary Mathematics*, vol. 453, pp. 299–306, 2008.
- [102] Power Grid Lib, 2022. GitHub repository, available at: (<https://github.com/power-grid-lib/pglib-opf>).
- [103] Gurobi Optimization, LLC, “Gurobi Optimizer Reference Manual,” 2022.
- [104] Y. Zhang, S. Shen, and J. L. Mathieu, “Data-driven optimization approaches for optimal power flow with uncertain reserves from load control,” in *2015 American Control Conference (ACC)*, pp. 3013–3018, IEEE, 2015.

- [105] J. Luedtke, “A branch-and-cut decomposition algorithm for solving chance-constrained mathematical programs with finite support,” *Mathematical Programming*, vol. 146, pp. 219–244, Aug. 2014.
- [106] A. Atamtürk, G. L. Nemhauser, and M. W. P. Savelsbergh, “Conflict graphs in solving integer programming problems,” *European Journal of Operational Research*, vol. 121, pp. 40–55, Feb. 2000.
- [107] North American Reliability Corporation (NERC), “Standard BAL-005 - Automatic Generation Control.” [Online]. Available: <https://www.nerc.com/pa/Stand/Pages/Default.aspx>, 2009.
- [108] R. Kannan, J. R. Luedtke, and L. A. Roald, “Stochastic DC optimal power flow with reserve saturation,” *Electric Power Systems Research*, vol. 189, p. 106566, 2020.
- [109] L. Roald, S. Misra, M. Chertkov, and G. Andersson, “Optimal power flow with weighted chance constraints and general policies for generation control,” in *2015 54th IEEE conference on decision and control (CDC)*, pp. 6927–6933, IEEE, 2015.
- [110] K. Margellos, V. Rostampour, M. Vrakopoulou, M. Prandini, G. Andersson, and J. Lygeros, “Stochastic unit commitment and reserve scheduling: A tractable formulation with probabilistic certificates,” in *2013 European Control Conference (ECC)*, pp. 2513–2518, 2013.
- [111] G. A. Hanasusanto, V. Roitch, D. Kuhn, and W. Wiesemann, “Ambiguous joint chance constraints under mean and dispersion information,” *Operations Research*, vol. 65, no. 3, pp. 751–767, 2017.
- [112] L. Roald, S. Misra, M. Chertkov, S. Backhaus, and G. Andersson, “Chance constrained optimal power flow with curtailment and reserves from wind power plants,” *arXiv preprint arXiv:1601.04321*, 2016.
- [113] OASYS, “Data of 118-node power system,” *GitHub repository* ([https://github.com/groupoasys/AGC\\_and\\_Manual\\_Reserve\\_CC](https://github.com/groupoasys/AGC_and_Manual_Reserve_CC)), 2023.
- [114] L. Roald, S. Misra, T. Krause, and G. Andersson, “Corrective control to handle forecast uncertainty: A chance constrained optimal power flow,” *IEEE Transactions on Power Systems*, vol. 32, no. 2, pp. 1626–1637, 2016.